

This electronic thesis or dissertation has been downloaded from the King's Research Portal at <https://kclpure.kcl.ac.uk/portal/>



## Particle phenomenology from M theory inspired models

Bozek, Krzysztof

*Awarding institution:*  
King's College London

The copyright of this thesis rests with the author and no quotation from it or information derived from it may be published without proper acknowledgement.

### END USER LICENCE AGREEMENT



Unless another licence is stated on the immediately following page this work is licensed

under a Creative Commons Attribution-NonCommercial-NoDerivatives 4.0 International

licence. <https://creativecommons.org/licenses/by-nc-nd/4.0/>

You are free to copy, distribute and transmit the work

Under the following conditions:

- Attribution: You must attribute the work in the manner specified by the author (but not in any way that suggests that they endorse you or your use of the work).
- Non Commercial: You may not use this work for commercial purposes.
- No Derivative Works - You may not alter, transform, or build upon this work.

Any of these conditions can be waived if you receive permission from the author. Your fair dealings and other rights are in no way affected by the above.

### Take down policy

If you believe that this document breaches copyright please contact [librarypure@kcl.ac.uk](mailto:librarypure@kcl.ac.uk) providing details, and we will remove access to the work immediately and investigate your claim.

KING'S COLLEGE LONDON

DOCTORAL THESIS

---

**Particle phenomenology from  
M theory inspired models**

---

*Author:*

**Krzysztof Bożek**

*Supervisor:*

**Prof. Bobby Acharya**



*A thesis submitted in fulfilment of the requirements for*

*the degree of Doctor of Philosophy in the*

Theoretical Particle Physics and Cosmology Group

Department of Physics

**London, April 2018**

**TO MY GRANDPARENTS**  
**MOIM DZIADKOM**

---

# Acknowledgements

This thesis would not be possible without help and support of my supervisor, Bobby Acharya. I am very grateful to him for providing me with many research opportunities, sharing his extensive knowledge and being always so understanding.

I owe my deepest gratitude to my fellow PhD student, Chakrit Pongkitivanichkul, for various illuminating discussions, collaborations and his help with my understanding of many aspects of theoretical high-energy physics.

I would like to thank Miguel Crispim Romão, Prof. Stephen King and Kazuki Sakurai who made this thesis possible through fruitful collaborations. It has been a great pleasure to work with all of you and I learned so much from you.

I am also very grateful to Professor Steven Abel and Professor Benjamin Allanach for their time and efforts on reading through this thesis and providing me with constructive feedback.

I would like to acknowledge many other professors, most notably John Ellis, Malcolm Fairbairn, Krzysztof Kutak, Nikolaos Mavromatos, Wiesław Płaczek and Riccardo Sapienza, for various illuminating discussions and their help through my studies.

I highly appreciate various discussions and support provided by fellow PhD students and postdocs from Kings's College London. And I will be definitely missing the crazy lunchbrakes together!

I am also very grateful to Alex Chaushev, Junwu Huang and Anna Ogorzałek for encouraging and help in PhD applications.

I owe my sanity thanks to many friends, in particular Pooya Azarhoosh, Marcello Davide Caio, Chandni Hindocha, Alix Le Marois, and the *DESY Proszę!* team, for adding colours into my life.

I am also very grateful to the admin staff of the Department of Physics, especially Megan Grace-Hughes, Julia Kilpatrick and Rowena Peake, for their exceptional commitment to work and for providing such a nice company.

Finally, and most importantly, I would like to thank to my parents for their unconditional love and persistent support, even at the most difficult for me times.

## Abstract

This thesis focuses on low-energy particle phenomenology arising from  $G_2$  compactifications of M theory. We construct a supersymmetric  $SO(10)$  model that can be naturally realised in this framework. An appropriate discrete symmetry combined with a symmetry breaking Wilson line suppresses the  $\mu$ -term and dangerous triplet–matter interactions at the compactification scale. Stabilised moduli introduce back the forbidden terms providing the  $\mu$ -term with the phenomenologically expected value of  $\mathcal{O}(\text{TeV})$ . In our model triplets are light and regenerated triplet interactions induce proton decay but safely within experimental constraints. In order to restore gauge unification we introduce extra, light, vector-like matter multiplets that together with the (unstable) lightest supersymmetric particle (LSP) can provide interesting experimental signatures. We also present a mechanism that generates high scale vacuum expectation values (VEV)s for the scalar components of right-handed neutrinos  $N$  of the vector-like pair that further break the gauge symmetry into the Standard Model  $SU(3)_C \times SU(2)_Y \times U(1)_Y$  as well as can induce the correct neutrino masses. The other significant part of the thesis is focused on collider phenomenology of string/M theory inspired models. In particular we study a prospect for electroweakino discovery at a proposed 100 TeV collider with three leptons plus missing transverse energy signature. We design simple but effective signal regions for this case and using simplified detector-level analysis we evaluate discovery reach and exclusion limits. Assuming  $3000 \text{ fb}^{-1}$  of integrated luminosity, W-inos could be discovered (excluded) up to 1.1 (1.8) TeV if the spectrum is not compressed.

# Contents

<b>1</b>	<b>Introduction</b>	<b>1</b>
1.1	SUSY . . . . .	4
1.2	Supergravity . . . . .	7
1.3	MSSM . . . . .	9
1.4	M theory on $G_2$ manifold . . . . .	11
1.4.1	Moduli stabilisation . . . . .	12
1.4.2	Observable sector . . . . .	15
1.5	Outline of the thesis . . . . .	17
<b>2</b>	<b>GUT models from M theory</b>	<b>19</b>
2.1	Introduction . . . . .	19
2.1.1	Symmetry breaking through Wilson lines . . . . .	20
2.1.2	Witten's solution of the doublet-triplet splitting problem . . . . .	21
2.1.3	Effective $\mu$ and trilinear terms . . . . .	25
2.2	SO(10) SUSY GUTs from M theory on $G_2$ -manifolds . . . . .	26
2.2.1	Additional vector-like family . . . . .	31
2.3	Consequences of $U(1)_X$ breaking . . . . .	33
2.3.1	The see-saw mechanism . . . . .	33
2.3.2	R-parity violation . . . . .	34
2.4	Effective light families . . . . .	38
2.5	Conclusion . . . . .	40
<b>3</b>	<b>Neutrino mass from M theory SO(10)</b>	<b>41</b>
3.1	Introduction and Motivation . . . . .	41
3.2	$U(1)_X$ Breaking scenarios and mechanisms . . . . .	42
3.3	Neutrino-neutralino mass matrix . . . . .	47
3.3.1	The mass matrix hierarchies . . . . .	51
3.4	Numerical Results . . . . .	54
3.4.1	$\nu$ component of the lightest state . . . . .	55
3.4.2	Matter Neutrino Yukawas and B-RPV couplings . . . . .	57
3.5	Conclusions and Discussion . . . . .	60
<b>4</b>	<b>Electroweakinos</b>	<b>62</b>
4.1	Introduction . . . . .	62
4.2	The cross sections and branching ratios . . . . .	64
4.2.1	The model setup . . . . .	64

4.2.2	The cross sections . . . . .	65
4.2.3	The branching ratios . . . . .	65
4.3	The simulation setup . . . . .	68
4.4	The kinematic distributions . . . . .	70
4.5	The limit and discovery reach . . . . .	73
4.5.1	The event selection . . . . .	73
4.5.2	The result . . . . .	74
4.6	Conclusion . . . . .	75
<b>5</b>	<b>Summary and outlook</b>	<b>77</b>
	<b>Appendices</b>	<b>80</b>
A.1	Charge fields Wilson Line absorption . . . . .	80
A.2	The lepton isolation requirement . . . . .	81
A.3	The visible cross sections . . . . .	83
	<b>Bibliography</b>	<b>86</b>

# Chapter 1

## Introduction

The Standard Model (SM) of particle physics [1–3] is a hugely successful theory of all known fundamental interactions except gravity. It is a quantum field theory based on  $SU(3)_C \times SU(2)_L \times U(1)_Y$  gauge group with the Higgs mechanism breaking down the gauge group to  $SU(3)_C \times U(1)_{EM}$  at low-energies. Since its formulation over 40 years ago its predictions for various observables like cross-sections, decay widths, asymmetries or magnetic moments of particles, to mention just a few, has been successfully confronted with experimental observations, often at an unprecedented level of accuracy. For long time the Standard Model provided guidance to the physics community for directions of future studies having predicted many particles and phenomena later to be discovered. The observation of the SM-like-Higgs boson has completed the Standard Model filling the last remaining gap.

Despite its success, as the SM does not include gravity, it can only be an effective low-energy theory. From the perspective of particle physics at the typical scale of SM,  $M_{EW} \sim \mathcal{O}(100 \text{ GeV})$ , the effects of gravity are too weak to be considered or indeed measurable. However, at the Planck scale,  $m_{pl} = \sqrt{\frac{hc}{8\pi G}} \approx 2 \cdot 10^{18} \text{ GeV}$ , gravity is expected to be comparable in strength to other fundamental interactions and cannot be possibly ignored. Now, there is a huge gap between  $M_{EW}$  and  $m_{pl}$ . In principle one can naively expect the SM to be valid up to the scale close to  $m_{pl}$  at which point a new, more fundamental theory enters the game. However, the existence of the Higgs boson in the SM, a scalar particle, raises concerns about validity of such an approach. The mass of a scalar particle is not protected by gauge symmetries and receives quantum corrections from new physics at a higher scale. In particular, if there is no new physics before the Planck scale, one would expect the mass of the Higgs to contain a term of order  $m_{pl}$ . It is thus difficult to imagine, unless some miraculous cancellations with the Higgs bare mass happen, that the physical mass of the Higgs is the observed 125 GeV, almost  $10^{16}$  times smaller than  $m_{pl}$ . This apparent fine-tuning is the infamous hierarchy problem. Setting aside anthropic solutions to this problem, one generally expects a new physics, i.e. supersymmetry, technicolor, or large extra dimensions, at about TeV scale for the fine-tuning not to be too large.



In addition to the hierarchy problem, that some would argue is just an aesthetic one, there are several other shortcomings of the SM. It does not contain suitable candidates for dark matter, dark energy or inflation required by cosmology observations. Similarly, it does not contain enough sources to create the asymmetry between the abundance of matter and antimatter observed in our universe. The Standard Model also does not address the question why there are three families of fermions and why they have such different masses.

It seems clear that SM has to be extended in some way. Over the years many proposals for beyond Standard Model (BSM) physics were made and those based on low-energy supersymmetry (SUSY) seem to be the most promising ones. Not only does SUSY provide solutions to the hierarchy problem and some of the other issues listed above, but it also contains attractive features like radiative electroweak symmetry breaking and gauge unification. In the simplest supersymmetric world, each particle has a superpartner which differs in spin by  $1/2$ . Since supersymmetry relates scalar and fermionic sectors, the masses of scalars are protected by the same gauge symmetries protecting fermions. However, if SUSY is realised in nature it has to be broken in order to split the mass of superpartners and their corresponding SM particles. Unfortunately, since the mechanism of SUSY breaking is unknown, one has to potentially add a significant number of new parameters (on top of the usual  $\sim 30$  SM parameters) in order to include all possible soft SUSY breaking terms. In the simplest case of the Minimal Supersymmetric Standard Model (MSSM) there are 105 new parameters. It also means that SUSY alone cannot be our ultimate theory of everything. From a complete theory of fundamental interactions we should require explanations of the observed values of parameters as well as unified description of gravity and particle physics.

Currently only string/M theory is known to provide a consistent, UV complete framework that unifies particle physics and gravity. In String/M theory one and more dimensional objects, the strings and D-branes, are fundamental, unlike in the case of QFT, where zero dimensional particles are<sup>1</sup>. In principle there is only one input parameter in the theory, the string tension  $T$ , which sets-up a characteristic energy scale of strings  $\sim m_{pl}$  and this is when the extended nature of strings should be visible. At lower (our) energies, however, different vibrational modes of strings appear as different (zero dimensional) particles.

There are only five possible formulations of string theories, so called corners: Type I, Type IIA, Type IIB, Heterotic  $SO(32)$  and Heterotic  $E_8$  all of which require 10D supersymmetric spacetime. Different corners, thanks to various dualities, are believed to be related to each other and unified into 11D M-theory. If String/M Theory is to be considered as the theory that describes our world, at low energies it should look like a four dimensional one, or in other words, the extra 6/7 dimensions have to be compactified. The compactification, because it can be done in many ways, introduces a lot of ambiguity. In order to avoid the hierarchy problem one usually requires the resulting theory to be supersymmetric, which restricts the class

---

<sup>1</sup>See for example [4] for a pedagogical introduction to string/M theory.

of allowed manifolds of extra, compactified dimensions to either Calabi-Yau 6-dimensional manifolds [5], or 7-dimensional manifolds with holonomy of  $G_2$  [6].

From the process of compactification, at the resulting four dimensional effective theory one is left with plethora of scalar fields, so called moduli. These are “leftovers” of the higher dimensional parameterisation of the compactified manifold. Since we have not observed any fundamental scalar fields, except for the SM-like Higgs, those moduli have to be made massive. On top of that, all parameters (masses, coupling constants) of the low energy theory depend on moduli, and thus, values of moduli fields have to be fixed. One can calculate and try to minimise the potential of moduli directly from string/M theory. Unfortunately, though, because details of compactifications are not well studied, one, naively, ends up with a large number of possible modulus (vacuum) configurations. This is what is known as the string landscape. Estimates are that there are about  $10^{\mathcal{O}(100)}$  (maybe  $\infty$ ?) possible configurations [7], and we know that our world is described only by one of those solution.

The fact that the natural scale of strings is way beyond our current (and probably even future) reach together with the enormous number of solution of string/M theory at lower energies made a lot of people believe that string/M theory is not testable. This is, however, not necessary true. The point here is that we actually know how our world works at low energies. Gravity is described by General Relativity (GR) and other forces and matter content by the Standard Model with the gauge group  $SU(3)_C \times SU(2)_L \times U(1)_Y$ . One can try to classify string vacua, and check whether the class of vacua that could describe our world has any interesting properties<sup>2</sup>. Could we impose some very general, simple but robust assumptions on string/M theory solutions and get meaningful predictions for particle physics and cosmology?

Results over the past decade or so have shown that this is indeed possible and string/M theory can in fact be a very useful guide to constructing models [10–14]. Namely, it leads to effective models with distinctive features and very few parameters. In this thesis we will study some examples of such string/M theory inspired models, in particular focusing on supersymmetric Grand Unified Theory (GUT) models arising from M theory compactified on  $G_2$ . A significant portion of the thesis, based on published work [15, 16], will be centred around construction and analysis of  $SO(10)$  SUSY GUT models in which I made a significant contribution. Those models have nice properties of unifying all fermions from a SM family into a single GUT representation,  $\mathbf{16}$  of  $SO(10)$ , as well as containing right-handed neutrino fields that provide left-handed neutrino with masses necessary to describe observed neutrino oscillations. In the other section of the thesis, based on publication [17] in which I made a significant contribution, we will focus on collider phenomenology that can arise from  $G_2$  compactification of M theory. As the particle physics community reviews possibilities of a future hadron collider, we believe that models arising from the UV completion by string/M

---

<sup>2</sup>Details of this approach is explained for example in [7, 8]. In [9] it is actually conjectured that this class of vacua is finite.

theory might help set out priorities and expectations for such a machine.

In the rest of this introduction we will review some of the concepts that will be used in the rest of the thesis. In particular we introduce basic concepts and notation of supersymmetry and supergravity used. We will also briefly discuss the generic results that arise from M theory compactified on  $G_2$  holonomy manifolds. Finally we will conclude with the outline for the rest of the thesis.

## 1.1 SUSY

In this section we will introduce basic ideas and notation of supersymmetry. The interested reader can consult [18] for more information.

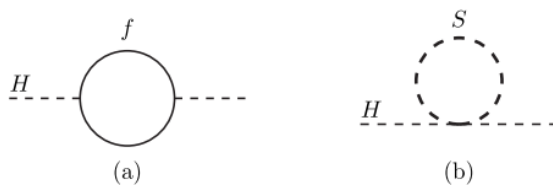


Figure 1.1: One loop quantum corrections to the Higgs squared mass parameter  $m_H^2$  coming from interactions with (a) a Dirac fermion  $f$ , (b) a scalar  $S$ .

The SM hierarchy problem is that the scalar Higgs boson receives big quantum corrections from virtual effects of every particle that couples to it, either directly or indirectly. For example, if there is a new fermion  $f$  at the scale  $\Lambda_{UV}$  that couples to the Higgs via  $-\lambda_f H \bar{f} f$  term, the correction to the Higgs mass square coming from the fermion loop shown in Fig. 1.1 (a) is

$$\Delta m_H^2 = -\frac{|\lambda_f|^2}{8\pi^2} \Lambda_{UV}^2 + \dots \quad (1.1)$$

If one expects  $\Lambda_{UV}$  to be of order of  $m_{pl}$  this gives a massive correction. Similarly, if instead of a new fermion one considers a new scalar  $S$  that couples to the Higgs via  $-\lambda_S H^2 S^2$  term, from the loop diagrams in Fig. 1.1 (b) one gets the correction to the Higgs mass:

$$\Delta_S m_H^2 = \frac{\lambda_S}{16\pi^2} [\Lambda_{UV}^2 - 2m_S^2 \ln(\Lambda_{UV}/m_S) + \dots] \quad (1.2)$$

Therefore, no matter what the nature of new states is, without miraculous cancellations, it is difficult to imagine the Higgs mass not to be pushed up to the scale of the new physics.

Supersymmetry provides a very attractive solution to this problem. Since corrections to the Higgs mass in Equations (1.1) and (1.2) have opposite signs SUSY relates fermions with bosons giving a symmetry reason for the cancellation to occur.

Supersymmetry is a global space-time symmetry that relates fermions to bosons:

$$\begin{aligned} Q|\text{fermion}\rangle &\sim |\text{boson}\rangle, \\ Q|\text{boson}\rangle &\sim |\text{fermion}\rangle. \end{aligned}$$

In its simplest realisation, so called  $\mathcal{N} = 1$  supersymmetry, the transformation is generated by two anticommuting spinors  $Q$  and its hermitian conjugate  $Q^\dagger$  which satisfy following relations:

$$\{Q_\alpha, Q_{\dot{\beta}}^\dagger\} = -2(\sigma^\mu)_{\alpha\dot{\alpha}}P_\mu, \quad (1.3)$$

$$\{Q_\alpha, Q_\beta\} = \{Q_{\dot{\alpha}}^\dagger, Q_{\dot{\beta}}^\dagger\} = 0, \quad (1.4)$$

$$[P^\mu, Q_\alpha] = [P^\mu, Q_{\dot{\alpha}}^\dagger] = 0, \quad (1.5)$$

$$[Q_\alpha, M^{\mu\nu}] = (\sigma^{\mu\nu})_\alpha{}^\beta Q_\beta, \quad (1.6)$$

where  $P_\mu$  and  $M_{\mu\nu}$  are Poincare operators,  $\sigma^\mu = \{\mathbf{1}, \sigma^i\}$  is the four vector of Pauli matrices, and  $\sigma^{\mu\nu}$  is an antisymmetrized product of  $\sigma^\mu$  matrices:

$$(\sigma^{\mu\nu})_\alpha{}^\beta = \frac{i}{4} (\sigma^\mu \bar{\sigma}^\nu - \sigma^\nu \bar{\sigma}^\mu), \quad (1.7)$$

with  $\bar{\sigma}^\mu$  defined as  $\bar{\sigma}^\mu = \{\mathbf{1}, -\sigma^i\}$ . Irreducible representations of the supersymmetry algebra are called supermultiplets. Each supermultiplet contains both fermions and bosons which are called superpartners of each other. In the superfield formalism, different field components are unified into a single object, superfield, using the notion of superspace where the Minkowski coordinates are combined with the anticommuting spinorial coordinates  $\theta^\alpha, \theta_{\dot{\alpha}}^\dagger$ . A single superfield contains equal number of fermionic and bosonic degrees of freedom.

Since the generator of spacetime translations,  $P_\mu$ , commutes with generators of supersymmetry, if SUSY is not broken, particles in a single multiplet have to have the same mass. Moreover, supersymmetry generators  $Q$  and  $Q^\dagger$  commutes also with the generators of gauge transformations. Therefore supermultiplets coincide with irreducible representations of gauge groups thus superpartners have the same electric charge, weak isospin, and color degrees of freedom.

There are two possibilities for global  $\mathcal{N} = 1$  SUSY irreducible representations:

- The chiral multiplet  $\Phi$

It contains a complex scalar  $\phi$ , a two-component Weyl fermion  $\psi$  and an auxiliary field  $F$ . In the superspace notation it reads:

$$\Phi(x^\mu, \theta, \theta^\dagger) = \phi(y) + \sqrt{2}\theta\psi(y) + \theta\theta F(y), \quad (1.8)$$

where  $y^\mu \equiv x^\mu + i\theta^\dagger\bar{\sigma}^\mu\theta$ .

The Lagrangian for a free chiral multiplet can be written as:

$$\mathcal{L}_{\text{free}}^{\Phi} = [\Phi^* \Phi]_D = -\partial^\mu \phi^* \partial_\mu \phi + i\psi^\dagger \bar{\sigma}^\mu \partial_\mu \psi + F^* F, \quad (1.9)$$

where we have introduced the notation:

$$[\mathbb{G}]_D = \int d^2\theta d^2\theta^\dagger \mathbb{G}. \quad (1.10)$$

- The vector/gauge multiplet  $V$

It consists of gauge bosons  $A_\mu^a$ , two-component Weyl spinors  $\lambda^a$  and auxiliary fields  $D^a$ . The index  $a$  here runs over the adjoint representation of the gauge group (e.g.  $a = 1, \dots, 8$  for  $SU(3)_C$ ). In general there are additional auxiliary fields contained in the gauge multiplet, but they can be supergauged away in so called Wess-Zumino gauge. In this gauge the vector supermultiplet takes the following form:

$$V_{WZ}(x^\mu, \theta, \theta^\dagger) = \theta^\dagger \bar{\sigma}^\mu \theta A_\mu(x) + \theta^\dagger \theta^\dagger \theta \lambda(x) + \theta \theta \theta^\dagger \lambda^\dagger(x) + \frac{1}{2} \theta \theta \theta^\dagger \theta^\dagger D(x). \quad (1.11)$$

The Lagrangian for a free gauge supermultiplet  $V$  can be constructed as:

$$\mathcal{L}_{\text{free}}^V = \frac{1}{4} [\mathcal{W}^\alpha \mathcal{W}_\alpha]_F + c.c., \quad (1.12)$$

where  $\mathcal{W}^\alpha$  is a field strength corresponding to the vector field:

$$\mathcal{W}^\alpha = \bar{D}_{\dot{\beta}} \bar{D}^{\dot{\beta}} (e^{-V} D^\alpha e^V), \quad (1.13)$$

with  $D$ 's denoting the supersymmetric covariant derivatives, defined as:

$$D_\alpha = \frac{\partial}{\partial \theta^\alpha} - i(\sigma^\mu \theta^\dagger)_\alpha \partial_\mu, \quad D^\alpha = -\frac{\partial}{\partial \theta_\alpha} + i(\theta^\dagger \bar{\sigma}^\mu)^\alpha \partial_\mu, \quad (1.14)$$

and

$$\bar{D}^{\dot{\alpha}} = \frac{\partial}{\partial \theta_{\dot{\alpha}}^\dagger} - i(\bar{\sigma}^\mu \theta)_{\dot{\alpha}} \partial_\mu, \quad \bar{D}_{\dot{\alpha}} = -\frac{\partial}{\partial \theta^{\dagger \dot{\alpha}}} + i(\theta \sigma^\mu)_{\dot{\alpha}} \partial_\mu. \quad (1.15)$$

The subscript F in Eq. (1.12) implies integration over the superspace index:

$$[\mathbb{G}]_F = \int d^2\theta \mathbb{G}|_{\theta^\dagger=0}. \quad (1.16)$$

In Wess-Zumino gauge, Lagrange density Eq. (1.12) corresponds to:

$$\mathcal{L}_{\text{WZ, free}}^V = D^a D_a + 2i\lambda^a \sigma^\mu \nabla_\mu \lambda^{\dagger a} - \frac{1}{2} F^{a\mu\nu} F_{\mu\nu}^a. \quad (1.17)$$

The most general renormalisable, supersymmetric Lagrangian with a chiral multiplet  $\Phi$

charged under a gauge group with vector fields  $V^a$ , can be written as:

$$\mathcal{L}_{ren} = \left[ \Phi^{*i} (e^{2g_a T^a V^a})^j \Phi_j \right]_D + ([W(\Phi_i)]_F + c.c.) + \left( \frac{1}{4} - i \frac{g_a \vartheta_a}{32\pi^2} \right) (\text{Tr}[W^{a\alpha} \mathcal{W}_\alpha^a]_F + c.c.) - 2\kappa[V]_D, \quad (1.18)$$

where  $W(\Phi_i)$ , the so called superpotential, is an arbitrary holomorphic function of mass dimension 3 and  $\kappa$  is a constant of mass dimension 2.  $\vartheta$  is a CP-violating parameter, that if not made small can lead to the strong CP problem in the Standard Model. The last term in Eq. (1.18), the Fayet-Iliopoulos term, can be present only in the case the gauge symmetry is that of  $U(1)$ . Notice that, neglecting the Fayet-Iliopoulos term, the Lagrangian is completely specified by the superpotential  $W$ .

In the case of  $M$  different chiral superfields the most general superpotential  $W$  can be written as:

$$W(\Phi_i) = \sum_{n=1}^{\infty} \prod_{0 \leq i_1, \dots, i_n \leq M} c_{i_1 \dots i_n} \Phi_{i_1} \dots \Phi_{i_n},$$

where coefficients  $c$  non-zero only if the corresponding combination of superfields is gauge invariant. Since chiral superfields have mass dimension 1, only terms with at most three superfields are renormalisable.

After the superspace integration and integrating out auxiliary fields, the Lagrangian 1.18 reads:

$$\begin{aligned} \mathcal{L} = & \text{Tr} \left[ -\frac{1}{4} F_{\mu\nu}^a F^{a\mu\nu} - i\lambda^a \sigma^\mu \nabla_\mu \lambda^{\dagger a} \right] + \frac{\vartheta_a g_a^2}{32\pi^2} \text{Tr} \left[ F_{\mu\nu}^a \tilde{F}^{a\mu\nu} \right] + \\ & + \nabla_\mu \phi^{*i} \nabla^\mu \phi_i - i\psi^{\dagger i} \bar{\sigma}^\mu \nabla_\mu \psi_i + i\sqrt{2} g_a q_i \left( \phi^{*i} \psi_i \lambda^a - \lambda^{\dagger a} \psi^{\dagger i} \phi_i \right) + \\ & - \frac{1}{2} \left( \frac{\delta^2 W}{\delta \phi_i \delta \phi_j} \psi_i \psi_j - \frac{\delta^2 W^*}{\delta \phi_i^* \delta \phi_j^*} \psi_i^\dagger \psi_j^\dagger \right) + V(\phi, \phi^*), \end{aligned}$$

where the scalar potential  $V(\phi, \phi^*)$  is

$$V(\phi, \phi^*) = \left( \frac{\delta W^*}{\delta \phi^{*i}} \right) \left( \frac{\delta W}{\delta \phi_i} \right) + \frac{1}{2} \left( \kappa - g \sum_a |\phi^{*i} (T^a)_j^i \phi^j|^2 \right)^2, \quad (1.19)$$

with  $T^a$  being gauge symmetry generators and  $\tilde{F}_{\mu\nu}^a = \frac{1}{2} \epsilon_{\mu\nu\rho\sigma} F^{a\rho\sigma}$ .

## 1.2 Supergravity

When supersymmetry is promoted to be a local symmetry, a new supermultiplet, containing spin-2 graviton and its spin-3/2 superpartner – gravitino, is allowed. Therefore, the resulting

theory, called supergravity (SUGRA)<sup>3</sup>, is able to account for gravity. Supergravity action is non-renormalisable and thus it is only an effective theory with a cut-off at the Planck scale. It is, however, interesting to be studied as often string/M theory is effectively described by SUGRA at low-energies.

The most general supergravity lagrangian, which we will not write here, depends only on three functions of superfields that should be specified by an UV complete theory:

- The superpotential  $W(\Phi_i)$  which is, as in the global SUSY case, an arbitrary holomorphic function of superfields that is invariant under the gauge symmetries of the theory and has mass dimension 3. This function encodes non-gauge interactions between chiral multiplets, e.g. Yukawa interactions and Higgs  $\mu$  terms.
- The Kähler potential  $K(\Phi_i, \tilde{\Phi}^{j*})$  that is a real, dimension  $[\text{mass}]^2$ , supergauge invariant function of chiral, antichiral and vector superfields. The Kähler potential gives rise to chiral kinetic terms and gauge interactions.
- The gauge kinetic function  $f_{ab}(\Phi_i)$ . It is a dimensionless holomorphic function of chiral superfields. It captures possibilities of kinetic mixing between Abelian components of the gauge groups as well as gives rise to nonrenormalisable couplings of the gauge supermultiplets to the chiral supermultiplets.

In addition to the superpotential  $W$ , Kähler potential  $K$ , and gauge kinetic function  $f_{ab}$ , for each  $U(1)$  gauge supermultiplet  $V^{(1)}$  one can specify real scalar constants  $\xi$  that appears in Fayet-Iliopoulos terms  $\mathcal{L} \supset [\xi V^{(1)}]_D$ .

We will be interested in the supergravity scalar potential, the generalisation of the global SUSY potential, Eq. (1.19), that reads,

$$V(\phi, \phi^*) = m_{pl}^4 e^G \left[ G^i (G^{-1})^j_i G_j - 3 \right] + \frac{1}{4} (f_{ab} \hat{D}^a \hat{D}^b + c.c.), \quad (1.20)$$

where  $G$  is defined as

$$G = \frac{K}{m_{pl}^2} + \ln \left( \frac{W(\phi)}{m_{pl}^3} \right) + \ln \left( \frac{W^*(\phi^*)}{m_{pl}^3} \right), \quad (1.21)$$

and it is called Kähler function. From  $G$  one can construct its derivatives,  $G^i = \delta G / \delta \phi_i$ ,  $G_j = \delta G / \delta \phi^{*j}$ , and  $G_i^j = \delta^2 G / \delta \phi^{*i} \delta \phi_j = \delta^2 K / \delta \phi^{*i} \delta \phi_j$ . The inverse of  $G_i^j$  is denoted by  $(G^{-1})^j_i$ . Finally,  $\hat{D}^a$  is defined as

$$\hat{D}^a = -G^i (T^a)_i^j \phi_j. \quad (1.22)$$

---

<sup>3</sup>See for example [19] and [20] for introduction to supergravity

Name	spin 0	spin 1/2	$SU(3)_C, SU(2)_L, U(1)_Y$	B	L
$Q$	$(\tilde{u}_L \tilde{d}_L)$	$(u_L d_L)$	$(\mathbf{3}, \mathbf{2}, \frac{1}{6})$	$+\frac{1}{3}$	0
$u^c$	$\tilde{u}_R^*$	$u_R^\dagger$	$(\bar{\mathbf{3}}, \mathbf{1}, -\frac{2}{3})$	$-\frac{1}{3}$	0
$d^c$	$\tilde{d}_R^*$	$d_R^\dagger$	$(\bar{\mathbf{3}}, \mathbf{1}, \frac{1}{3})$	$-\frac{1}{3}$	0
$L$	$(\tilde{\nu} \tilde{e}_L)$	$(\nu e_L)$	$(\mathbf{1}, \mathbf{2}, -\frac{1}{2})$	0	+1
$e^c$	$\tilde{e}_R^*$	$e_R^\dagger$	$(\mathbf{1}, \mathbf{1}, 1)$	0	-1
$H_u$	$(H_u^+ H_u^0)$	$(\tilde{H}_u^+ \tilde{H}_u^0)$	$(\mathbf{1}, \mathbf{2}, +\frac{1}{2})$	0	0
$H_d$	$(H_d^0 H_d^-)$	$(\tilde{H}_d^0 \tilde{H}_d^-)$	$(\mathbf{1}, \mathbf{2}, -\frac{1}{2})$	0	0

Table 1.1: Chiral supermultiplets in the MSSM. The column labelled with B (L) shows the barion (lepton) number assignment for the corresponding supermultiplet.

Field	spin 1/2	spin 1	$SU(3)_C, SU(2)_L, U(1)_Y$
gluino, gluon	$\tilde{g}$	g	$(\mathbf{8}, \mathbf{1}, 0)$
winos, W boson	$\tilde{W}^\pm \tilde{W}^0$	$W^\pm W^0$	$(\mathbf{1}, \mathbf{3}, 0)$
bingo, B boson	$\tilde{B}^0$	$B^0$	$(\mathbf{1}, \mathbf{1}, 0)$

Table 1.2: Gauge supermultiplets in the MSSM.

### 1.3 MSSM

The Minimal Supersymmetric Standard Model (MSSM) is a minimal, consistent supersymmetric extension of the SM. It expands the field content of the SM by including spin 0 superpartners, sleptons or squarks, for fermions and spin 1/2 superpartners, gauginos, for gauge bosons, see Tables 1.1 and 1.2.

In order to avoid  $SU(2)_L - SU(2)_L - U(1)_Y$  and  $U(1)_Y - U(1)_Y - U(1)_Y$  gauge anomalies, i.e. requiring that  $Tr[T_3^2 Y] = Tr[Y^3] = 0$ , as well as to provide Yukawa couplings to all fermions, the Higgs sector of the SM in the MSSM has to be expanded to include two chiral supermultiplets  $H_u$  and  $H_d$  with the opposite sign hypercharges.

The superpotential for the MSSM reads then:

$$W_{MSSM} = u^c \mathbf{y}_u Q H_u - d^c \mathbf{y}_d Q H_d - e^c \mathbf{y}_e L H_d + \mu H_u H_d \quad (1.23)$$

where the dimensionless Yukawa couplings  $\mathbf{y}_u$ ,  $\mathbf{y}_d$  and  $\mathbf{y}_e$  are  $3 \times 3$  matrices in family space, while  $\mu$  is mass dimension 1 parameter and its the supersymmetric version of the Higgs boson mass in SM.

There are potentially other terms that can be included in the MSSM superpotential, lepton



and baryon number violating operators:

$$W_{\Delta L=1} = \frac{1}{2}\lambda^{ijk}L_iL_je_k^c + \lambda'^{ijk}L_iQ_jd_k^c + \mu'^iL_iH_u, \quad (1.24)$$

$$W_{\Delta B=1} = \frac{1}{2}\lambda''^{ijk}u_i^c d_j^c d_k^c, \quad (1.25)$$

where  $i, j, k$  are generation indices. Those terms are dangerous as, if present simultaneously, they can induce proton decay  $p^+ \rightarrow e^+\pi^0$  with the rate orders of magnitude above current limits. For example, the decay rate in the case of the down-type squark mediator, with analogous contributions for other sparticle mediators, can be estimated to be:

$$\Gamma_{p \rightarrow e^+\pi^0} \sim \frac{m_p^5}{m_{d_i}^4} |\lambda'^{11i}\lambda''^{11i}|^2. \quad (1.26)$$

For order one  $\lambda$ s and TeV scale squarks this gives the lifetime of proton below 1 second.

In order to suppress such terms, a symmetry is required, so called R-parity. For each particle in the MSSM we assign a multiplicative, conserve quantum number

$$P_R = (-1)^{3(B-L)+2s}, \quad (1.27)$$

where  $s$  is the spin of the particle. The R-parity even particles corresponds to the SM fields and MSSM Higgses, while all sparticles are R-parity odd. If the R-parity is exactly conserved, there is no mixing between sparticles and particles. This leads to the lightest supersymmetric particle (LSP) being stable which also makes it a candidate for a dark matter particle.

Finally, in order for the MSSM to be viable model of nature, the supersymmetry needs to be broken. If SUSY was not broken and sparticles were mass degenerate with their corresponding particle counterparts we should have already seen light scalar sparticles in experiments. In order not to loose the original motivation behind SUSY, its ability to cancel quadratic corrections to the Higgs mass, it cannot be broken arbitrary. It should be broken spontaneously, meaning that the underlying theory is invariant under supersymmetry, but the vacuum state is not. Throughout this thesis we will assume that the underlying theory is that of M-Theory compactified on a  $G_2$  holonomy manifold, which leads to a four dimensional  $N = 1$  supersymmetry [6]. It was shown in [10, 21, 22] how, in this setup, the supersymmetry can be broken spontaneously in a hidden sector and gravity mediated to the visible one. In low-energy limit ( $\ll m_{pl}$ ) we will be interested in here, we can parameterise the supersymmetry breaking contributions by introducing extra terms, called soft terms, to the, otherwise supersymmetric, visible sector lagrangian that explicitly break the supersymmetry. Those terms cannot be arbitrary either, being at most mass-dimension three, so they do not reintroduce the quadratic divergences to scalar masses<sup>4</sup>.

---

<sup>4</sup>See [23] and reference therein for details and proofs

The most general soft supersymmetry-breaking Lagrangian reads:

$$\mathcal{L}_{soft} = - \left( \frac{1}{2} M_a \lambda^a \lambda^a + \frac{1}{6} a^{ijk} \phi_i \phi_j \phi_k + \frac{1}{2} b^{ij} \phi_i \phi_j + t^i \phi_i \right) + c.c. - (m^2)_j^i \phi^{j*} \phi_i, \quad (1.28)$$

and consists of gaugino masses  $M_a$ , scalar squared-mass terms  $(m^2)_j^i$  and  $b^{ij}$ , trilinear scalar couplings  $a^{ijk}$ , and tadpole couplings  $t^i$ . The terms in Eq. (1.28) clearly break SUSY as they involve only scalars and gauginos and not their respective superpartners.

## 1.4 M theory on $G_2$ manifold

In this section we would like to review the general phenomenological results coming from M theory compactified on a  $G_2$  holonomy manifold and compare them with results from other corners of string/M theory. More details could be found in [12, 24].

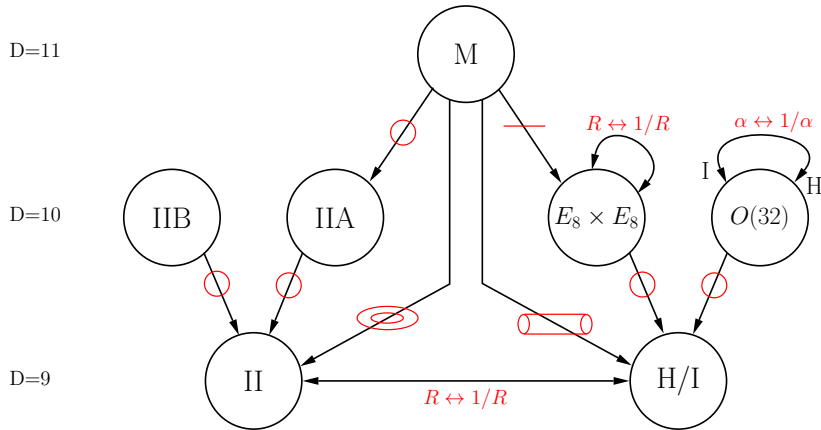


Figure 1.2: Dualities between various string/M theories. In particular, M theory with one spatial dimension compactified to a circle is equivalent to the type IIA string theory, while with one dimension reduced to a line to the heterotic  $E_8 \times E_8$ . Similarly, a 9-dimensional theory arises from M theory compactified on a two-dimensional tori  $T^2$  can also be constructed from either the type IIA or IIB compactified on circle. M teory on a cylinder results in a nine-dimensional theory that can be constructed from the Type I or heterotic string theories. Figure reproduced from [25]. Originally from [26] where one can find extensive discussion on string dualities.

M theory is a 11 dimensional theory that unifies all consistent verison of superstring theory. Although there is currently no complete formulation of M theory, various limits have been extensively studied using so called string dualities, see Fig. 1.2. M theory can also be studied in the low-energy limit where it can be approximated by eleven-dimensional supergravity. Most of the results that we are going to discuss here assumes the validity of the SUGRA limit.

In order to make contact with the everyday-life four-dimensional world, seven extra dimen-

sions of 11D M theory have to be compactified. The simplest option would be to compactify extra dimensions on a seven-torus, but this would leave all high-dimensional SUSY generators resulting in a phenomenologically uninteresting  $\mathcal{N} = 8$  SUSY in four dimensions. Much more attractive scenarios emerge when compactification is on a  $G_2$  holonomy manifold.  $G_2$  manifolds are seven dimensional manifolds with holonomy group equal to the exceptional Lie group  $G_2$ . A holonomy group describes how vectors and spinors transform under parallel transportation around closed curves. The size of the holonomy group constrains the number of covariantly constant spinors, SUSY generators, that survive the compactification. In the case of M theory compactified on  $G_2$  this results in a  $\mathcal{N} = 1$  supersymmetric theory in the uncompactified four dimensional spacetime [6].  $G_2$  corresponds here to six-dimensional Calabi-Yau manifolds (of holonomy  $SU(3)$ ) used in 10D heterotic string theories that also result in effective 4D  $\mathcal{N} = 1$  SUSY [5].

When M theory is compactified on a smooth  $G_2$  manifold, the resulting theory does not contain low-energy non-abelian gauge fields, that are present in the Standard Model. However, a realistic 4D theory can arise if the  $G_2$  manifolds contains special kinds of singularities [27]. In particular, non-abelian ADE, i.e.  $SU(n)$ ,  $SO(2n)$ ,  $E_6$ ,  $E_7$  or  $E_8$ , gauge fields can be realised along three-dimensional submanifolds of  $G_2$  where there are orbifold singularities [28, 29]. Chiral matter, charged under a non-abelian gauge symmetry, is localised at points where the corresponding orbifold singularity is enhanced [30, 31]. From the phenomenological point of view it is interesting to realise that two three-dimensional manifolds of orbifold singularities embedded in a seven-dimensional manifold do not generically intersect with each other. This means that, first of all, chiral matter is generically not charged under two gauge symmetries arising from different orbifolds. This implies that the supersymmetry breaking in a hidden sector is likely to be gravity, not gauge, mediated to the visible sector. Secondly, if gauge coupling unification is to be motivated theoretically, and not accidental, the gauge groups of the Standard Model have to come from a simple gauge group arising from a single orbifold singularity.

Although no explicit realisation of compact  $G_2$  manifolds with all singularities required for phenomenology is currently known, such manifolds are expected to exist based on dualities with the heterotic and type IIA string theories [27]. Here we will assume that appropriate compact  $G_2$  manifolds do indeed exist and enough is known about the physics that arises from them.

### 1.4.1 Moduli stabilisation

When string/M theories are compactified on a manifold, the shape and size of the manifold is parameterised by vacuum expectation values (VEVs) of scalar fields, the moduli. Since the low-energy physics, i.e. particle masses and couplings, is characterised by the compactified manifold, moduli VEVs need to be fixed, or, in the jargon, stabilised. One possible stabil-

isation mechanism, successfully used in the context of the type IIB theory, is to use fluxes of warped geometries [32]. In the context of M theory on  $G_2$  fluxes were shown to stabilise moduli [33], however they also lead to a phenomenologically uninteresting Planck-scale SUSY breaking in the visible sector. On the other hand, the compactification on a  $G_2$  manifold without fluxes, where moduli are stabilised with a non-perturbative superpotential generated by strong dynamics in a hidden sector results in the supersymmetry being broken at a hierarchically small scale [21]. In this thesis we will thus focus on fluxless  $G_2$  compactification scenarios.

As explained in [10, 21, 22], a minimal viable model that stabilises moduli fields in M theory on  $G_2$  involves a hidden sector with two non-abelian asymptotically free gauge groups,  $SU(Q) \times SU(P+1)$ , and a pair of vector-like quark fields  $\Phi_{hid}, \tilde{\Phi}_{hid}$  charged under  $SU(P+1)$ . At low energies strong gauge dynamics generates a non-perturbative superpotential:

$$W = m_{pl}^3 \left( A_1 P \phi^{2/P} e^{ib_1 f_1} + A_2 Q e^{ib_2 f_2} \right), \quad b_1 = \frac{2\pi}{P}, \quad b_2 = \frac{2\pi}{Q}, \quad (1.29)$$

where the matter field  $\phi$  represents the degrees of freedom of an effective meson field, coming from condensation of  $\Phi_{hid}$  and  $\tilde{\Phi}_{hid}$  quarks when the interaction becomes strong.  $A_1$  and  $A_2$  are numerical constants that are calculable for a given  $G_2$  manifold, while  $f_1$  and  $f_2$  are gauge kinetic functions of the two hidden sectors. In general, the gauge kinetic functions  $f_1$  and  $f_2$  are different from each other, but analysis greatly simplifies when the two three-cycles on which the hidden sector gauge fields are localised are in the same homology class. This then implies that

$$f_1 = f_2 \equiv f_{hid} = \sum_{i=1}^N N_i (t_i + i s_i), \quad (1.30)$$

what we will assume. In the above equation,  $s_i$  are the  $N$  geometric moduli of the  $G_2$  manifold, while  $t_i$  are axions coming from the 3-form field of the eleven-dimensional supergravity. The  $N_i$  are constants fixed by a particular choice of the  $G_2$  manifold.

In order to calculate the supergravity potential, Eq. (1.20), we need to specify the Kähler potential. Based on results from [34] we will assume that it reads:

$$K/m_{pl}^2 = -3 \ln \left( 4\pi^{1/3} V_7 \right) + \tilde{K}_{hid}(s_i) \bar{\phi} \phi, \quad (1.31)$$

where  $V_7$  is the volume of the  $G_2$  manifold in units of the eleven-dimensional Planck length and a homogeneous function of moduli of degree  $7/3$ , i.e.

$$V_7 = \prod_i (s^i)^{a_i}, \quad \text{where } \sum_i a_i = 7/3. \quad (1.32)$$

$\tilde{K}_{hid}(s_i)$  is a homogeneous function of the moduli of degree zero which will generally be of order one and vary adiabatically.

Having specified all necessary ingredients one can now calculate and try to minimise the scalar potential for moduli. It was shown in [22] that in such, fairly general, setup, all moduli can be indeed stabilise with VEVs of order

$$\langle s_i \rangle \simeq 0.1 m_{pl}. \quad (1.33)$$

The requirement that the vacua that support this have a small cosmological constant lead to large  $F$ -term VEVs for the hidden sector meson fields,  $F_\phi$ . This imply breaking of supersymmetry and a non-zero gravitino mass

$$m_{3/2} = \frac{\langle F_\phi \rangle}{\sqrt{3} m_{pl}} = e^{K/2 m_{pl}} \frac{|W|}{m_{pl}^2}, \quad (1.34)$$

that the scale for scalar masses in supergravity. Interestingly, in this setup,  $\langle F_\phi \rangle$  is much bigger than VEVs of modulus  $F$ -terms,  $F_s$ , i.e.  $\langle F_\phi \rangle \gg \langle F_s \rangle$ . This hierarchy between  $\langle F_s \rangle$  and  $\langle F_\phi \rangle$  is responsible for the particular pattern of the soft supersymmetry breaking terms in the models coming from M theory compactification on  $G_2$ , as we will see in section 1.4.2, below.

Following general supergravity results, after the supersymmetry is broken  $m_{3/2}$  set the scale for scalar fields. In particular, moduli get masses, with the lightest modulus mass estimated to be [35]:

$$m_{s;min}^2 = \mathcal{O}(1) m_{3/2}^2. \quad (1.35)$$

The lightest moduli and its mass is of profound importance for cosmology, as it can potentially dominate the early Universe, leading to a non-thermal cosmological history. In order for the successful Big-Bang Nucleosynthesis (BBN) predictions not to be ruined, the mass of the lightest modulus has to be bigger than about 30 TeV.

The moduli stabilisation mechanism stabilises all moduli but gives a mass of  $\mathcal{O}(m_{3/2})$  to only one combination of axions. The masses of the other axions are generated by higher order instanton effects which make them exponentially suppressed relative to  $m_{3/2}$  [36]. One of these light axions could naturally serve as the QCD axion, thus solving the strong CP-problem.

The requirement for the lightest modulus not to spoil the success of BBN predictions gave us, since  $m_{s;min}^2 \sim m_{3/2}^2$ , the lower limit on  $m_{3/2}$ . The axion relic abundance, proportional to a positive power of  $m_{3/2}$ , gives rise to an  $\mathcal{O}(1)$  fraction of dark matter only when  $m_{3/2} \lesssim 100$  TeV [36]. Therefore the phenomenological input constrains the gravitino mass to be:

$$30 \text{ TeV} \lesssim m_{3/2} \lesssim 100 \text{ TeV}. \quad (1.36)$$

This condition can be easily satisfied by the formula Eq. (1.34) in the moduli stabilisation discussed above. See [35] for detailed discussion.

Finally, it is interesting to realise that comparing to other string theory compactifications,

the moduli stabilisation in M theory is the most straight forward one. In M theory there is only one type of moduli (all arise as massless fluctuations of the metric of the extra dimensions) and only one stabilisation mechanism is required to stabilised them all. In other corners of string/M theory multiple types of moduli arise and multiple stabilisation mechanisms are usually required. For example, in the case of Type IIB compactifications three different types of moduli, complex structure, dilaton and Kähler are present. Non-zero fluxes can stabilise complex structure and dilaton moduli, but generically not all Kähler moduli can be stabilised this way and other mechanisms have to be used in parallel. In case of heterotic and Type IIA theories compelling scenarios for stabilisation of all moduli have to be found yet. For details see [24] and reference therein.

### 1.4.2 Observable sector

Having all moduli fields stabilised we can now turn our attention to the visible sector that includes the Standard Model. Because of the apparent gauge unification, especially in the supersymmetric version of SM, it is reasonable to assume that all SM gauge fields arise from a single orbifold singularity. This setting provides a GUT theory at the compactification scale. In this work we will be mainly interested in  $SO(10)$  GUTs, but we will also review previous results on  $SU(5)$  GUTs.

In order to avoid potentially large gauge interaction between the visible and hidden sector matter, the visible sector should also reside on a 3-manifold (corresponding to an orbifold singularity) that is different from the one supporting the hidden sector. Since two 3-manifold embedded inside a 7-manifold do not generically intersect with each other, this implies that there should be no gauge connection between the visible and hidden sectors.

The full  $\mathcal{N} = 1$  supergravity at the compactification scale which includes both sectors is defined by the following Kähler, superpotential and gauge kinetic functions [11]:

$$K/m_{pl}^2 = \left(-3 \ln(4\pi^{1/3} V_7) + \bar{\phi}\phi\right) + \tilde{K}_{\bar{\alpha}\beta}(s_i)\bar{\Phi}^{\bar{\alpha}}\Phi^\beta + (Z(s_i)H_u H_d + h.c.) + \dots \quad (1.37)$$

$$W = m_{pl}^3 \left(A_1 P \phi^{-(2/P)} e^{ib_1 f_1} + A_2 Q e^{ib_2 f_2}\right) + Y'_{\alpha\beta\gamma} \Phi^\alpha \Phi^\beta \Phi^\gamma \quad (1.38)$$

$$f_1 = f_2 \equiv f_{hid} = \sum_i N^i z_i; \quad \text{Im}(f_{vis}^0) = \sum_i N_{vis}^i s_i \equiv V_{\hat{Q}_{vis}} \quad (1.39)$$

where  $\Phi$ 's are chiral matter fields of the visible sector, while  $K_{\bar{\alpha}\beta}$ ,  $Y'_{\alpha\beta\gamma}$  and  $f_{vis}^0$  are, respectively, their Kähler metric, un-normalised Yukawa couplings and tree-level gauge kinetic functions. The Yukawa couplings arise from membrane instantons which connect singularities, points inside gauge 3-manifolds, where chiral superfields are supported. They are given by:

$$Y'_{\alpha\beta\gamma} = C_{\alpha\beta\gamma} e^{2\pi i \sum_i l_i^{\alpha\beta\gamma} \langle t_i + i s_i \rangle} \quad (1.40)$$

where  $C \sim \mathcal{O}(1)$  and  $l$ -s are integers characterising the 3-cycle encapsulating the three singu-

larities supporting the chiral multiplets  $\Phi^\alpha, \Phi^\beta$  and  $\Phi^\gamma$ . Due to the exponential dependence on the moduli it is natural to obtain a hierarchical structure of Yukawa couplings.

With the visible and hidden sectors not being charged under the same gauge symmetries, the supersymmetry breaking is mediated to the visible sector via Planck suppressed interactions, i.e. gravity mediated. Based on general supergravity formulas [37] one can compute soft-parameters that need to be introduced into the visible sector Lagrangian. In particular, soft scalar masses can be written as:

$$m_{\bar{\alpha}\beta}^2 = \left(m_{3/2}^2 + V_0\right) \delta_{\bar{\alpha}\beta} - \langle \mathcal{U}^\dagger \Gamma_{\bar{\alpha}\beta} \mathcal{U} \rangle, \quad (1.41)$$

$$\Gamma_{\bar{\alpha}\beta} = e^{\hat{K}} F^{\bar{m}} (\partial_{\bar{m}} \partial_n \tilde{K}_{\bar{\alpha}\beta} - \partial_{\bar{m}} \tilde{K}_{\bar{\alpha}\gamma} \tilde{K}^{\gamma\bar{\delta}} \partial_n \tilde{K}_{\bar{\delta}\beta}) F^n, \quad (1.42)$$

where indices  $\alpha, \beta, \gamma$  run through visible fields, while  $n$  and  $m$  iterates over moduli fields.  $\hat{K}$  denotes the hidden sector part of the Kähler potential, Eq. (1.37), while  $V_0$  is the VEV of the scalar potential, Eq. (1.20), i.e. the tree-level cosmological constant. Since the observed value of the cosmological constant is small, we are interested only in vacua with this term set to (or close to) zero [22]. Matrix  $\mathcal{U}$  normalises the visible sector Kähler matrix, i.e.  $\mathcal{U}^\dagger \tilde{K} \mathcal{U} = 1$ .

Although non-diagonal contributions are difficult to compute in generic string/M theory vacua, since the modulus F-term VEVs are suppressed compared to that of the hidden-sector meson fields,  $\langle F_s \rangle \ll \langle F_\phi \rangle$ , they should be negligible compared to the diagonal contributions. This leads to

$$m_{\bar{\alpha}\beta} \approx m_{3/2} \delta_{\bar{\alpha}\beta}. \quad (1.43)$$

Suppression of moduli  $F_s$  simplifies computation of scalar trilinear soft-terms as well, leading to [10]

$$\tilde{A}_{\alpha\beta\gamma} \approx \left\langle (\mathcal{U}_{\alpha\alpha'} \mathcal{U}_{\beta\beta'} \mathcal{U}_{\gamma\gamma'}) e^{\hat{K}} F^\phi \hat{K}_\phi Y'_{\alpha'\beta'\gamma'} \right\rangle \quad (1.44)$$

$$\approx 1.48 m_{3/2} Y_{\alpha\beta\gamma}, \quad (1.45)$$

where matrix  $\mathcal{U}$  normalises the visible sector Kähler matrix, and  $Y_{\alpha\beta\gamma}$  is the normalised Yukawa coupling.

As we have seen, in  $G_2$  vacua the scalar masses and reduced scalar-trilinear couplings,  $A_{\alpha\beta\gamma} = \frac{\tilde{A}_{\alpha\beta\gamma}}{Y_{\alpha\beta\gamma}}$ , are of order of  $m_{3/2}$ . On the other hand, gauginos, with gravity mediated contribution to soft masses given by [22]:

$$M_{1/2}^{grav} = \left\langle \frac{e^{\hat{K}/2} F^{s_i} \partial_{s_i} f_{vis}}{2i \text{Im} f_{vis}} \right\rangle \approx -0.0307 \times m_{3/2}, \quad (1.46)$$

are suppressed compared to  $m_{3/2}$ . This is because Eq. (1.46) does not depend on the hidden sector meson  $F$ -terms,  $F_\phi$ , while the moduli  $F$ -terms are suppressed,  $\langle F_{s_i} \rangle \ll \langle F_\phi \rangle$ .

Since the tree-level gaugino masses are suppressed, other contributions, e.g. anomaly

mediation and threshold effects can be important. Those contributions were analysed in [22] leading to

$$M_1 \approx \left( -0.03156\eta + \alpha_{GUT}(-0.22497 + 0.52313(1-c)) \right) \times m_{3/2}, \quad (1.47)$$

$$M_2 \approx \left( -0.03156\eta + \alpha_{GUT}(-0.03409 + 0.55483(1-c)) \right) \times m_{3/2}, \quad (1.48)$$

$$M_3 \approx \left( -0.03156\eta + \alpha_{GUT}(-0.10226 + 0.47557(1-c)) \right) \times m_{3/2}, \quad (1.49)$$

where  $\eta$  comes from the threshold corrections coming from the Kaluza-Klein modes and can be computed analytically. The constant  $c$  controls the size of the higher order corrections ( $\propto \frac{\phi\bar{\phi}}{V_X}$ ) to the matter Kähler potential and depends on details of a specific model considered. As one can see, the contribution from anomaly mediation makes the gaugino masses non-universal. Typically, one should expect, after RG running to the electroweak scale, to have  $M_1$  and  $M_2$  of order of few hundred GeV and gluinos that are heavier than that.

Since the observed Higgs mass is small compared to the unification scale, the Higgs/Higgsino  $\mu$ -term in the superpotential should be absent at the unification scale. When moduli get their VEVs, they can generate effective  $\mu$ -term. In the supergravity approximation [37]:

$$\mu = \langle m_{3/2} K_{H_u H_d} - F^{s_i} K_{H_u H_d s_i} \rangle. \quad (1.50)$$

If one allows for  $\frac{s}{m_{pl}} H_u H_d \subset K/m_{pl}^2$ , where  $s$  is a modulus field, and having in mind the suppression of  $\langle F^s \rangle \ll m_{3/2}$ , one can get

$$\mu \approx 0.1 m_{3/2} \sim \mathcal{O}(TeV). \quad (1.51)$$

With  $M_1, M_2 \sim \mathcal{O}(100 \text{ GeV})$ , the LSP and NLSP will be typically form of Wino and Bino. However, if the effective  $\mu$ -term, Eq. (1.51) is suppressed, Higgsino could also become the LSP. This can, for example, happen when the  $H_u H_d$  term in the Kähler potential does not, because of a symmetry, contain one, but two moduli fields, i.e.  $\frac{ss'}{m_{pl}^2} H_u H_d$ , leading to  $\mu \sim \mathcal{O}(100 \text{ GeV})$ .

## 1.5 Outline of the thesis

This thesis is organised as follows.

In chapter 2, based on publications [15, 16], we study GUT models arising from M theory compactified on a  $G_2$  holonomy manifold focusing on the issue of doublet-triplet splitting. We start with the review of the Witten's proposal of using a discrete symmetry enhanced by a symmetry breaking Wilson line that has been previously successfully applied in the context of  $SU(5)$  GUTs. In this case, the mechanism allows for the Higgs  $\mu$ -term to be forbidden from the superpotential while at the same time allowing for compactification scale masses for triplets.



When moduli are stabilised they regenerate Higgs  $\mu$ -term from the Kähler potential leading to phenomenologically viable models. We then extend those results to the case of  $SO(10)$  gauge group and realise that the solution to the double-triplet splitting problem is substantially different as triplets cannot be decoupled at high scale. Instead, we suppress possible triplet-matter interactions and check explicitly that even when those terms are reintroduced by moduli, experimental constraints are not violated. In order to restore the gauge coupling unification spoiled by light triplets we introduce extra vector-like matter multiplets and argue that flavour observables should not be affected in a significant way. We discuss how the high-scale VEVs in scalar components of right-handed neutrinos from the vector-like multiplets can break the gauge group down to the SM and induce Majorana masses required for the see-saw mechanism. At the same time, however, those VEVs induce potentially dangerous R-parity violating terms. Finally, we comment on how, in the framework of M theory one can naturally induce realistic Yukawa textures.

In chapter 3, based on the publication [16], we provide details of the high-scale breaking mechanism of the  $U(1)_X$  in our  $SO(10)$  SUSY GUT models. The mechanism is similar to that of Kolda-Martin with higher order terms in the superpotential inducing VEVs of right-handed components of extra vector-like multiplets. Depending on which of the non-renormalisable terms are allowed different values of VEVs can be achieved and we present several distinct scenarios. Masses of physical neutrinos are greatly influenced, through subsequently induced R-parity violating terms and Majorana masses, by the  $U(1)_X$  breaking. We derive, including all possible contributions, the resulting  $11 \times 11$  dimensional neutrino-neutralino mass matrix. We perform a numerical scan of the parameter space of  $SO(10)$  SUSY GUTs showing that models with the phenomenologically viable neutrino masses are indeed possible.

In chapter 4, based on the publication [17], we study the prospect of observing electroweakinos at a proposed 100 TeV hadron collider in the  $WZ$  channel. Partially motivated by results from  $G_2$  compactified M theory we focus on a model where squarks and sleptons are decoupled and one of the neutralinos becomes the LSP. We also assume that the mass hierarchy is such that  $M_2 > \mu$  and  $M_2 - \mu \gg m_Z$ , which maximises the discovery reach. We calculate branching ratios for W-inos and, because of its clear experimental signature, the fully leptonic  $WZ$  channel is chosen for the analysis. We study different kinematic distributions of the signal and background samples, generated at the (simplified) detector level. Based on that we design simple but effective signal regions and evaluate discovery reach and exclusion limits. We conclude that assuming  $3000 \text{ fb}^{-1}$  of integrated luminosity, W-inos could be discovered (excluded) up to 1.1 (1.8) TeV if the spectrum is not compressed.

Finally, in chapter 5 we provide the summary of results and discuss possible future directions of study.

## Chapter 2

# GUT models from M theory

### 2.1 Introduction

As argued in chapter 1, M Theory compactified on a  $G_2$  holonomy manifold leads to an effective 4D  $\mathcal{N} = 1$  SUSY, where gauge fields and chiral fermions are supported by different types of singularities in the compactified space. Simple gauge groups arising in this framework naturally lead to GUT types of models, where all fundamental interactions (but gravity) are unified. The moduli fields, that are low-energy remnants of compactification and govern the size of low-energy parameters, are stabilised leading to phenomenologically viable models [21]. In this chapter, we will extend the scope of the  $M$  theory approach from the previously considered  $SU(5)/\text{MSSM}$  case arising from  $M$  theory on  $G_2$  manifolds [11, 38] to  $SO(10)$ , where an entire fermion family  $Q, u^c, d^c, L, e^c, N$ , including a charge conjugated right-handed neutrino  $N$ , is unified within a single  $\mathbf{16}$  representation denoted  $\mathbf{16}^m$ .

One of the main issues in constructing GUT models, commonly referred to as the doublet-triplet splitting problem, is how to embed SM Higgses into GUT representations. On doing so, one is inevitably led to interactions not present in the SM. For example, in the simplest  $SU(5)$  case, GUT multiplets that incorporate SM Higgs doublets,  $\mathbf{5}$  and  $\bar{\mathbf{5}}$ , unify Higgses with colour triplets  $D, \bar{D}$ . The  $SU(5)$  invariance dictates that if Yukawa couplings, needed for fermion masses, are allowed, triplets have renormalisable couplings to matter that can mediate proton decay, usually at a rate much faster than the current experimental constraints. In many models, including those originating in string/ $M$  theory, this problem is often solved by making the colour-triplet very massive [39–41], something often achieved with a discrete symmetry with effective action on the triplets that is different from that on the doublets. We will see that in the case of  $SO(10)$  the solution turns out to be necessarily quite different, leading to distinct phenomenological constraints and predictions, considered previously from a phenomenological point of view in [42] and also [43–45].

The outline of this chapter is the following. In the rest of this section we review the doublet-splitting problem in the context of  $SU(5)$  GUT models. We start with the GUT

breaking mechanism, Wilson lines, naturally applicable to M Theory models on  $G_2$  before focusing on Witten's solution to the doublet-triplet splitting problem. We also show how effective Higgs  $\mu$ -term can be generated from the Kähler potential, despite being forbidden in the superpotential by Witten's solution. In section 2.2 we extend the discussion to the case of  $SO(10)$  GUTs where we are naturally led to a novel solution involving additional vector-like matter fields. The model constructed contains an extra  $U(1)_X$  gauge group and the consequences of its breaking are discussed in section 2.3. In section 2.4 we propose a mechanism that allows accommodating complicated Yukawa textures in this model, before concluding in section 2.5.

### 2.1.1 Symmetry breaking through Wilson lines

In order for a GUT model to be considered viable one has to specify a mechanism which breaks the GUT group into the SM  $SU(3)_C \times SU(2)_L \times U(1)_Y$ . Potentially, the choice of the breaking mechanism can also provide one with a solution to the doublet-triplet splitting problem. In the context of M theory where one has gauge fields propagating in extra dimensions (above the usual four), GUT groups are usually broken using so called Wilson lines [5, 46, 47]<sup>1</sup> which we are going to review below. We will see that Wilson lines will be indeed essential in solving the doublet triplet splitting problem, both in models of  $SU(5)$  and  $SO(10)$ .

In M Theory on  $G_2$  gauge fields are localised along a three-dimensional subspace  $Q$  of a singular manifold  $X$  of holonomy  $G_2$  [28, 29] (thus including the usual Minkowski spacetime  $M^4$  gauge fields propagate along  $M^4 \times Q$ ). If the space  $Q$  is **not** simply connected, i.e. it can be considered as a quotient  $Q = Q_0/\Gamma$  of a simply connected manifold  $Q_0$  by a discrete free-acting symmetry group  $\Gamma$ , it can admit a flat vacuum gauge configuration with non-trivial holonomy, Wilson lines  $\mathcal{W}$ . This means that one can find a non-contractible path  $\gamma$  in  $Q$  along which one can construct a non-trivial path ordered quantity

$$\mathcal{W}_\gamma = \mathcal{P} \exp \left( i \int_\gamma B_m dx^m \right) \neq 1, \quad (2.1)$$

where  $B_m$  is a non-trivial, flat background gauge field (that cannot be gauged away),  $m$  goes over the space  $Q$  and  $\mathcal{P}$  represents the path ordering. For a given vacuum configuration  $B_m$  there can be many inequivalent Wilson lines  $\mathcal{W}_\gamma$ , one for each class of non-contractible loops  $\gamma \in \pi_1(Q)$  with Eq. (2.1) providing a homomorphic map  $\gamma \rightarrow \mathcal{W}_\gamma$  between the fundamental group  $\pi_1(Q)$  and GUT group  $G$ . The homomorphism (2.1) provides the group operation for the

---

<sup>1</sup>One might be tempted to use the usual four dimensional spontaneous symmetry breaking. In M theory on  $G_2$ , however, only representations smaller than the adjoint are realised [30, 48, 49] making the spontaneous symmetry breaking difficult without breaking the SM gauge group as well. An alternative possibility of GUT breaking without higher dimensional representations include a non-standard Higgs breaking, e.g. flipped  $SU(5)$  [50] but we are not going to explore this possibility here.

discrete group  $\{\mathcal{W}_\gamma\}$  of inequivalent Wilson lines:

$$\mathcal{W}_{\gamma\gamma'} = \mathcal{W}_\gamma \cdot \mathcal{W}_{\gamma'}. \quad (2.2)$$

When the vacuum configuration  $B_m$  is fixed the GUT group  $G$  is broken to the subgroup  $H \subseteq G$  that commutes with  $\{\mathcal{W}_\gamma\}$ . If Wilson lines commute with each other (i.e. they are Abelian)  $[\mathcal{W}_\gamma, \mathcal{W}_{\gamma'}] = 0$ , they form part of the centre of the surviving group  $H$ . This implies that Abelian Wilson lines are generated by generators of surviving  $U(1)$  groups:

$$\mathcal{W}_\gamma = \exp\left(i \sum_k^n a_k^\gamma Q_k\right), \quad (2.3)$$

where  $Q_i$  are generator of  $n$   $U(1)$  groups that survive symmetry breaking and  $a_i^\gamma$  are numerical coefficients. Moreover, the set of generators  $\{Q_i\}$  can be extended to form a basis of the Cartan subalgebra of the unbroken group  $G$ , therefore implying the rank of the surviving group  $H$  and GUT groups  $G$  is the same <sup>2</sup>. In this work we are going to consider only such rank-preserving (i.e. Abelian) Wilson lines. In order for the surviving group to have rank less than the original GUT group one has to consider non-Abelian Wilson lines, for examples see [47].

Instead of working on the quotient space  $Q = Q_0/\Gamma$  one can equivalently consider the physics on the covering space  $Q_0$  with fields  $\psi(x)$  on  $Q_0$  satisfying boundary conditions [47]:

$$\psi(\gamma(x)) = \psi(x), \quad \gamma \in \Gamma = \pi_1(Q). \quad (2.4)$$

One cannot gauge away the background field  $B_\mu$  with boundary conditions (2.4) imposed, however, the field  $B_\mu$  can be put to zero in  $Q_0$  if the boundary conditions change at the same time:

$$\psi(\gamma(x)) = \mathcal{W}_\gamma \psi(x), \quad \text{for } \psi \text{ in fundamental repr.} \quad (2.5)$$

Therefore we can view the Wilson line breaking either 1) as non-zero expectation value of GUT group gauge bosons (in the quotient space  $Q$ ), or 2) GUT gauge fields vanishing in vacuum, but with charge fields absorbing Wilson lines when transformed under the fundamental group of the manifold, in line with Eq. (2.5). A toy model in 5D space  $M^4 \times S^1$  showing explicitly the Wilson line absorption mechanism is presented in Appendix A.1

### 2.1.2 Witten's solution of the doublet-triplet splitting problem

The Wilson line breaking mechanism reviewed so far can be applied to break gauge symmetries when gauge bosons propagate in extra dimensions, which is common setting in String/M-Theory framework. Let's now focus on whether the Wilson line breaking can be used for solving the doublet-triplet splitting problem.

---

<sup>2</sup>As the rank of a group is equal to the dimension of its Cartan subalgebra.

One possibility, often used in heterotic string theories, is to project out unwanted fields (i.e. Higgs triplets) from low-energy physics by virtue of compactification [5, 46, 47]. In this context gauge unification arises only in some dimensions higher than the usual four, and is broken to the SM using Wilson lines present along the compactified dimensions. If the symmetry of the compactified dimensions is chosen appropriately the dangerous colour triplets can be projected out from the low-energy spectrum of 4D theory, i.e. the Kaluza-Klein zero mode Higgs triplets are not compatible with transformation (2.5), while leaving Higgs doublets intact. In the case of M-theory compactified on  $G_2$ , however, this mechanism is not viable, as it requires matter fields to propagate along extra dimensions, In M-theory matter fields are localised at a singular point of extra dimensions [27, 30, 31], i.e. propagate only along visible four dimensions, and are not zero modes of Kaluza-Klein tower of fields.

An alternative solution of doublet-triplet splitting that can be used in the context of M-Theory was proposed by Witten [38], and is based on a discrete symmetry of the  $G_2$  manifold. If this symmetry is isomorphic to the fundamental group of the extra dimensional manifold  $Q$ , then the action of the discrete symmetry can be altered by the Wilson lines when acting on the matter fields that absorbed them. This means that the Wilson line phases will effectively act as charges of the discrete symmetry. Since Wilson lines do not commute with the original GUT group  $G$ , the resulting discrete symmetry will not commute with  $G$  either. Different components of a GUT multiplet will acquire different discrete charges, giving us a leverage over doublet-triplet splitting.

Let us review here in more details the results of [38] as this will be a starting point for our studies into  $SO(10)$  GUT models. For concreteness for now we will assume that the GUT group  $G$  is  $SU(5)$ , and only in section 2.2 we will extend these results to the  $SO(10)$  case. As discussed already, in order for a non-trivial Wilson line to develop, we need  $Q$  to be non-simply connected. An example of such can be a quotient of a three-sphere  $\mathbf{S}^3$  with fundamental group  $L \cong Z_N$ :

$$Q = S^3/L, \quad (2.6)$$

where if we parameterise the three sphere  $S^3$  by two complex numbers  $z_1$  and  $z_2$  satisfying  $|z_1|^2 + |z_2|^2 = 1$ , then the action of  $L$  on  $S^3$  is given by:

$$L : z_i \rightarrow e^{2\pi i/N} z_i, \quad i = 1, 2, \quad (2.7)$$

and  $L$  acts freely on  $Q$ <sup>3</sup>.  $Q$  is then not-simply connected with the fundamental group  $\pi_1(Q)$  being finite, abelian  $Z_n$ . In this case it is enough to consider a single Wilson line  $\mathcal{W} = \mathcal{W}_\gamma$  defined along the path  $\gamma = \{x \rightarrow Lx\}$ , with the rest of them being generated through Eq. (2.2). Also, since  $L^n x = x$ , it must be that  $\mathcal{W}^n = 1$ .

As we know from Eq. (2.3), the Wilson line that breaks the  $SU(5)$  to the SM gauge group

---

<sup>3</sup>If one relax the requirement for  $L$  to act freely one can get the generalisation of the Wilson line breaking, so called orbifold breaking, see e.g. [51, 52]

$H = SU(3)_C \times SU(2)_L \times U(1)_Y$  will be generated by  $U(1)_Y$  generators. Using the standard embedding of SM  $SU(3)_C \times SU(2)_L \times U(1)_Y$  in  $SU(5)$  [53] we can break  $G \rightarrow H$  using the Wilson line:

$$\mathcal{W} = \text{diag}(\eta^{2\rho}, \eta^{2\rho}, \eta^{2\rho}, \eta^{-3\rho}, \eta^{-3\rho}), \quad (2.8)$$

where  $\eta = e^{2\pi i/N}$ .

This breaking pattern results in the following decomposition of  $SU(5)$  irreps:

$$\bar{\mathbf{5}} : L = (\mathbf{1}, \mathbf{2})_{(-\frac{1}{2})} \oplus d^c = (\bar{\mathbf{3}}, \mathbf{1})_{(\frac{1}{3})} \quad (2.9)$$

$$\bar{\mathbf{5}}_d : H_d = (\mathbf{1}, \mathbf{2})_{(-\frac{1}{2})} \oplus \bar{D} = (\bar{\mathbf{3}}, \mathbf{1})_{(\frac{1}{3})} \quad (2.10)$$

$$\mathbf{5}_u : H_u = (\mathbf{1}, \mathbf{2})_{(\frac{1}{2})} \oplus D = (\mathbf{3}, \mathbf{1})_{(-\frac{1}{3})} \quad (2.11)$$

$$\mathbf{10} : e^c = (\mathbf{1}, \mathbf{1})_{(1)} \oplus Q = (\mathbf{3}, \mathbf{2})_{(\frac{1}{6})} \oplus u^c = (\bar{\mathbf{3}}, \mathbf{1})_{(-\frac{2}{3})} \quad (2.12)$$

containing all matter fields of SM ( in  $3 \times (\bar{\mathbf{5}} + \mathbf{10})$ ) and Higgses together with Higgs triplets (in  $\mathbf{5}_u$  and  $\bar{\mathbf{5}}_d$ ).

Now, in order to split Higgs doublets and triplets, Witten proposed [38] using a geometric symmetry of the manifold  $F \cong \pi_1(Q)$ . In our case, where  $Q$  is a quotient of  $S^3$  defined in Equations (2.6) and (2.7), we can construct  $F$  to act on  $Q$  in the following way:

$$F : z_1 \rightarrow z_1, z_2 \rightarrow e^{2\pi i/N} z_2. \quad (2.13)$$

Comparing Equations (2.7) and (2.13) we can see that up to transformation (2.7) there are two sets of fixed points of  $Q$  under  $F$ . The first one, a circle  $S_1$  defined by  $|z_1| = 1, z_2 = 0$  is clearly left invariant by  $F$ , while the second one, a circle  $S_2$  defined by  $z_1 = 0, |z_2| = 1$  is left fixed up to the equivalence relation (2.7). In Eq. (2.5) we have seen that when a GUT symmetry breaking Wilson line is introduced a fundamental field transforms under a fundamental group  $\pi_1(Q)$  with absorption of the Wilson line phases. This means that a discrete symmetry  $F'$  that survives the Wilson line breaking act as  $F$  at  $S_1$ , but as  $F \times \mathcal{W}$  at  $S_2$ . If we now place all chiral fields on  $S_1$  or  $S_2$  (we would break the discrete symmetry  $F'$  if we do otherwise), then all components of a multiplet localised on  $S_1$  will transform with the same  $Z_n$  charge due to the action of  $F$ . On the other hand, components of a multiplet on  $S_2$  will have discrete charges of  $F'$  split by the action of the Wilson line. If matter fields are put on  $S_1$  and  $S_2$  appropriately one can use the surviving discrete charges of  $F'$  to constrain interaction of the low energy superpotential, i.e. solve the doublet-triplet splitting problem, as we will see in the  $SU(5)$  example below.

Following [38] we can put  $\bar{\mathbf{5}}^w$ , the multiplet containing  $H_d$  and  $\bar{D}$ , at points on  $S_2$ , while all other multiplets, including  $\mathbf{5}^h$ , containing  $H_u$  and  $D$ , as well as matter multiplets  $\bar{\mathbf{5}}^m$  and  $\mathbf{10}^m$ , at points on  $S_1$ . Then the transformation rules for these multiplets under  $F$ , Eq. (2.13),

are:

$$\begin{aligned}
\bar{\mathbf{5}}^w &\rightarrow \eta^\omega \left( \eta^\delta H_d^w \oplus \eta^\gamma \bar{D}^w \right), \\
\mathbf{5}^h &\rightarrow \eta^\chi \mathbf{5}^h, \\
\bar{\mathbf{5}}^m &\rightarrow \eta^\tau \bar{\mathbf{5}}^m, \\
\mathbf{10}^m &\rightarrow \eta^\sigma \mathbf{10}^m,
\end{aligned} \tag{2.14}$$

where  $\eta \equiv e^{2\pi i/N}$ ,  $\{\omega, \chi, \tau, \sigma, \delta, \gamma\} \in \mathbb{Z} \bmod N$ .  $\omega, \chi, \tau, \sigma$  are arbitrary charges, while  $\delta$  and  $\gamma$  have to satisfy the condition  $2\delta + 3\gamma = 0 \bmod N$  as they arise from the Wilson line, Eq. (2.8). By requiring that Yukawa couplings, Majorana neutrino masses, and colour-triplet masses must be present, we obtain constraints on the charges as can be seen in Table 2.1 where we chose  $\omega = 0$ .

Coupling		Constraint
up-type Yukawas	$H_u^h \mathbf{10}^m \mathbf{10}^m$	$2\sigma + \chi = 0 \bmod N$
down-type Yukawas	$H_d^w \mathbf{10}^m \bar{\mathbf{5}}^m$	$\sigma + \tau + \delta = 0 \bmod N$
neutrino Majorana masses	$H_u^w H_u^w \bar{\mathbf{5}}^m \bar{\mathbf{5}}^m$	$2\chi + 2\tau = 0 \bmod N$
colour-triplet masses	$\bar{D}^w D^h$	$\chi + \gamma = 0 \bmod N$

Table 2.1: Couplings and charges for  $SU(5)$  operators required for phenomenological reasons.

One can solve these by writing all angles in terms of, say,  $\sigma$

$$\begin{aligned}
\chi &= -\gamma = -2\sigma \bmod N, \\
\delta &= -3\sigma + N/2 \bmod N, \\
\tau &= 2\sigma + N/2 \bmod N.
\end{aligned} \tag{2.15}$$

For this model to be phenomenologically viable we need to forbid Higgs  $\mu$  term (as we do not want Higgs to have a mass of order  $M_{GUT} \approx 10^{16}$  GeV, and to at last realise the doublet-triplet splitting), as well as dangerous proton decay operators. Table 2.2 lists the operators that need to be forbidden together with their overall discrete charge assuming conditions given by Eq. (2.15). Choice of  $N = 4$  and  $\sigma = 1$  gives an example of charges that meet all constraints listed.

Coupling		Constraint
$\mu$ -term	$H_u^h H_d^w$	$-5\sigma + N/2 \neq 0 \bmod N$
dimension-5 proton decay	$\mathbf{10}^m \mathbf{10}^m \mathbf{10}^m \bar{\mathbf{5}}^m$	$5\sigma + N/2 \neq 0 \bmod N$
bilinear R-parity violation	$\mathbf{5}^h \bar{\mathbf{5}}^m$	$N/2 \neq 0 \bmod N$
trilinear R-parity violation	$\mathbf{10}^m \bar{\mathbf{5}}^m \bar{\mathbf{5}}^m$	$5\sigma \neq 0 \bmod N$

Table 2.2: Couplings and charges for  $SU(5)$  operators that should not be present for phenomenological reasons. Charges follow constraints given by Eq. (2.15).

### 2.1.3 Effective $\mu$ and trilinear terms

In the  $SU(5)$  model constructed so far, we have decoupled Higgs triplets  $D$  and  $\bar{D}$  by allowing their mass term in the superpotential using a geometric symmetry of the  $G_2$  manifold. At the same time the symmetry forbids Higgs doublet  $\mu$ -term providing a natural explanation of why the Higgs is lighter than  $m_{pl}$  and different in behaviour compare to triplets. However, the discrete symmetry forces  $\mu = 0$ , phenomenologically though,  $\mu \geq \mathcal{O}(100)$  GeV from direct limits on the masses of charged Higgsinos from colliders. The symmetry must therefore be broken at low energy.

Since moduli fields need to be stabilised and acquire non-zero VEVs [22], they are the natural choice for the fields responsible for breaking the discrete symmetry [10]. Since the discrete symmetry is a geometric symmetry of the extra dimensions, the moduli fields are naturally charged under it and after being stabilised, generically, they will break the symmetry. This then generates an effective  $\mu$  term from, e.g. Kähler potential operators of the form:

$$K \supset \frac{s}{m_{pl}} H_u H_d + h.c., \quad (2.16)$$

à la Giudice-Masiero [54], where  $s$  denotes a  $G_2$ -manifold modulus field of the appropriate charge<sup>4</sup>. Note that such terms are forbidden in the superpotential [27]. In  $M$  theory compactifications on  $G_2$ -manifolds *without* fluxes, all of the moduli fields  $s_j$  reside in chiral superfields  $S_j = t_j + i s_j$  which contain axions,  $t_j$ . This implies that terms polynomial in moduli fields ( $s_j = S_j - \bar{S}_j$ ), such as in Eq. (2.16), are forbidden in the superpotential due to holomorphy and the axion shift symmetries,  $t_j \rightarrow t_j + a_j$ .

From the standard supergravity Lagrangian when taking the flat limit of supergravity [37] we get an effective  $\mu$ -term:

$$\mu = \langle m_{3/2} K_{H_u H_d} - F^{s_i} K_{H_u H_d s_i} \rangle. \quad (2.17)$$

When we plug in Eq. (2.16) it leads to:

$$\mu \sim \frac{\langle s \rangle}{m_{pl}} m_{3/2} + \frac{\langle F^s \rangle}{m_{pl}}. \quad (2.18)$$

As discussed in Sec. 1.4.1, in  $M$  Theory on  $G_2$  one expects the modulus  $F$ -term VEVs,  $\langle F^s \rangle$ , being subleading compare to  $\langle s \rangle \sim 0.1 m_{pl}$ . One therefore gets,

$$\mu \sim 0.1 m_{3/2} \sim \mathcal{O}(TeV). \quad (2.19)$$

An important thing to notice is that similar analysis can be performed for other vector

---

<sup>4</sup>One expects  $\mathcal{O}(100)$  different moduli fields coming from a realistic compactification, therefore, generically, there should be a moduli with the discrete charge suitable for the Eq. (2.16)



like pairs  $X\bar{X}$ , if present in a model. In particular, this means that bilinear R-parity violating operators, like the one in Table 2.2, will be generically present with the coupling  $\sim \mu$ . On top of that, if one adds extra vector-like pairs, beyond the MSSM spectrum, they will face a potentially dangerous mixing between SM particles and the new states generated through the moduli VEV, even if such mixing is not initially allowed in the superpotential. We will study those challenges when we construct an  $SO(10)$  model below.

Similarly to the  $\mu$ -term above, also effective trilinear terms, e.g. Yukawa and trilinear R-parity violating terms, can be generated in our framework. Let's consider the contribution to the Kähler potential:

$$K \subset \frac{s}{m_{pl}^2} XYZ + \text{h.c.}, \quad (2.20)$$

with  $s$  a moduli, likely to be a different one compare to Eq. (2.16), and  $X, Y, Z$  are chiral supermultiplets. Following [37] we can write the effective trilinear coupling  $\lambda_{XYZ}^{(K)}$  to be:

$$\lambda_{XYZ}^{(K)} = \frac{(\langle s \rangle m_{3/2} + \langle F^s \rangle)}{m_{pl}^2}. \quad (2.21)$$

As before,  $F$ -term VEV contribution is sub-leading compare to  $\langle s \rangle$  and we can estimate:

$$\lambda_{XYZ}^{(K)} \sim \frac{\langle s \rangle m_{3/2}}{m_{pl}^2} \sim 0.1 \frac{m_{3/2}}{m_{pl}} \sim 10^{-15}. \quad (2.22)$$

Although this value is numerically small, it will have deep impact on the LSP lifetime as we will see in chapter 3. At the same time, the smallness of Eq. (2.22) imply that this mechanism is not suitable to generate physical Yukawas, and those should be rather allowed at tree level, in line with what was required so far, e.g. see Table 2.1.

## 2.2 $SO(10)$ SUSY GUTs from M theory on $G_2$ -manifolds

Ideas reviewed so far were used to construct the  $G_2$ -MSSM [11, 55], SUSY  $SU(5)$  models arising in M Theory on a  $G_2$  manifold. We now turn into an extension of the program to the  $SO(10)$  GUT group, while referring to previous work on  $G_2$  compactifications and consequent predictions for the parameters [12, 22].

In the remainder of this section, we focus on the GUT group  $G = SO(10)$ . Using an abelian Wilson line to break the GUT group, the simplest case of a surviving group that is the most resembling to the SM is

$$SO(10) \rightarrow SU(3)_c \times SU(2)_L \times U(1)_Y \times U(1)_X, \quad (2.23)$$

under which the branching rules of the GUT irreps read

$$\begin{aligned}
\mathbf{10} : H_u &= (\mathbf{1}, \mathbf{2})_{(\frac{1}{2}, 2)} \oplus H_d = (\mathbf{1}, \mathbf{2})_{(-\frac{1}{2}, -2)} \oplus D = (\mathbf{3}, \mathbf{1})_{(-\frac{1}{3}, 2)} \oplus \bar{D} = (\bar{\mathbf{3}}, \mathbf{1})_{(\frac{1}{3}, -2)} , \quad (2.24) \\
\mathbf{16} : L &= (\mathbf{1}, \mathbf{2})_{(-\frac{1}{2}, 3)} \oplus e^c = (\mathbf{1}, \mathbf{1})_{(1, -1)} \oplus N = (\mathbf{1}, \mathbf{1})_{(0, -5)} \oplus u^c = (\bar{\mathbf{3}}, \mathbf{1})_{(-\frac{2}{3}, -1)} \oplus \\
&\oplus d^c = (\bar{\mathbf{3}}, \mathbf{1})_{(\frac{1}{3}, 3)} \oplus Q = (\mathbf{3}, \mathbf{2})_{(\frac{1}{6}, -1)} , \quad (2.25)
\end{aligned}$$

and the subscripts are the charges under  $U(1)_Y \times U(1)_X$ , which are normalised as  $Q_Y = \sqrt{\frac{5}{3}}Q_1$ ,  $Q_X = \sqrt{40}\tilde{Q}_X$ , where  $Q_1, \tilde{Q}_X$  are  $SO(10)$  generators.

Following the discussion around Eq. (2.3), the Wilson line has to be generated by generators of surviving  $U(1)$  groups, in this case  $U(1)_Y$  and  $U(1)_X$ :

$$\mathcal{W} = \exp \left[ \frac{i2\pi}{N} (aQ_Y + bQ_X) \right] = \sum_{m=0}^{\infty} \frac{1}{m!} \left( \frac{i2\pi}{N} \right)^m (aQ_Y + bQ_X)^m , \quad (2.26)$$

where the coefficients  $a, b$  specify the parameterisation of the Wilson line and are only constrained by the requirement that  $\mathcal{W}^N = 1$  assuming the fundamental group of the manifold supporting the Wilson line to be  $\mathbb{Z}^N$ , in line with Eq. (2.6). Under the linear transformation:

$$\frac{1}{2}a + 2b \rightarrow \alpha , \quad (2.27)$$

$$\frac{1}{3}a - 2b \rightarrow \beta , \quad (2.28)$$

its action on the fundamental irrep then reads

$$\mathcal{W}_{10} = \eta^\alpha H_u \oplus \eta^{-\alpha} H_d \oplus \eta^{-\beta} D \oplus \eta^\beta \bar{D} , \quad (2.29)$$

where  $\eta$  is, as before, the  $N$ th root of unity.

Likewise the Wilson line matrix acts on the 16 irrep as

$$\mathcal{W}_{16} = \eta^{-\frac{3}{2}\beta} L \oplus \eta^{\alpha+\frac{3}{2}\beta} e^c \oplus \eta^{-\alpha+\frac{3}{2}\beta} N \oplus \eta^{-\alpha-\frac{1}{2}\beta} u^c \oplus \eta^{\alpha-\frac{1}{2}\beta} d^c \oplus \eta^{\frac{1}{2}\beta} Q , \quad (2.30)$$

which could be simplified a bit further by replacing  $\beta \rightarrow 2\beta$  without loss of generality, in order for the parameters to read as integers.

Similarly to the  $SU(5)$  case we can construct a discrete symmetry that can split components of an irrep. Following the language of section 2.1.2, if we place a matter multiplet on a circle  $S_1$ , the discrete charges are not affected by the Wilson line, and states from this multiplet will have identical discrete charges after GUT group is broken. On the other hand, if a GUT multiplet is put on  $S_2$ , the discrete symmetry absorbs Wilson line phases, modifying discrete charges of different components accordingly.

Having all the ingredients required to employ Witten's discrete symmetry proposal, we

would like to have a consistent implementation of a well-motivated doublet-triplet splitting mechanism as it was done for  $SU(5)$ . Unfortunately the customary approach to the problem does not seem to work with  $SO(10)$ . To understand this first notice that Witten's splitting mechanism can only work in order to split couplings between distinct GUT irreps. This is understood as  $\mathcal{W}$  has the form of a gauge transformation of the surviving group and so it will never be able to split self bilinear couplings of a GUT irrep. For example, if one takes a  $\mathbf{10}$  with Wilson line phases, denoted  $\mathbf{10}^\omega$ , to contain the MSSM Higgses, following Eq. (2.29) it will transform as:

$$\mathbf{10}^\omega \rightarrow \eta^\omega \left( \eta^\alpha H_u \oplus \eta^{-\alpha} H_d \oplus \eta^{-\beta} D \oplus \eta^\beta \bar{D} \right) \quad (2.31)$$

under the surviving discrete symmetry, with  $\omega \in \{0, \dots, N-1\}$  being an overall charge for the multiplet from the original discrete symmetry  $F$ , Eq. (2.13). One can see that mass terms for the Higgses and coloured triplets are simultaneously allowed or disallowed and thus doublet-triplet splitting is not realised.

We can, in principle, add extra  $\mathbf{10}$  multiplets and forbid some couplings between the different members of the various  $\mathbf{10}$  multiplets, but one can see that there will typically be more than one pair of light Higgs doublets which tend to destroy gauge coupling unification. Consider one additional  $\mathbf{10}$ , denoted  $\mathbf{10}^h$  without Wilson line phases<sup>5</sup>:  $\mathbf{10}^h \rightarrow \eta^\xi \mathbf{10}^h$ . We have eight possible gauge invariant couplings with a  $\mathbf{10}^w$  and  $\mathbf{10}^h$  that can be written in matrix form as

$$W \supset \mathbf{H}_d^T \cdot \mu_H \cdot \mathbf{H}_u + \bar{\mathbf{D}}^T \cdot M_D \cdot \mathbf{D}, \quad (2.32)$$

where  $\mu_H$  and  $M_D$  are two  $2 \times 2$  superpotential mass parameters matrices,  $\mathbf{H}_{u,d}^T = (H_{u,d}^w, H_{u,d}^h)$ ,  $\bar{\mathbf{D}}^T = (\bar{D}^w, \bar{D}^h)$ , and  $\mathbf{D}^T = (D^w, D^h)$ . The entries of the matrices are non-vanishing depending on which of the following discrete charge combinations are zero (mod  $N$ )

$$\begin{aligned} D^w \bar{D}^w, H_u^w H_d^w &: 2\omega, \\ D^h \bar{D}^h, H_u^h H_d^h &: 2\xi, \\ H_u^w H_d^h &: \alpha + \omega + \xi, \\ H_u^h H_d^w &: -\alpha + \omega + \xi, \\ D^w \bar{D}^h &: -\beta + \omega + \xi, \\ D^h \bar{D}^w &: \beta + \omega + \xi. \end{aligned} \quad (2.33)$$

The naive doublet-triplet splitting solution would be for  $\mu_H$  to have only one zero eigenvalue, with  $M_D$  having all non-zero eigenvalues. One finds that there is no choice of constraints in Eq. (2.33) that accomplishes this.

---

<sup>5</sup>In the language of section 2.1.2  $\mathbf{10}^h$  is placed on the circle  $S_2$ .

We could consider that in order to split the Higgses,  $H_u$  and  $H_d$ , from the coloured triplets  $-D, \bar{D}$  – we would need to add another  $\mathbf{10}$ , but it was shown that this cannot be achieved and so we are ultimately left with light coloured triplets. As adding more  $\mathbf{10}$  does not seem to help, we will consider only a single light  $\mathbf{10}^\omega$  at low energy.

In order to allow for light  $D, \bar{D}$  we need to guarantee that they are sufficiently decoupled from matter to prevent proton-decay. To accomplish this, we can use the discrete symmetry to forbid certain couplings, namely to *decouple  $D$  and  $\bar{D}$  from matter*. Such couplings arise from the  $SO(10)$  invariant operator  $\mathbf{10}^\omega \mathbf{16} \mathbf{16}$ , with  $\mathbf{16}$  denoting the three  $SO(10)$  multiplets, each containing a SM family plus right handed neutrino  $N$ . At the same time we would like to allow for Yukawa interactions, that in the  $SO(10)$  case for the up-type quarks and right-handed neutrinos look like:

$$y_u^{ij} H_u^w \mathbf{16}_i \mathbf{16}_j \equiv y_u^{ij} H_u^w (Q_i u_j^c + L_i N_j + i \leftrightarrow j), \quad (2.34)$$

and similarly for down-type quarks and charged leptons. If  $\mathbf{16}$  transforms as  $\eta^\kappa \mathbf{16}$ , the couplings and charge required to fulfil the constraints mentioned are shown in the Table 2.3.

Coupling		Constraint
up-type Yukawas	$H_u^w \mathbf{16} \mathbf{16}$	$2\kappa + \alpha + \omega = 0 \pmod N$
down-type Yukawas	$H_d^w \mathbf{16} \mathbf{16}$	$2\kappa - \alpha + \omega = 0 \pmod N$
triplets–matter interaction	$D^w \mathbf{16} \mathbf{16}$	$2\kappa - \beta + \omega \neq 0 \pmod N$
	$\bar{D}^w \mathbf{16} \mathbf{16}$	$2\kappa + \beta + \omega \neq 0 \pmod N$ ,

Table 2.3: Minimal constraints on discrete charges for the  $SO(10)$  model.

The suppression of colour triplet couplings to matter was previously considered by Dvali in [42] and also [43–45] from a bottom-up perspective.

As discussed in section 2.1.3, the couplings forbidden at a renormalizable tree-level by the discrete symmetry are generically regenerated from Kähler interactions through the Giudice-Masiero mechanism [54]. While this provides the Higgsinos a TeV scale  $\mu$ -term mass, it also provides effective trilinear couplings with an  $\mathcal{O}(10^{-15})$  coefficient. As these are generic, we need to systematically study their physical implications at low energies, such as proton-decay, R-parity violation, and flavour mixing.

For proton decay, the effective superpotential will be generate by the following Kähler potential

$$K \supset \frac{s}{m_{pl}^2} \bar{D} d^c u^c + \frac{s}{m_{pl}^2} D e^c u^c + \frac{s}{m_{pl}^2} D Q Q + \frac{s}{m_{pl}^2} \bar{D} Q L + \frac{s}{m_{pl}^2} D N d^c + \text{h.c.} , \quad (2.35)$$

where we assume  $\mathcal{O}(1)$  coefficients and take one family for illustrative purposes. As the moduli

acquire non-vanishing VEVs, these become

$$W_{eff} \supset \lambda D Q Q + \lambda D e^c u^c + \lambda D N d^c + \lambda \bar{D} d^c u^c + \lambda \bar{D} Q L, \quad (2.36)$$

with  $\lambda$  in analogy to Eq. (2.22) can be estimated to be:

$$\lambda \approx \frac{1}{m_{pl}^2} (\langle s \rangle m_{3/2} + \langle F_s \rangle) \sim 10^{-15}. \quad (2.37)$$

Notice that contrary to the  $SU(5)$  case, there is no extra contribution from the bilinear term  $\kappa L H_u$  since it is not allowed by gauge invariance.

Based on diagrams like one given in Fig. 2.1 we estimate the scalar triplet mediated proton decay rate to be:

$$\Gamma_p \simeq \frac{|\lambda^2|^2 m_p^5}{16\pi^2 m_D^4} \simeq (10^{42} \text{ yrs})^{-1}, \quad (2.38)$$

where we took the mass of the colour triplets to be  $m_D \simeq 10^3$  GeV, as it is expected to be of order of  $\mu$ , Eq. (2.19). This satisfies current experimental limits [56],  $\Gamma_p^{(\text{exp.})} \lesssim (10^{33} \text{ yrs})^{-1}$ .

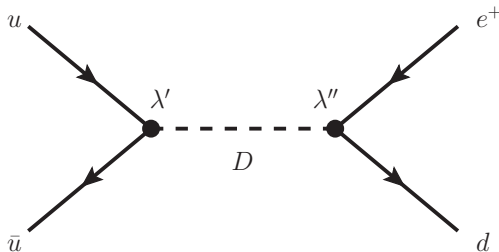


Figure 2.1: Diagram contributing to proton decay in the  $SO(10)$  model. Couplings  $\lambda'$ ,  $\lambda''$  have the same order of magnitude, given by Eq. (2.37).

Another limit for triplet scalar comes from the cosmological constraints on its decay. As we have seen from proton-decay operators, Eq. (2.36), triplet scalars can decay into quarks. If they start to decay during the Big Bang Nucleosynthesis (BBN) then nucleons could be disassociated, spoiling the predictions for light element abundances. We can estimate another limit on the triplet scalar mass by calculating its lifetime as it decay through the processes  $D \rightarrow e^c u^c, Q Q, Q L, d^c u^c$ , and we get

$$\Gamma \simeq \lambda^2 m_D \simeq (10^{-3} \text{ sec})^{-1}, \quad (2.39)$$

which is consistent with BBN constraint. They will also give interesting collider signatures due to their long-lived nature.

### 2.2.1 Additional vector-like family

Gauge coupling unification is in general spoiled by light colour triplets, unless they are also accompanied by additional light doublet states. The 1-loop renormalisation group (RG) equations for the SM gauge couplings  $g_1, g_2, g_3$  written in terms of quantities  $\alpha_a^{-1} = g_a^2/4\pi$  reads [57]:

$$\frac{d}{dt}\alpha_a^{-1}(\mu) = \frac{1}{16\pi^2}b_a, \quad (2.40)$$

where  $t = \ln\left(\frac{\mu}{\mu_0}\right)$  and  $\mu, \mu_0$  being some energy scales. For models with low-energy MSSM particle content  $(b_1, b_2, b_3) = (33/5, 1, -3)$  and gauge couplings appear to unify at  $Q \sim 10^{16}$  GeV. This is, for example the case of the  $G_2$ -MSSM. However, in our  $SO(10)$  case we have additional light triplets that ruin the unification. In the present framework, the only way we know of, to circumvent this issue is the presence of light additional states which complete the triplets into complete GUT multiplets.

Happily, this can also be achieved by use of the discrete symmetry. First we notice that the down-type quarks  $-d_X^c, \bar{d}_X^c$  have the same SM quantum numbers as the coloured triplet pair  $-D, \bar{D}$  coming from the  $\mathbf{10}^w$ . Therefore, we introduce a vector-like pair of  $\mathbf{16}$ 's, labelled as  $\mathbf{16}_X + \overline{\mathbf{16}}_X$ . Next a GUT-scale mass is given to their colour triplet components  $d_X^c, \bar{d}_X^c$  whilst keeping the remaining particles light. Suitable charges under the discrete symmetry can forbid the appropriate mass terms and the large mass can arise from membrane instantons if the  $\mathbf{16}_X$  and  $\overline{\mathbf{16}}_X$  are close by on the  $G_2$  manifold [39].

We take  $\mathbf{16}_X$  to be localised along a Wilson line, and following Eq. (2.30) we find that it transforms under the discrete symmetry as

$$\mathbf{16}_X \rightarrow \eta^x \left( \eta^{-3\gamma} L \oplus \eta^{3\gamma+\delta} e^c \oplus \eta^{3\gamma-\delta} N \oplus \eta^{-\gamma-\delta} u^c \oplus \eta^{-\gamma+\delta} d^c \oplus \eta^\gamma Q \right). \quad (2.41)$$

Assuming  $\overline{\mathbf{16}}_X$  transforms without Wilson line phases,  $\overline{\mathbf{16}}_X \rightarrow \eta^{\bar{x}} \overline{\mathbf{16}}_X$ , the condition for the mass term is

$$\bar{d}_X^c d_X^c : x - \gamma + \delta + \bar{x} = 0 \pmod{N}, \quad (2.42)$$

whilst forbidding all the other self couplings that would arise from  $\mathbf{16}_X \overline{\mathbf{16}}_X$ .

The light  $D^w$  and  $\bar{D}^w$  from the original  $\mathbf{10}^w$  then “complete” the  $\mathbf{16}_X + \overline{\mathbf{16}}_X$  pair. The light states in the  $\mathbf{16}_X$  and  $\overline{\mathbf{16}}_X$  obtain masses via the Kähler potential of order of TeV, via the Giudice-Masiero mechanism as in Eq. (2.19). The low-energy spectrum is then the one of MSSM plus this vector-like family, which in turn preserves unification albeit with a larger gauge coupling at the GUT scale (relative to the MSSM), see Fig. 2.2.

In analogy to effective mass term for light states of  $\mathbf{16}_X, \overline{\mathbf{16}}_X$ , an effective  $\mu$ -terms of the form  $\mu_X^i \mathbf{16}_i \overline{\mathbf{16}}_X$  is also induced by moduli vevs, which might rise concerns about mixing of extra states with SM quarks and leptons. However, one finds that all the light components of the extra matter decouple from ordinary matter, with mixings suppressed by terms of order

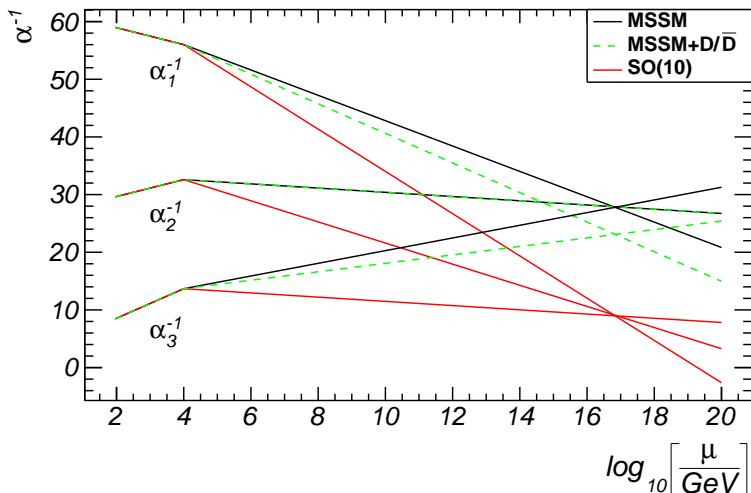


Figure 2.2: Renormalisation group evolution of the inverse gauge coupling  $\alpha_i^{-1}(\mu)$  in MSSM (black solid lines),  $SO(10)$  model with light triplets  $D, \bar{D}$ , labeled MSSM+ $D/\bar{D}$  (green dashed lines), and  $SO(10)$  model with extra  $\mathbf{16}_X$  and  $\overline{\mathbf{16}}_X$ , labeled  $SO(10)$  (red solid lines). We assume that all new states beyond SM (including SUSY partners) are introduced at about  $10^4$  GeV.

(2.37). For example, consider the up-type quark sector. The superpotential contribution to the mass matrix is, schematically,  $U_L \cdot M_u \cdot U_R^T$ , with  $U_L = (u^i, u_X, \bar{u}_X^c) \subset (\mathbf{16}, \mathbf{16}_X, \overline{\mathbf{16}}_X)$ ,  $U_R = ((u^c)^i, \bar{u}_X, u_X^c) \subset (\mathbf{16}, \overline{\mathbf{16}}_X, \mathbf{16}_X)$ , and

$$M_u = \begin{pmatrix} y_u^{ij} \langle H_u \rangle & \mu_{XQ}^i & 0 \\ 0 & \mu_{XXQ} & 0 \\ \mu_{Xu}^j & 0 & \mu_{Xu} \end{pmatrix}. \quad (2.43)$$

Here  $\mu_{XQ}^i, \mu_{Xu}^j, \mu_{XXQ}, \mu_{Xu}$  are moduli induced  $\mu$ -type parameters of  $\mathcal{O}(\text{TeV})$  while the vanishing entries are non-zero only to first order in moduli-induced trilinear interactions that are vanishingly small,  $\mathcal{O}(10^{-15})$ . We have found numerically that flavour changing neutral currents (FCNCs) are highly suppressed by this structure. This can be understood analytically in the approximation that the electroweak masses can be ignored, since  $y_u \langle H_u \rangle / \mu \sim \mathcal{O}(0.1)$ . In this approximation, the third lightest  $u$ -quark will be given by the two component Weyl quarks

$$t = u'_3 \simeq \frac{1}{\sqrt{(\mu_X^3)^2 + (\mu_{XXQ})^2}} ((\mu_{XXQ})u_3 - (\mu_X^3)u_X), \quad (2.44)$$

$$t^c = (u_3^c)' \simeq \frac{1}{\sqrt{(\mu_{Xu}^3)^2 + (\mu_{Xu})^2}} ((\mu_{Xu}(u^c)_3 - (\mu_{Xu}^3)u_X^c), \quad (2.45)$$

and as a result the light  $up$ -quark, which we denote  $t$ , does not result in a mixing including  $\overline{u^c}_X$ . This is important, since  $\overline{u^c}_X$  in  $U_L$  couples to  $Z$  differently, only through the electromagnetic contribution to the neutral current and not via the  $J_3^\mu$  contribution. Consequently, FCNCs will be naturally suppressed and the CKM matrix should have only small deviations from unitarity. Furthermore we note that the resulting matter states couple to the Higgses and  $Z$  as in the MSSM.

## 2.3 Consequences of $U(1)_X$ breaking

Introducing the  $\mathbf{16}_X$  and  $\overline{\mathbf{16}}_X$  will play a crucial role in breaking the extra  $U(1)$  subgroup of  $SO(10)$  and generating right-handed neutrino masses. We assume that a mechanism similar to the one proposed by Kolda-Martin [58] is in effect, such that the right-handed neutrino components acquire a non-trivial high-scale vev along the D-flat direction,  $\langle N_X \rangle \approx \langle \overline{N}_X \rangle = v_X$ <sup>6</sup>, which in turn breaks the rank. We will discuss in great details models incorporating this mechanism in chapter 3. Before doing so, however, we shall comment on generic implications of  $U(1)_X$  breaking and expectations for the scale  $v_X$ .

### 2.3.1 The see-saw mechanism

Presence of the  $\mathbf{16}_X$  and  $\overline{\mathbf{16}}_X$  with vevs in their right-handed neutrino components gives us the possibility of having a see-saw mechanism [59–63] for light physical neutrino masses. Such a mechanism is welcome since representations  $\mathbf{45}$  and larger are absent in  $M$  theory [30, 48, 49]. Depending on the details of symmetry breaking mechanism and neutrino masses this mechanism might be of huge relevance. For example, if we start with an  $SO(10)$  invariant theory the Yukawas are unified for each family leading to at least one very heavy Dirac neutrino mass,  $m_\nu^D \sim \mathcal{O}(175 \text{ GeV})$ . However, if the right-handed conjugated neutrino has a heavy Majorana mass, then the physical left-handed neutrino mass will be small through a type I see-saw mechanism. In order to accomplish this, one has to allow the following terms in the superpotential

$$W \supset y_\nu H_u L N + M N N, \quad (2.46)$$

where  $y_\nu$  are the neutrino Yukawas,  $L$  the matter lepton doublets,  $N$  the right-handed conjugated neutrino, and  $M$  its Majorana mass, which we take  $M \gg m_\nu^D = y_\nu \langle H_u \rangle$ . With the above ingredients, a mostly left-handed light neutrino will have a physical mass

$$m_{phy}^\nu \simeq \frac{(m_\nu^D)^2}{M}. \quad (2.47)$$

---

<sup>6</sup>In fact, the D-flat condition reads  $\langle N_X \rangle^2 + \langle N \rangle^2 = \langle \overline{N}_X \rangle^2$ , but we will see that the VEV of  $N$  needs to be much smaller compare to  $\langle N_X \rangle$  and  $\langle \overline{N}_X \rangle$ .



One of the most appealing features of  $SO(10)$  models is that each family is in a  $\mathbf{16}$  which includes a natural candidate for the right-handed conjugated neutrino, the  $N$ . In order to employ a type I see-saw mechanism, we need to generate a Majorana mass term for the matter right-handed conjugated neutrino through the operator  $W \supset \overline{\mathbf{16}}_X \overline{\mathbf{16}}_X \mathbf{16}^m \mathbf{16}^m$ ,<sup>7</sup> that requires discrete charges to satisfy:

$$2\bar{x} + 2\kappa = 0 \pmod{N}. \quad (2.48)$$

The term in the superpotential leads to the operator

$$\frac{1}{m_{pl}} \overline{N}_X \overline{N}_X N N, \quad (2.49)$$

from which the Majorana mass for the (CP conjugated) right-handed neutrino field  $N$  emerges as

$$M \simeq \frac{\langle \overline{N}_X \rangle^2}{m_{pl}}. \quad (2.50)$$

The requirement of a realistic neutrino masses with this mechanism puts constraints on the value of the D-flat VEVs  $\langle N_X \rangle = \langle \overline{N}_X \rangle = v_X$ . Since the physical neutrino mass in type I see-saw mechanism is given by Eq. (2.47), assuming  $m_\nu^D \simeq \mathcal{O}(100 \text{ GeV})$ , and knowing that the upper bound on the neutrino masses  $m_\nu^{phy} \lesssim 0.1 \text{ eV}$ , one finds

$$M \gtrsim 10^{14} \text{ GeV} \Rightarrow v_X \gtrsim 10^{16} \text{ GeV}. \quad (2.51)$$

The above argument suggests that we need to break the  $U(1)_X$  close to the GUT scale. Since the Wilson line breaking mechanism is rank-preserving, we need to look for an alternative solution. One possibility is to break the gauge group with a non-zero Fayet-Iliopolous term generated with the Green-Schwarz mechanism [64–66] required for anomaly cancellation of an anomalous  $U(1)$ . In the context of M-Theory on  $G_2$ , however, there are no anomalous  $U(1)$  symmetries [67, 68] making this option not viable in your model. Instead, we use a modified Kolda-Martin mechanism [58] where higher order operators can break the symmetry. We discuss details of this mechanism in chapter 3 where we also study its implication on neutrino masses.

### 2.3.2 R-parity violation

Despite the existence of an effective matter parity symmetry inside  $SO(10)$ , the presence of a vector-like family will lead to R-parity violating [69] (RPV) interactions though the VEV of the  $N_X, \overline{N}_X$  components in the presence of moduli generated interactions. Furthermore,

---

<sup>7</sup>Given that in  $M$  Theory one does not account for irreps larger than the adjoint, this is the lowest order term that can generate a right-handed neutrino Majorana mass.

as we will see in detail in section 3.2, the scalar component of the matter conjugate right-handed neutrino,  $N$ , will also, although usually suppressed compared to  $v_X$ , acquire a VEV. These VEVs break  $SO(10)$  and will inevitably generate RPV. These interactions will mediate proton-decay, enable the lightest supersymmetric particle (LSP) to decay, and generate extra contributions to neutrino masses. In our framework RPV is generic, not only arising from allowed superpotential terms but as well from Kähler interactions involving moduli fields.

The interactions that break R-parity can either be trilinear or bilinear (B-RPV), and have different origins in our framework. The first contribution we can find comes from the tree-level renormalizable superpotential allowed by the discrete symmetry. Since we will encounter  $\langle N \rangle \neq 0$ , this means that even in a minimal setup, there will be an B-RPV contribution from matter Dirac mass coupling

$$W \supset y_\nu N H_u L , \quad (2.52)$$

reading

$$W \supset y_\nu \langle N \rangle H_u L . \quad (2.53)$$

Next we turn our attention to the Kähler potential, where interactions otherwise forbidden by the discrete symmetry might arise if there is a modulus with required charge. In such case, there is another contribution arising from the non-vanishing VEVs of  $N$ ,  $N_X$  and  $\bar{N}_X$  in conjugation with moduli VEVs. To see this, notice that in the Kähler potential there are generically interactions of the form

$$K \supset \frac{1}{m_{pl}} N H_u L + \frac{s}{m_{pl}^2} N_X H_u L + \frac{s}{m_{pl}^2} \bar{N}_X^\dagger H_u L + \text{h.c.} , \quad (2.54)$$

where while the first term exists in zeroth order in moduli (otherwise there would be no neutrino Dirac mass in the superpotential), the last two are otherwise forbidden by the discrete symmetry, and  $s$  denotes a generic modulus for each coupling. These terms will generate contributions to B-RPV as  $N$ ,  $N_X$  and  $\bar{N}_X$  acquire VEVs.

There are two types of contribution arising from the terms above. The first is generated through the Giudice-Masiero mechanism. As the moduli acquire VEVs, new holomorphic couplings will appear in the superpotential

$$W_{eff,1} = \frac{m_{3/2}}{m_{pl}} \langle N \rangle H_u L + 0.1 \frac{m_{3/2}}{m_{pl}} \langle N_X \rangle H_u L + 0.1 \frac{m_{3/2}}{m_{pl}} \langle \bar{N}_X^\dagger \rangle H_u L , \quad (2.55)$$

where  $m_{3/2} \simeq \mathcal{O}(10^4)$  GeV, and since  $s/m_{pl} \simeq 0.1$  in  $M$  Theory. Notice that in principle we would also have a term in the Kähler potential involving  $N$ , but this can be found to be subleading in comparison to the term arising from the Dirac mass, Eq. (2.53).

The second contribution arises if the F-terms of the fields  $N_X$ ,  $N$ ,  $\bar{N}_X$  are non-vanishing.

In this case, we expect the appearance of the contributions

$$W_{eff,2} = \frac{\langle F_N \rangle}{m_{pl}} H_u L + 0.1 \frac{\langle F_{N_X} \rangle}{m_{pl}} H_u L + 0.1 \frac{\langle F_{\bar{N}_X^\dagger} \rangle}{m_{pl}} H_u L, \quad (2.56)$$

and its magnitude will depend on how much F-breaking provoked by our symmetry breaking mechanism. Here we are considering that the case where  $\bar{N}_X^\dagger H_u L$  cannot exist in the Kähler potential in zeroth order in a modulus field.

Putting all together, the B-RPV interactions account to the B-RPV parameter

$$W \supset \kappa_m H_u L \quad (2.57)$$

with

$$\kappa_m = \left( y_\nu + \frac{m_{3/2}}{m_{pl}} \right) \langle N \rangle + 0.1 \frac{m_{3/2}}{m_{pl}} \langle N_X \rangle + 0.1 \frac{m_{3/2}}{m_{pl}} \langle \bar{N}_X^\dagger \rangle + \frac{\langle F_N \rangle}{m_{pl}} + 0.1 \frac{\langle F_{N_X} \rangle}{m_{pl}} + 0.1 \frac{\langle F_{\bar{N}_X^\dagger} \rangle}{m_{pl}}, \quad (2.58)$$

and the relative strength of each contribution is model detail dependent, namely on neutrino Yukawa textures, symmetry breaking details, and F-flatness deviation.

In a similar manner, trilinear RPV couplings will be generated when  $N$ ,  $N_X$  and  $\bar{N}_X$  acquire VEVs. In order to systematically study this, we notice that the trilinear RPV couplings come from the term

$$\mathbf{16} \mathbf{16} \mathbf{16} \mathbf{16}, \mathbf{16}_X \mathbf{16} \mathbf{16} \mathbf{16}, \overline{\mathbf{16}}_X^\dagger \mathbf{16} \mathbf{16} \mathbf{16} \quad (2.59)$$

as the scalar component of  $N_X$ ,  $N$  acquires non-vanishing VEVs. Notice that the last term lives in the Kähler potential. These are made forbidden at tree-level using the discrete symmetry of the compactified space. However, just like the  $\mu$  terms and the B-RPV terms shown above, these terms will in general be present in the Kähler potential and will effectively be generated as the moduli acquire VEVs. This happens again through the Giudice-Masiero mechanism and we will find

$$\mathcal{O} \left( \frac{m_{3/2}}{m_{pl}^2} (\langle N \rangle + \langle N_X \rangle + \langle \bar{N}_X^\dagger \rangle) \right) \{ L L e^c, L Q d^c, u^c d^c d^c \}, \quad (2.60)$$

where  $m_{3/2}/m_{pl} \simeq \mathcal{O}(10^{-14})$ . The apparent suppression of trilinear RPV is understood as these terms can only be generated by non-renormalizable terms in an  $SO(10)$  context.

Similarly to the B-RPV case, there will be further contributions if the F-terms of  $N_X$ ,  $N$ ,  $\bar{N}_X$  are non-vanishing. Namely we find

$$\mathcal{O} \left( \frac{\langle F_N \rangle + \langle F_{N_X} \rangle + \langle F_{\bar{N}_X^\dagger} \rangle}{m_{pl}^2} \right) \{ L L e^c, L Q d^c, u^c d^c d^c \}, \quad (2.61)$$

and again we expect these to be sub-leading even if the F-terms are not vanishing.

We see then that the values of all RPV couplings are strictly related to the details of the breaking mechanism employed to break the extra  $U(1)_X$ , leading to further constraints. In particular, the magnitude of the B-RPV term, Eq. (2.57), is constrained as it contributes to the physical neutrino masses [69–71]. The constraint is  $\kappa_m \lesssim \mathcal{O}(1 \text{ GeV})$ , which, assuming the leading contribution to  $\kappa_m \approx \lambda v_X$ , leads to the upper bound  $v_X \lesssim 10^{15} \text{ GeV}$ . This is in contradiction with the see-saw requirement  $v_X \sim 10^{16} \text{ GeV}$  assumed in the estimates, section 2.3.1. However, there is a natural way within this framework to further suppress the bilinear RPV terms. This happens when the charges of the moduli fields under the discrete symmetry are such that the leading order terms in  $K$ , which are linear in the moduli i.e.  $\frac{s}{m_{pl}^2} v_X L H_u$ , are *forbidden* by the symmetry, with the leading term arising at higher order in the moduli. If the leading term arises at quadratic order or higher, (e.g.  $K \sim \frac{s^2}{m_{pl}^3} v_X L H_u$ ) then the suppression will be sufficient. Furthermore, some moduli may have smaller vevs than others in a detailed model, leading to additional suppression. The complete picture of neutrino masses, including B-RPV operators, will be discussed in section 3.3.

Under the assumption that  $\kappa_m \ll \mu$ , performing a small rotation, of  $\mathcal{O}(\kappa_m/\mu)$ , in  $(H_d, L)$  space, the B-RPV term, Eq. (2.57), can be absorbed by  $\mu H_d H_u$ . As a consequence, the trilinear RPV terms will be enhanced by the Yukawa couplings  $y_e H_d L e^c$ , etc., leading to

$$W \supset y_e \frac{\kappa_m}{\mu} L L e^c + y_d \frac{\kappa_m}{\mu} L Q d^c + \lambda \frac{v_X}{m_{pl}} u^c d^c d^c, \quad (2.62)$$

and we have dropped the  $\mathcal{O}(1/m_{pl})$  contributions to the first two terms since now the Yukawa rotated contributions are much larger. Also, we kept the last term with the parameterisation  $v$  describing all contributions. These will be very small, for example in the case the VEVs are high-scale,  $\langle N_X \rangle \simeq 10^{16} \text{ GeV}$ , the trilinear RPV coupling strength is of  $\mathcal{O}(10^{-17})$ . A direct consequence of this result is that proton decay will be within experimental limits, even when the  $\Delta L = 1$  terms are enhanced.

While the proton is relatively stable, the enhanced terms will provide a decay channel for the LSP, which is now unstable. In the limit that we can take the final states to be massless, and considering that the LSP is a neutralino mainly composed of neutral gauginos, the LSP lifetime through the decay  $\tilde{\chi}^0 \rightarrow d^c Q L$  can be estimated from a tree-level diagram involving a virtual  $\tilde{d}^c$  with mass  $m_0$ <sup>8</sup>,

$$\tau_{LSP} \simeq (3.9 \times 10^{-15}) \left( \frac{\mu}{g_w y_d \kappa_m} \right)^2 \left( \frac{m_0}{10 \text{ TeV}} \right)^4 \left( \frac{100 \text{ GeV}}{m_{LSP}} \right)^5 \text{ sec}, \quad (2.63)$$

where  $g_w$  is a weak gauge coupling. The LSP lifetime is bounded to be either  $\tau_{LSP} \lesssim 1 \text{ sec}$  or  $\tau_{LSP} \gtrsim 10^{25} \text{ sec}$  [70, 72], from Big Bang Nucleosynthesis (BBN) and indirect Dark Matter

<sup>8</sup>See, for example, the diagrams in [18].

(DM) experiments, respectively. If we take  $m_{LSP} \simeq 100$  GeV,  $m_0 \simeq 10$  TeV,  $y_d = y_b \simeq 10^{-2}$ ,  $g_w \simeq 0.1$ , we find that  $\kappa_m$  is constrained to be either

$$\kappa_m \gtrsim 6 \times 10^{-2} \text{ GeV} \quad (2.64)$$

$$\text{or } \kappa_m \lesssim 2 \times 10^{-14} \text{ GeV}, \quad (2.65)$$

for a short- and long-lived LSP, respectively<sup>9</sup>. This in turn constrains the magnitude of VEVs of  $N$ ,  $N_X$  and  $\bar{N}_X$  following Eq. (2.58).

We can use the above result to infer some parametric dependence on the scale of the  $U(1)_X$  breaking. If we have the leading contribution to the B-RPV coupling to be  $\kappa_m \simeq \langle N_X \rangle \lambda$ , then from Eq. (2.64),  $\langle N_X \rangle \gtrsim 10^{13}$  GeV. In this case, the LSP is too short lived to be a good DM candidate, but decays quickly enough to not spoil BBN predictions. On the other-hand, a low-scale VEV is bound to be  $\langle N_X \rangle \lesssim 1$  GeV in order to allow for a long-lived LSP. This would imply the abelian gauge boson associated with extra  $U(1)_X$  to be light,  $m_{Z'} < \mathcal{O}(1)$  GeV. This last scenario is completely excluded from experimental searches.

The lack of a good DM candidate in the visible sector indicates us that DM is realised elsewhere.  $M$  theory usually provides axion dark matter candidates [36, 73]. It has also been recently suggested that, in the context of String/ $M$  Theory, the generic occurrence of hidden sectors could account for the required DM mechanics [74, 75].

## 2.4 Effective light families

So far we have considered a relatively simple SUSY  $SO(10)$  model that includes three pairs of matter irreps  $\mathbf{16}^m$ , single  $\mathbf{10}^w$  on a Wilson line containing Higgs multiplets, and a vector like pair  $\mathbf{16}_X, \bar{\mathbf{16}}_X$ . We have also discussed several conditions that need to be imposed on discrete charges in order to get satisfactory phenomenological results. These are Table 2.3, Eq. (2.42), Eq. (2.48) as well as suppression of the RPV operators and cross-terms between the visible matter,  $\mathbf{16}_X$  and  $\bar{\mathbf{16}}_X$  necessary for Eq. (2.43). We emphasize that one can explicitly solve for all of the conditions. A solution example is given by

$$(N, \omega, \alpha, \beta, \kappa, x, \gamma, \delta, \bar{x}) = (16, 4, 0, 1, 6, 2, 1, 13, 2). \quad (2.66)$$

which is also anomaly free, as can be checked by explicit calculations [76].

It is well known, however, that for such simple  $SO(10)$  models where each family is unified into a simple irrep with universal soft masses the electroweak symmetry is difficult to break [77–82]. Since the two Higgs soft masses are unified at GUT scale and have similar beta function due to Yukawa unification, either both masses are positive at electroweak scale and

---

<sup>9</sup>In the above estimate we used the fact that the decay involving the bottom Yukawa is the largest contribution to the decay width.

symmetry is not broken or both masses are negative and the potential becomes unbounded from below. Another aspect of the Yukawa unification problem lies in the fact that low energy spectrum of quarks and leptons requires some degree of tuning in parameter space when their RG runnings are considered. A customary solution to these problems is the use of higher dimensional representations [83], which are not present in our framework.

The EWSB and Yukawa textures issues are naturally solved if each family is not contained in one single complete  $\mathbf{16}$ , but is instead formed of states from different Ultra Violet (UV) complete  $\mathbf{16}$ s. In order to implement this in our framework, first we assume the existence of multiple  $\mathbf{16}$  with independent and different Wilson line phases, alongside the existence of multiple  $\overline{\mathbf{16}}$ . Second, we employ Witten's proposal to turn on some vector-like masses such that three effective light  $\mathbf{16}$  survive. Since in  $M$  Theory the strength of the Yukawa couplings is given by membrane instantons, and are therefore related to distances between the singularities supporting the respective superfields, by constructing effective families from different UV  $\mathbf{16}$ s one can obtain different Yukawa couplings within each family.

Such solution can be achieved if one considers  $M$  complete  $\overline{\mathbf{16}}_j$  and  $M + 3$  complete  $\mathbf{16}_i$  UV irreps. Allowing for masses between different states of these UV irreps to appear, one has schematically the mass terms in the superpotential

$$\mathbf{16}_i \mu_{ij} \overline{\mathbf{16}}_j, \quad (2.67)$$

but since  $i = 1, \dots, M$  while  $j = 1, \dots, M + 3$  the mass matrix  $\mu_{ji}$  can only have at most rank  $M$  and hence there will be three linear combinations composing three  $\mathbf{16}$  that will remain massless. If these masses are truly  $SO(10)$  invariant, i.e.

$$\mathbf{16}_i \mu_{ij} \overline{\mathbf{16}}_j = \mu_{ij} (Q_i \overline{Q}_j + L_i \overline{L}_j + \dots), \quad (2.68)$$

each effective light family will be  $SO(10)$  invariant. Consequently each family will retain unified Yukawa textures, and so this does not solve our problem of splitting the Yukawa couplings within each family.

However, Witten's proposal endows our framework with a GUT breaking discrete symmetry which can be employed to ensure that the superpotential mass matrices between the UV states

$$\mu_{ij}^Q Q_i \overline{Q}_j + \mu_{ij}^L L_i \overline{L}_j + \dots, \quad (2.69)$$

are not the same, leading to different diagonalisations of  $Q$ ,  $L$ , etc which in turn break the Yukawa  $SO(10)$  invariance. In order to accomplish that, take for example that the  $\mathbf{16}_i$  absorb distinct and independent Wilson line phases, while  $\overline{\mathbf{16}}_j$  do not, i.e. the UV irreps will

transform under the discrete symmetry as

$$\mathbf{16}_i \rightarrow \eta^{m_i} \left( \eta^{-3\gamma_i} L_i \oplus \eta^{3\gamma_i+\delta_i} e_i^c \oplus \eta^{3\gamma_i-\delta_i} N_i \oplus \eta^{-\gamma_i-\delta_i} u_i^c \oplus \eta^{-\gamma_i+\delta_i} d_i^c \oplus \eta^{\gamma_i} Q_i \right) \quad (2.70)$$

$$\overline{\mathbf{16}}_j \rightarrow \eta^{\overline{m}_j} \overline{\mathbf{16}}_j, \quad (2.71)$$

and look for solutions for the discrete charges where different states have different mass matrices. Since explicit examples can only be given by solving extensive modular linear systems, which are computationally prohibitive, a fully working example with three light-families is not provided.

## 2.5 Conclusion

In this chapter we have discussed the origin of an  $SO(10)$  SUSY GUT from  $M$  theory on a  $G_2$  manifold. We started with a review of  $M$  theory results behind  $SU(5)$  SUSY GUT models, dubbed  $G_2$ MSSM. Extending those results into the  $SO(10)$  case we were naturally led to a novel solution of the doublet-triplet splitting problem involving an extra  $\mathbf{16}_X + \overline{\mathbf{16}}_X$  vector-like pair where discrete symmetries of the extra dimensions were used to prevent proton decay by suppressing the Yukawa couplings of colour triplets. Such models maintain gauge coupling unification but with a larger GUT coupling than predicted by the MSSM. Extra light states with the quantum numbers of a  $\mathbf{16}_X + \overline{\mathbf{16}}_X$  vector-like pair that might be accessible in future LHC searches provide a prominent prediction of this approach. We argue that these extra multiplets, also required to break the additional  $U(1)_X$  gauge symmetry, inevitably lead to R-parity violating operators. Even though the moduli potential generically breaks the discrete symmetry, we have seen that one naturally satisfies the constraints from the proton lifetime and decays affecting BBN. We also have found a consistent scenario for neutrino masses arising from the high scale see-saw mechanism, with sufficiently suppressed RPV contributions. We argue, however, that this simple scenario, having soft masses and Yukawas unified among each family, fails short in explaining the nature of EWSB and low-energy Yukawa textures. Instead, a more complicated models might be manufactured in the context of M Theory with low-energy matter  $\mathbf{16}$ s being effective irreps composed of different UV complete  $\mathbf{16}$ s. This gives us more leverage in accommodating observable phenomena. including all mixing term potentially contributing to the result. In the following chapter we are going to embark on scrupulous studies of neutrino mass generation including all mixing term arising from the broken  $U(1)_X$ . For these to be meaningful we also present there the details of the  $U_X$  breaking mechanism.

## Chapter 3

# Neutrino mass from M theory SO(10)

### 3.1 Introduction and Motivation

In this chapter we address the problem of  $U(1)_X$  breaking and neutrino masses arising from the  $SO(10)$  GUT, following the construction in chapter 2, although our approach to solving these problems may be more general than the specific example studied. To break the  $U(1)_X$  gauge symmetry, we employ a (generalised) Kolda-Martin mechanism [58], where higher order operators can break the symmetry, inducing vacuum expectation values (VEVs) in the scalar right-handed neutrino components of both the matter  $\mathbf{16}$  and the extra  $\mathbf{16}_X$ , as well as their conjugate partners. The subsequent induced R-parity violation provides additional sources of neutrino mass, in addition to that arising from the seesaw mechanism discussed in section 2.3.1. The resulting  $11 \times 11$  neutrino mass matrix is analysed for one neutrino family (nominally the third family) and it is shown how a phenomenologically acceptable neutrino mass can emerge. We defer any discussion of flavour mixing to a possible future study of flavour from  $M$  theory. Here we only show that symmetry breaking and viable neutrino masses can arise within the framework of  $M$  theory  $SO(10)$ , which is a highly non-trivial result, given the constrained nature of  $M$  theory constructions.

It is worth remarking that there are other alternative ways that have been proposed to study neutrino masses in string theory, which are complementary to the approach followed here. For example, it is possible to obtain large Majorana mass terms from instanton effects [21, 84–87], large volume compactification [88], or orbifold compactifications of the heterotic string [87]. However the origin of Majorana mass terms in  $SO(10)$  has been non-trivial to realise from the string theory point of view. In GUTs all matter fields are unified in  $\mathbf{16}$  multiplets whereas Higgs fields and triplet scalars are unified in  $\mathbf{10}$ . Since string theory does not predict light chiral multiplets in higher representations than the adjoint, the traditional renormalisable terms involving  $\mathbf{126}, \overline{\mathbf{126}}, \mathbf{210}$ , e.g.,  $W \sim \mathbf{126} \mathbf{16} \mathbf{16}$ , are not possible. The



dominant higher order operators are quartic ones such as  $W = \overline{\mathbf{16}} \overline{\mathbf{16}} \mathbf{16} \mathbf{16}$ . Assuming that the supersymmetric partner of the right handed neutrino singlet gets a VEV, the Majorana mass is given by  $M \sim \frac{\langle \overline{N} \rangle^2}{M_{PL}}$ . However, as seen in section 2.3 previously, the required values of neutrino masses imply  $M > 10^{14}$  GeV, which gives  $\langle \overline{N} \rangle \sim \sqrt{M m_{pl}} \sim 10^{16}$  GeV. This leads to the requirement of high scale breaking that we need to realise here. Before doing so, however, we want to acknowledge that the implementation of the seesaw mechanism in other corners of string compactification has also been discussed previously [89–91].

The layout of the remainder of the chapter is as follows. In section 3.2, the mechanism for  $U(1)_X$  breaking will be given. The neutrino mass matrix will be analysed in section 3.3, and the numerical results presented in section 3.4. Finally we conclude in section 3.5.

### 3.2 $U(1)_X$ Breaking scenarios and mechanisms

As has been shown in section 2.3, BBN constraints on the LSP lifetime as well as the requirement for the see-saw mechanism to sufficiently suppress neutrino masses require a breaking mechanism for the extra  $U(1)_X$  in which the breaking VEV is stabilised at high values, more or less close to the GUT scale. In order to do so, we will look into the D-flat direction of the potential that breaks the extra  $U(1)_X$ . It was shown [58, 92] that in the D-flat direction, non-renormalisable operators can provide such scenario. In its simplest inception, the Kolda-Martin mechanism [58] relies on a vector-like pair which lowest order term allowed in the superpotential is non-renormalizable

$$W = \frac{c}{m_{pl}} (\Phi \bar{\Phi})^2 \quad (3.1)$$

and alongside the soft-term Lagrangian

$$-\mathcal{L}_{soft} = m_{\Phi}^2 |\Phi|^2 + m_{\bar{\Phi}}^2 |\bar{\Phi}|^2, \quad (3.2)$$

it is immediate to find that along the D-flat direction the potential has a non-trivial minimum which fixes the VEVs at a high scale

$$\langle \Phi \rangle^2 = \sqrt{-\frac{(m_{\Phi}^2 + m_{\bar{\Phi}}^2) m_{pl}^2}{12c^2}}, \quad (3.3)$$

where if we take  $m_{\Phi} \simeq m_{\bar{\Phi}} \simeq m_{3/2} \simeq 10^4$  GeV, as expected from M-Theory on  $G_2$  where gravity mediates SUSY breaking [22], the VEVs are estimated at  $\langle \Phi \rangle \simeq 10^{11}$  GeV.

There are some caveats to this mechanism as presented above. First, there is significant F-breaking as  $\langle F \rangle \simeq \mathcal{O}(10^{15})$  GeV. While this is not a problem if the vector-like family does not share gauge interactions with ordinary matter, in our case non-vanishing F-terms will originate undesirable interactions, cf. section 2.3.2. We shall therefore focus on F-flat

solutions.

Second, the mechanism is not complete in the absence of higher order corrections from the SUGRA [37], beyond the soft terms, that at the high VEV scale compete with the non-renormalisable terms in the scalar potential arising from the superpotential. One has to include

$$-\mathcal{L} \supset C \frac{1}{m_{pl}} \Phi^2 \bar{\Phi}^2 + \text{h.c.}, \quad (3.4)$$

with the estimated value of  $C \simeq \mathcal{O}(m_{3/2})$  at the GUT scale. Although this term, of mass dimension four, is technically non-soft [23], it is not relevant for low-energy,  $\mathcal{O}(\text{TeV})$  global SUSY, in which the limit  $m_{pl} \rightarrow \infty$  is valid. Because of that, as well as the common origin with the regular soft breaking terms we will write this term in the soft-lagrangian part  $\mathcal{L}_{soft}$ .

Finally the model presented differs from ours as  $\mu$ -terms are generically generated by moduli VEVs even if they are disallowed by the discrete symmetry of the compactified space.

In order to proceed, we turn to a more complete version of the mechanism. To do so, we include the  $\mu$ -term

$$W = \mu \Phi \bar{\Phi} + \frac{c}{m_{pl}} (\Phi \bar{\Phi})^2 \quad (3.5)$$

and the more complete soft Lagrangian,

$$-\mathcal{L}_{soft} = m_{\Phi}^2 |\Phi|^2 + m_{\bar{\Phi}}^2 |\bar{\Phi}|^2 - (B\mu \Phi \bar{\Phi} + \text{h.c.}) + \frac{C}{m_{pl}} \Phi^2 \bar{\Phi}^2 + \text{h.c.} \quad (3.6)$$

Due to the presence of the  $\mu$ -term, the F-term

$$\langle F_{\Phi} \rangle = \mu \bar{\Phi} + \frac{2c}{m_{pl}} \Phi \bar{\Phi}^2 \quad (3.7)$$

can be set to zero for two different field configurations

$$\langle F_{\Phi} \rangle = 0 \Rightarrow \begin{cases} \langle \bar{\Phi} \rangle = 0 \\ \langle \Phi \bar{\Phi} \rangle = -\frac{\mu m_{pl}}{2c} \end{cases} \quad (3.8)$$

and the non-trivial VEV can be estimated. Taking  $\mu \simeq \mathcal{O}(10^3)$  GeV, this leads to  $\langle \Phi \rangle = 10^{10.5}$  GeV. This looks very similar to the original Kolda-Martin case, with the exception being that the F-term can vanish, and the parametric dependence on the VEV is now on  $\mu$  instead of a soft-mass. In general there might be a non-SUSY preserving vacuum elsewhere in field space, but we will work under the assumption that the SUSY vacua discovered with this approach are at least stable enough to host phenomenologically viable models.

We wish to assess if we can minimise the potential in this SUSY-preserving field configuration. For that, we need to check if the above field configuration will also extremise the

soft-term Lagrangian. To see this we take

$$-\partial_{\Phi}\mathcal{L}_{soft} = m_{\Phi}^2\Phi^* - B\mu\bar{\Phi} + \frac{2C}{m_{pl}}\Phi\bar{\Phi}^2 = 0 \quad (3.9)$$

and, in the limit the VEVs are real, we find a trivial and a non-trivial solutions

$$-\partial_{\Phi}\mathcal{L}_{soft} = 0 \Rightarrow \begin{cases} \langle\Phi\rangle = 0 \\ \langle\Phi\rangle^2 = -\frac{(m_{\Phi}^2 - B\mu)m_{pl}}{2C} \end{cases} \quad (3.10)$$

and the second one seems very similar to the non-trivial configuration derived through the F-term. In fact, both conditions can be met. To see this, we reparameterise the soft-terms by factoring out their dimensionful dependence on  $m_{3/2}$

$$B\mu = m_{3/2}\mu b \quad (3.11)$$

$$C = m_{3/2}\tilde{c} \quad (3.12)$$

$$m_{\Phi} = m_{3/2}a, \quad (3.13)$$

where  $a, b, \tilde{c}$  are dimensionless, and from SUGRA [37] formulae they are  $\mathcal{O}(1)$  at the GUT scale. Of course they will evolve with the scale through RGE evolution, so they need not to be always of the same order. The condition that both the F-flatness and soft-term stabilisation are jointly achieved boils down to be a relation between parameters

$$\frac{\tilde{c}}{c} = \frac{2am_{\Phi} - \mu b}{\mu}, \quad (3.14)$$

which is generically valid.

In order for the above non-trivial VEV be a minimum, we need the trivial VEV solution to account for a maximum. This is to say that the mass matrix for the system  $(\Phi, \bar{\Phi}^*)$  evaluated at the origin has a negative eigen-value. In our case this accounts for allowing its determinant to be negative

$$(|\mu|^2 + m_{\Phi}^2)(|\mu|^2 + m_{\bar{\Phi}}^2) - B\mu^2 < 0. \quad (3.15)$$

We notice as well that the above discussion can be immediately extended for the case that the lowest order non-renormalisable term allowed by the discrete symmetry

$$W \supset \frac{c}{m_{pl}^{2n-3}}(\Phi\bar{\Phi})^n \Rightarrow \Phi \simeq (\mu m_{pl}^{2n-3})^{\frac{1}{2n-2}} \quad (3.16)$$

happens for  $n \geq 2$ , and not only for  $n = 2$ . Even so, the presented implementation of the Kolda-Martin mechanism only accounts for a vector-like pair of superfields, while in our case the system breaking the extra  $U(1)_X$  is composed of  $N, N_X, \bar{N}_X$  states.

Therefore, we want to find similar solutions starting with the superpotential

$$W = \mu_{Xm}^N N \bar{N}_X + \mu_X^N N_X \bar{N}_X + \frac{c_{2,2}}{m_{pl}} (N \bar{N}_X)^2 + \frac{c_{n,k}}{m_{pl}^{2n-3}} (N_X \bar{N}_X)^{n-k} (N \bar{N}_X)^k \quad (3.17)$$

where  $n \geq 2$  and  $k < n$ . The third term generates a Majorana mass for the matter right-handed conjugated neutrino,  $N$ . The full soft-term Lagrangian for this theory is

$$-\mathcal{L}_{soft} = m_N^2 |N|^2 + m_{N_X}^2 |N_X|^2 + m_{\bar{N}_X}^2 |\bar{N}_X|^2 - (B \mu_{Xm}^N N \bar{N}_X + \text{h.c.}) - (B \mu_X^N N_X \bar{N}_X + \text{h.c.}) \\ + \left( \frac{C_{2,2}}{m_{pl}} (N \bar{N}_X)^2 + \text{h.c.} \right) + \left( \frac{C_{n,k}}{m_{pl}^{2n-3}} (N_X \bar{N}_X)^{n-k} (N \bar{N}_X)^k + \text{h.c.} \right) \quad (3.18)$$

where again  $C_{i,j}$  coefficients are  $\mathcal{O}(m_{3/2})$  at the GUT scale.

The F-terms now read

$$F_N = \mu_{Xm}^N \bar{N}_X + \frac{2c_{2,2}}{m_{pl}} N \bar{N}_X^2 + \frac{k c_{n,k}}{m_{pl}^{2n-3}} N_X^{n-k} N^{k-1} \bar{N}_X^n \quad (3.19)$$

$$F_{N_X} = \mu_X^N \bar{N}_X + \frac{(n-k) c_{n,k}}{m_{pl}^{2n-3}} N_X^{n-k-1} N^k \bar{N}_X^n \quad (3.20)$$

$$F_{\bar{N}_X} = \mu_{Xm}^N N + \mu_X^N N_X + \frac{2c_{2,2}}{m_{pl}} N^2 \bar{N}_X + \frac{n c_{n,k}}{m_{pl}^{2n-3}} N_X^{n-k} N^k \bar{N}_X^{n-1} \quad (3.21)$$

which have a significantly more challenging look than the simplified version presented above. Nonetheless, the same conclusions hold. The above F-terms become more tractable for the  $k = 0$  and  $k = n - 1$  cases. In these cases it is possible to get algebraic expressions for the VEVs estimates. For the  $k = 0$ , the F-flatness conditions alone give us

$$\langle N \bar{N}_X \rangle = -\frac{\mu_{Xm}^N m_{pl}}{2c_{2,2}} \quad (3.22)$$

$$\langle N_X \bar{N}_X \rangle = \left( -\frac{\mu_X^N m_{pl}^{2n-3}}{n c_{n,o}} \right)^{\frac{1}{n-1}} \quad (3.23)$$

while for  $k = n - 1$ , analogous expressions can be obtained

$$|\langle N \bar{N}_X \rangle| \simeq (\mu_{Xm}^N m_{pl}^{2n-3})^{\frac{1}{n-1}} \quad (3.24)$$

$$|\langle N_X \bar{N}_X \rangle| \simeq ((\mu_X^N)^{3-n} m_{pl}^{3n-5})^{\frac{1}{n-1}} \quad (3.25)$$

where the approximations mean we dropped  $\mathcal{O}(1)$  parameters and took all  $\mu$ -terms to be of the same order, which is expected.

$n$	$k$	$\langle N \rangle$ (GeV)	$\langle N_X \rangle$ (GeV)	$\langle \bar{N}_X \rangle$ (GeV)
2	0	$10^{10.5}$	$10^{10.5}$	$10^{10.5}$
	1	$10^{10.5}$	$10^{10.5}$	$10^{10.5}$
3	0	$10^{6.5}$	$10^{14.25}$	$10^{14.25}$
	1	$10^{10.2}$	$10^{15.5}$	$10^{15.5}$
	2	$10^{10.5}$	$10^{18}$	$10^{18}$
4	0	$10^{5.5}$	$10^{15.5}$	$10^{15.5}$
	1	$10^{10.1}$	$10^{16.5}$	$10^{16.5}$
	2	$10^{10.3}$	$10^{18}$	$10^{18}$
	3	$10^{10.5}$	$10^{20.5}$	$10^{20.5}$

Table 3.1: Estimate of the magnitude of the VEVs in SUSY vacua for different implementations of the modified Kolda-Martin mechanism. In all cases the scalar component of the (CP conjugated) right-handed neutrino field  $N$  develops a VEV, breaking R-parity, in addition to the  $N_X$  and  $\bar{N}_X$  VEVs.

In both cases, the ratio between the  $N_X$  and  $N$  VEV is follows the same dependency on  $n$

$$\left| \frac{\langle N_X \rangle}{\langle N \rangle} \right| \simeq \left( \frac{m_{pl}}{\mu} \right)^{\frac{n-2}{n-1}} \simeq \begin{cases} 1 & n = 2 \\ 10^{7.5} & n = 3 \\ 10^{10} & n = 4 \end{cases} \quad (3.26)$$

where we  $\mu$  is an  $\mathcal{O}(\mu_X^N, \mu_{Xm}^N)$  parameter. This result shows that there is a hierarchy between  $N_X$  and  $N$  VEVs, which is very desirable as  $N$  VEVs can generate large B-RPV couplings, cf. section 2.3.2.

Just like before, we use the D-flat direction

$$\left| \frac{\langle \bar{N}_X \rangle}{\langle N_X \rangle} \right|^2 = \left| \frac{\langle N \rangle}{\langle N_X \rangle} \right|^2 + 1, \quad (3.27)$$

which sets the magnitude of the three VEVs. The results for  $k = 0$  and  $k = n - 1$  can be immediately estimated algebraically, in contrast to the other cases. The full result of SUSY preserving configurations can be seen in Table 3.1. It is important to note that for  $n = 4$ , the only viable scenario is for  $k = 0$ , while for  $n = 3$  the  $k = 2$  is not viable as there are super-GUT VEVs. In the end we are only interested in the sensible cases, where the VEVs are below the GUT scale and therefore the mechanism is self-consistent.

The SUSY configurations above are expected to stabilise the soft-terms Lagrangian just before. The stabilisation conditions are

$$\begin{aligned}
m_{\Phi_1}^2 \Phi_1^* - B\mu_1 \bar{\Phi} + \frac{2C_{2,2}}{m_{pl}} \Phi_1 \bar{\Phi}^2 &= 0 \\
m_{\Phi_2}^2 \Phi_2^* - B\mu_2 \bar{\Phi} + \frac{nC_{n,0}}{m_{pl}^{2n-3}} \Phi_2^{n-1} \bar{\Phi}^n &= 0 \\
m_{\bar{\Phi}}^2 \bar{\Phi}^* - B\mu_1 \Phi_1 - B\mu_2 \Phi_2 + \frac{2C_{2,2}}{m_{pl}} \Phi_1^2 \bar{\Phi} + \frac{nC_{n,0}}{m_{pl}^{2n-3}} \Phi_2^n \bar{\Phi}^{n-1} &= 0
\end{aligned}$$

and reparameterising the dimensionful soft-terms just as before, the above conditions will resemble the F-flatness conditions in form and so they will be jointly respected taken the parameters of the theory respect relations between them.

As before, the condition that the above extrema are minima is that the potential has a runaway direction around the origin. This is the same to say that, when close to the origin the potential takes the form

$$V \simeq \mathbf{N}^* \cdot M_N \cdot \mathbf{N} \quad (3.28)$$

with  $\mathbf{N} = (N, N_X, \bar{N}_X^*)$ , such that  $M_N$  has at least one negative eigenvalue to account for a run-away behaviour at the trivial extremum. Boundness of the potential in the D-flat direction is achieved by noticing that – for each field direction – at least a quadratic term from the non-renormalisable interactions becomes the leading contribution, while keeping a run-away behaviour at the origin.

### 3.3 Neutrino-neutralino mass matrix

The different breaking scenarios discussed in the previous section rely on different superpotential terms, which are either present or suppressed depending on the discrete symmetry of the compactified  $G_2$  space. Furthermore, the generic presence of a matter field VEV,  $\langle N \rangle$ , will generate B-RPV terms, as described in section 2.3.2. In turn, these provide a new source of neutrino masses which has to be taken into account.

To be more precise we enumerate all the interactions that contribute to neutrino masses. First, we let the matter neutrino to have a Yukawa coupling at tree-level, of the form

$$W_{tree} \supset y_\nu N L H_u. \quad (3.29)$$

Next we have to consider the non-renormalizable terms that employ the KM mechanism for each scenario. Alongside this, we also keep a term that can generate a Majorana mass for the matter right-handed conjugated neutrino,  $N$ . On top of these, we include a set of non-renormalizable terms involving the Higgses or  $L$ -type fields, in first order of  $1/m_{pl}$ . The

non-renormalizable terms that will affect the neutral fermion mass matrix are then

$$\begin{aligned}
W_{non.ren.} \supset & \frac{c_{2,2}}{m_{pl}} (NN) (\bar{N}_X \bar{N}_X) + \frac{c_{n,k}}{m_{pl}^{2n-3}} (N_X \bar{N}_X)^{n-k} (N \bar{N}_X)^k \\
& + \frac{1}{m_{pl}} (b_1 H_d H_u L \bar{L}_X + b_2 L L \bar{L}_X \bar{L}_X + b_3 H_d H_u L_X \bar{L}_X + b_4 L L_X \bar{L}_X \bar{L}_X \\
& + b_5 L_X L_X \bar{L}_X \bar{L}_X + b_6 H_d H_u N \bar{N}_X + b_7 L \bar{L}_X N \bar{N}_X + b_8 L_X \bar{L}_X N \bar{N}_X \\
& + b_9 H_d H_u N_X \bar{N}_X + b_{10} L \bar{L}_X N_X \bar{N}_X + b_{11} L_X \bar{L}_X N_X \bar{N}_X). \tag{3.30}
\end{aligned}$$

The terms that are disallowed by discrete symmetry are generically re-generated as the moduli acquire VEVs. As such, the following Kähler potential terms will have an important contribution for neutrino masses

$$\begin{aligned}
K \supset & \frac{s}{m_{pl}} \bar{L}_X L_X + \frac{s}{m_{pl}} \bar{L}_X L + \frac{s}{m_{pl}} \bar{N}_X N_X + \frac{s}{m_{pl}} \bar{N}_X N + \frac{s}{m_{pl}} \bar{H}_u H_d \\
& + \frac{s}{m_{pl}^2} N_X L_X H_u + \frac{s}{m_{pl}^2} N L H_u + \frac{s}{m_{pl}^2} N_X L H_u + \frac{s}{m_{pl}^2} N L_X H_u + \frac{s}{m_{pl}^2} \bar{N}_X \bar{L}_X H_d, \tag{3.31}
\end{aligned}$$

where  $s$  denotes a generic modulus fields that counterbalances the discrete charge. This modulus field needs not to be the same for each coupling. As the moduli acquire VEVs as they are stabilised, the above terms will generate the effective superpotential

$$\begin{aligned}
W_{eff} \supset & \mu_{XX}^L \bar{L}_X L_X + \mu_{Xm}^L \bar{L}_X L + \mu_{XX}^N \bar{N}_X N_X + \mu_{Xm}^N \bar{N}_X N + \mu H_u H_d \\
& + \lambda_{\bar{X}\bar{X}} H_d \bar{L}_X \bar{N}_X + \lambda_\nu H_u L N + \lambda_{mX} H_u L N_X + \lambda_{Xm} H_u L_X N + \lambda_{XX} H_u L_X N_X \tag{3.32}
\end{aligned}$$

where the parameters can be estimated, analogously to the case in section 2.1.3, to lie inside the orders of magnitude

$$\mu \simeq m_{3/2} \frac{s}{m_{pl}} \simeq \mathcal{O}(10^3) \text{ GeV} \tag{3.33}$$

$$\lambda \simeq m_{3/2} \frac{s}{m_{pl}^2} \simeq \mathcal{O}(10^{-15}). \tag{3.34}$$

Therefore, the total superpotential, which includes all the interactions that contribute to the neutral fermion mass matrix is give by

$$W_{total} \supset W_{tree} + W_{non.ren.} + W_{eff}. \tag{3.35}$$

In our framework we have VEVs of the  $N$ -type fields that can be significantly large, depending on which implementation of the KM mechanism we assume. As such, B-RPV

couplings, mixing Higgses superfields with  $L$ -type superfields, appear in the superpotential as

$$\kappa_m H_u L + \kappa_X H_u L_X + \kappa_{\overline{X}} H_d \overline{L}_X \quad (3.36)$$

where the  $\kappa$ -parameters read

$$\kappa_m \simeq (y_\nu + \lambda_\nu) \langle N \rangle + \lambda_{mX} \langle N_X \rangle \quad (3.37)$$

$$\kappa_X \simeq \lambda_{Xm} \langle N \rangle + \lambda_{XX} \langle N_X \rangle \quad (3.38)$$

$$\kappa_{\overline{X}} \simeq \lambda_{\overline{X}\overline{X}} \langle \overline{N}_X \rangle \quad (3.39)$$

where we are dropping the  $F$ -terms contribution as the solutions for our KM mechanism presented in section 3.2 are aligned in the  $D$  and  $F$  directions. We also note that we are assuming no tree-level Yukawa couplings involving extra vector-like  $N_X$ ,  $\overline{N}_X$  for the KM scenarios, i.e. they are all forbidden by the discrete symmetry.

Furthermore, the presence of B-RPV induces a sub-EWS VEV on the scalar components of the  $\nu$ -type fields [93]. In our case, below the EWS, we expect all  $\nu$ -type scalars to acquire a non-vanishing VEV, generating a mixing between  $N$ -type fermions and Higgsinos through

$$\epsilon_m H_u^0 N + \epsilon_X H_u^0 N_X + \epsilon_{\overline{X}} H_d^0 \overline{N}_X \quad (3.40)$$

where the coefficients read

$$\epsilon_m \simeq (y_\nu + \lambda_\nu) \langle \nu \rangle + \lambda_{mX} \langle \nu_X \rangle \quad (3.41)$$

$$\epsilon_X \simeq \lambda_{Xm} \langle \nu \rangle + \lambda_{XX} \langle \nu_X \rangle \quad (3.42)$$

$$\epsilon_{\overline{X}} \simeq \lambda_{\overline{X}\overline{X}} \langle \overline{\nu}_X \rangle \quad (3.43)$$

and, as expected, they have the same generic form as the  $\kappa$ -parameters since both sets of parameters arise from trilinear and Yukawa couplings in the superpotential.

Finally, as in the MSSM, the presence of VEVs will mix some fermions with gauginos through kinetic terms, namely the Higgsinos with  $\tilde{B}_1$ ,  $\tilde{W}^0$  due to the Higgses VEVs. In our case we also have  $N$ -type and  $\nu$ -type scalar VEVs, which will mix gauginos with matter fermions through kinetic terms. We have, for the  $SU(2)$  states,

$$g' \tilde{B} \langle \nu_i \rangle \nu_i, \quad g \tilde{W}^0 \langle \nu_i \rangle \nu_i, \quad g'' \tilde{B}_X \langle \nu_i \rangle \nu_i \quad (3.44)$$

while for the  $N$ -states, which are singlets under the SM gauge group, the mixing with the gaugino of the extra  $U(1)_X$  gauge group

$$g'' \tilde{B}_X \langle N_i \rangle N_i \quad (3.45)$$



where, in both expressions, we used the shorthand  $g' = \sqrt{\frac{5}{3}}g_1$  and  $g'' = \frac{1}{2\sqrt{10}}g_X$ .

With all the above considerations, we can now construct the  $11 \times 11$  mass matrix for neutral fermions of our model. We define this matrix in the basis

$$\psi = (\tilde{B}, \tilde{W}^0, \tilde{B}_X, \tilde{H}_d^0, \tilde{H}_u^0, \nu, \nu_X, \bar{\nu}_X, N, N_X, \bar{N}_X), \quad (3.46)$$

and it has the schematic form

$$\mathbf{M}_{\chi-\nu} = \begin{pmatrix} \mathbf{M}_{\chi^0}^{5 \times 5} & \mathbf{M}_{\chi\nu}^{5 \times 6} \\ (\mathbf{M}_{\chi\nu}^{5 \times 6})^T & \mathbf{M}_{\nu}^{6 \times 6} \end{pmatrix}. \quad (3.47)$$

The usually called neutralino part of the matrix includes only mass terms involving gauginos and Higgsinos, and its form is very similar to the MSSM, except we have an extended gauge group with one more  $U(1)_X$  factor. It reads

$$\mathbf{M}_{\chi^0}^{5 \times 5} = \begin{pmatrix} M_1 & 0 & 0 & -\frac{1}{\sqrt{2}}g'v_d & \frac{1}{\sqrt{2}}g'v_u \\ 0 & M_2 & 0 & \frac{1}{\sqrt{2}}g'v_d & -\frac{1}{\sqrt{2}}g'v_u \\ 0 & 0 & M_X & -2\sqrt{2}g''v_d & 2\sqrt{2}g''v_u \\ -\frac{1}{\sqrt{2}}g'v_d & \frac{1}{\sqrt{2}}g'v_d & -2\sqrt{2}g''v_d & 0 & -\mu \\ \frac{1}{\sqrt{2}}g'v_u & -\frac{1}{\sqrt{2}}g'v_u & 2\sqrt{2}g''v_u & -\mu & 0 \end{pmatrix} \quad (3.48)$$

The next block is the one involving terms mixing the usual neutralino states with matter states. As such, they include B-RPV masses that mix matter with Higgses. The matrix reads

$$\mathbf{M}_{\chi\nu}^{5 \times 6} = \begin{pmatrix} -\frac{1}{\sqrt{2}}g\nu & -\frac{1}{\sqrt{2}}g'\nu_X & \frac{1}{\sqrt{2}}g'\bar{\nu}_X & 0 & 0 & 0 \\ \frac{1}{\sqrt{2}}g\nu & \frac{1}{\sqrt{2}}g'\nu_X & -\frac{1}{\sqrt{2}}g'\bar{\nu}_X & 0 & 0 & 0 \\ 3\sqrt{2}g''\nu & 3\sqrt{2}g''\nu_X & -3\sqrt{2}g''\bar{\nu}_X & -5\sqrt{2}g''N & -5\sqrt{2}g''N_X & 5\sqrt{2}g''\bar{N}_X \\ 0 & 0 & \kappa_{\bar{X}} & 0 & 0 & \epsilon_{\bar{X}} \\ \kappa_m & \kappa_X & 0 & \epsilon_m & \epsilon_X & 0 \end{pmatrix} \quad (3.49)$$

where, in order to de-clutter notation, we are taking the fields names as to represent the VEVs. We notice that the B-RPV couplings  $\kappa$  and  $\epsilon$  are superpotential terms, while the top three rows is generated by kinetic terms only.

The lower-right  $6 \times 6$  block is purely from the superpotential, and includes only the masses involving  $\nu$ -type and/or  $N$ -type fermions. To obtain the mass, one performs the usual SUSY rule for fermionic masses

$$(\mathbf{M}_{\nu}^{6 \times 6})_{ij} = -\frac{1}{2} \frac{\partial^2}{\partial \psi_i \partial \psi_j} W_{total} \quad (3.50)$$

where  $i, j = \{\nu, \nu_X, \bar{\nu}_X, N, N_X, \bar{N}_X\}$ .

This  $6 \times 6$  matrix has three main blocks: the  $\nu\nu$  block,  $\nu N$  block, and  $NN$  block. Schemat-

ically they are arranged, in our basis, as

$$\mathbf{M}_\nu^{6 \times 6} = -\frac{1}{2} \left( \begin{array}{c|c} M_{\nu\nu} & M_{\nu N} \\ \hline M_{\nu N}^T & M_{NN} \end{array} \right) \quad (3.51)$$

The actual form of the matrix is obtained using the full superpotential in Eq. (3.35). Doing so, one gets the following sub-blocks. First we have the  $\nu\nu$  block that has mixing between  $\bar{\nu}_X$  and  $\nu, \nu_X$ . In the sub-basis  $(\nu, \nu_X, \bar{\nu}_X)$  this reads

$$M_{\nu\nu} = \begin{pmatrix} 0 & 0 & \frac{b_7 \bar{N}_X N}{m_{pl}} + \frac{b_{10} \bar{N}_X N_X}{m_{pl}} + \mu_{Xm}^L \\ 0 & \frac{b_8 \bar{N}_X N}{m_{pl}} + \frac{b_{11} \bar{N}_X N_X}{m_{pl}} + \mu_X^L \\ & & 0 \end{pmatrix} \quad (3.52)$$

where we dropped the terms  $\nu^2/m_{pl}$ ,  $v_{u/d}^2/m_{pl}$  as they are irrelevant and to de-clutter, and since this block is symmetric we omit the lower left triangular part. But notice that the terms with coefficients  $b_7, b_8, b_{10}, b_{11}$  can play an important role as they can generate heavy Dirac masses, depending on the KM mechanism.

Next we have the  $\nu N$  block, where one can find the neutrino Dirac masses generated by the Higgses VEV at the EWS. Taking the rows to be along the basis  $(\nu, \nu_X, \bar{\nu}_X)$ , while the columns along  $(N, N_X, \bar{N}_X)$ , this block reads

$$M_{\nu N} = \begin{pmatrix} v_u y_\nu + \frac{b_7 \bar{N}_X \bar{\nu}_X}{m_{pl}} & \frac{b_{10} \bar{N}_X \bar{\nu}_X}{m_{pl}} & \frac{b_7 N \bar{\nu}_X}{m_{pl}} + \frac{b_{10} N_X \bar{\nu}_X}{m_{pl}} \\ \frac{b_8 \bar{N}_X \bar{\nu}_X}{m_{pl}} & \frac{b_{11} \bar{N}_X \bar{\nu}_X}{m_{pl}} & \frac{b_8 N \bar{\nu}_X}{m_{pl}} + \frac{b_{11} N_X \bar{\nu}_X}{m_{pl}} \\ \frac{b_7 \bar{N}_X \nu}{m_{pl}} + \frac{b_8 \bar{N}_X \nu_X}{m_{pl}} & \frac{b_{10} \bar{N}_X \nu}{m_{pl}} + \frac{b_{11} \bar{N}_X \nu_X}{m_{pl}} & \frac{b_7 N \nu}{m_{pl}} + \frac{b_{10} N_X \nu}{m_{pl}} + \frac{b_8 N \nu_X}{m_{pl}} + \frac{b_{11} N_X \nu_X}{m_{pl}} \end{pmatrix} \quad (3.53)$$

where we dropped the sub-leading terms  $v_{u/d} \lambda \simeq \mathcal{O}(10^{-13})$  GeV.

Finally we have the  $NN$  block, that involves Dirac and Majorana masses generated through the first two terms in Eq. (3.30). Ignoring the terms generated by Higgses and sneutrino VEVs, in the sub-basis  $(N, N_X, \bar{N}_X)$  this block reads

$$M_{NN} = \begin{pmatrix} \frac{c_{n,k}(k-1)k}{m_{pl}^{2n-3}} \bar{N}_X^n N_X^{n-k} N^{k-2} + \frac{2c_{2,2}}{m_{pl}} \bar{N}_X^2 & \frac{c_{n,k} k(n-k)}{m_{pl}^{2n-3}} \bar{N}_X^n N^{k-1} N_X^{-k+n-1} & \frac{c_{n,k} k n}{m_{pl}^{2n-3}} \bar{N}_X^{n-1} N_X^{n-k} N^{k-1} + \mu_{Xm}^N + \frac{4c_{2,2}}{m_{pl}} \bar{N}_X N \\ \frac{c_{n,k}(-k+n-1)(n-k)}{m_{pl}^{2n-3}} \bar{N}_X^n N^k N_X^{n-k-2} & \frac{c_{n,k} n(n-k)}{m_{pl}^{2n-3}} \bar{N}_X^{n-1} N_X^{-k+n-1} N^k + \mu_{XX}^N \\ \frac{c_{n,k}(n-1)n}{m_{pl}^{2n-3}} \bar{N}_X^{n-2} N_X^{n-k} N^k + \frac{2c_{2,2}}{m_{pl}} N^2 \end{pmatrix} \quad (3.54)$$

where the orders of magnitude of each entry will largely depend on which KM scenario is being considered. The matrix is symmetric so only the upper diagonal entries are displayed.

### 3.3.1 The mass matrix hierarchies

Following the description of the mass matrix above, we will now try to infer the hierarchies between the entries of the matrix. First we notice that, regardless of the case (i.e. the allowed

Kolda-Martin operators), the biggest entry in the mass matrix is always in the Gaugino- $N$  mixing block <sup>1</sup>. This result is understandable as we expect the breaking of the extra  $U(1)_X$  to transform a chiral superfield and a massless vector superfield into a single massive vector superfield. The degrees of freedom add up correctly, and would mean that below the  $U(1)_X$  breaking scale we can take  $\tilde{B}_X$  and the linear combination of  $N$ -states that break the  $U(1)_X$  to be integrated out jointly. The linear combination that breaks the extra  $U(1)_X$  depends on the exact values of the VEVs, but we can highlight some characteristics and how the mass-matrix will look like after this is integrated out.

In order to single out the correct linear combination that breaks the extra  $U(1)_X$ , one can perform a rotation in the last three states –  $N, N_X, \bar{N}_X$  – in order to retain only one mixing mass between these states and the  $\tilde{B}_X$ . In order to do so, in the limit the mass matrix is real, the rotation is

$$U = \begin{pmatrix} 1 & 0 & & & & \\ 0 & 1 & \cdots & & & \\ & \vdots & \ddots & & & \\ & & & \cos(\theta) & -\sin(\theta)\cos(\phi) & \sin(\theta)\sin(\phi) \\ & & & \sin(\theta) & \cos(\theta)\cos(\phi) & -\cos(\theta)\sin(\phi) \\ & & & 0 & \sin(\phi) & \cos(\phi) \end{pmatrix}$$

where the angles are determined by the strength of the mixing mass parameters. For instance, in the  $n = 2, k = 0$  Kolda-Martin mechanism presented before, the VEVs of the scalar components of  $N, N_X, \bar{N}_X$  are all of same order. In such case, taking  $\theta \simeq 3\pi/4$  and  $\phi \simeq \arctan \sqrt{2}$  will leave only one state mixing with  $\tilde{B}_X$ . For the other Kolda-Martin implementations, the  $N_X, \bar{N}_X$  VEVs are much larger than  $N$  VEV and so we can take  $\theta \simeq 0$  with  $\phi \simeq 3\pi/4$  to accomplish the same.

The rotation above affects only the last three columns and rows. Since the entries of last three columns of a given row will be mixed with at-most order 1 coefficients, whilst there might be cancellations there will be no order of magnitude enhancements. Once the rotation is performed one can then integrate out  $\tilde{B}_X$  jointly with its Dirac partner. This in turn will affect all the remainder of the matrix. For example, the entry  $i, j$  will receive a contribution from integrating out a Dirac mass at position  $a, b$  of order

$$-\frac{M_{i3}M_{bj}}{M_{3b}}$$

with some order one coefficients from the rotation. In this case we are setting one of the

---

<sup>1</sup>The caveat to this statement is if we allow for an order 1 Neutrino Yukawa, in that case the  $\kappa$  entry originated from  $y_\nu \langle N \rangle LH_u$ , will have the same order of magnitude. But since the B-RPV coupling above does not involve  $\tilde{B}_X, N, N_X$ , or  $\bar{N}_X$ , the magnitude of this coupling does not change the following discussion. We will return to B-RPV couplings further below.

indices to 3 as this is the position of  $\tilde{B}_X$  in our basis. The remaining index,  $b$ , refers to the position of the linear combination that breaks the extra  $U(1)_X$ . If, for example, the breaking linear combination that breaks the extra  $U(1)_X$  is mostly composed of  $N_X, \bar{N}_X$  states, the main contribution to the  $\nu$  Majorana mass is given by

$$\frac{b_{10}}{m_{pl}} \langle \nu \rangle \langle \bar{\nu}_X \rangle \ll 10^{-10} \text{ GeV}$$

even if we let the respective coupling on, i.e.  $b_{10} \simeq \mathcal{O}(1)$ . Therefore, after the above rotation and integrating out, the mass matrix remains schematically the same, but with the absence of  $\tilde{B}_X$  and a linear combination composed of  $N, N_X, \bar{N}_X$ .

After integrating out the Dirac fermion originated by the breaking, one can see that the Majorana and Dirac masses – generated at the  $U(1)_X$  breaking scale – involving only the surviving terms of the  $N, N_X, \bar{N}_X$  system are the leading entries of the mass matrix. These are present in the bottom-right-most  $2 \times 2$  block. These states will then be responsible for a type of see-saw mechanism involving the lighter  $SU(2)$  doublet states  $\nu, \nu_X, \bar{\nu}_X$ , with EW scale Dirac mass terms. In order to make sense of this see-saw mechanism, the  $\nu$ -states need to be protected from too much mixing with the remaining gauginos and higgsinos, such that the lightest mass eigenstate is dominantly composed of  $\nu$ . Actually the mixing between the  $\nu$ -type states with gauginos is negligible since it is generated by  $\nu$ -type VEVs and are therefore sub-EWS. But the mixing with Higgsinos is parametrically dependent on  $N$ -type VEVs through B-RPV terms, the so called  $\kappa$  mass parameters. In particular, the mixing with Higgsinos constrains  $\kappa_m$  to be at most  $\mathcal{O}(\text{GeV})$  [69–71].

The  $\kappa$  parameters defined in Equations (3.37), (3.38) and (3.39) can have other potentially undesirable consequences as they can spoil Higgs physics. Consider, for example, the matter B-RPV interaction, and assume that  $\kappa_m$  is significantly larger than any other mass involving  $H_u$ . If this were to happen, then  $L$  and  $H_u$  superfields would pair up to produce a heavy vector-like pair. Then  $H_u$  would be much heavier than the EWS physics and would spoil Higgs physics, where  $H_u$  and  $H_d$  are identified as a vector-like pair. In order to preserve viable Higgs physics, we need all  $\kappa$ -parameters to be much smaller than the remaining masses appearing in the Higgs potential.

Finally, there is risk that  $\nu, \nu_X, \bar{\nu}_X$  states will mix with each other too much. To see this consider the  $3 \times 3$  sub-block of the matrix as shown in Eq. (3.52). If all  $b_i$  couplings are suppressed, this matrix will maximally mix  $\nu$  and  $\nu_X$  through the  $\mu$ -terms. But it is important to note that while most of the  $b_i$  interactions will be generated by Higgses and  $\nu$ -type VEVs (making them naturally sub-leading even if they are allowed by discrete symmetry) there are two terms that can have important contributions

$$\frac{b_{10}}{m_{pl}} N_X \bar{N}_X \nu \bar{\nu}_X, \quad \frac{b_{11}}{m_{pl}} N_X \bar{N}_X \nu_X \bar{\nu}_X, \quad (3.55)$$

which for the KM cases can generate Dirac masses much greater than  $\mu$ -terms if the respective  $b_i$  coefficients are unsuppressed. This can then provide a natural mechanism to split  $\nu$  from  $\nu_X, \bar{\nu}_X$ , if the coupling  $b_{10}$  is forbidden while  $b_{11}$  is allowed by the discrete symmetry. In this case, we define

$$\mu_{11} = \frac{b_{11}}{m_{pl}} \langle N_X \rangle \langle \bar{N}_X \rangle \quad (3.56)$$

and the leading entries for Eq. (3.52) will take the form

$$\begin{pmatrix} 0 & 0 & \mu_{Xm}^L \\ 0 & 0 & \mu_{11} \\ \mu_{Xm}^L & \mu_{11} & 0 \end{pmatrix}, \quad (3.57)$$

which will then lead to  $\nu_X, \bar{\nu}_X$  to pair up and decouple from  $\nu$  as  $\mu_{11} \gg \mu_{Xm}^L$ .

### 3.4 Numerical Results

As the full mass matrix presents an intricate structure of relations and hierarchies between different states, it is ultimately impossible to obtain a simple and revealing analytic expression that describes how one should obtain good neutrino physics. Instead, we perform a numerical scan over space, ensuring that the above constraints are satisfied. In so doing, we divided the analysis into different realisations of the Kolda-Martin mechanism, parameterised by different values of  $(n, k)$ , corresponding to the scenarios in Table 3.1.

In all the cases, we considered a point of the parameter space to be good if the mass of the lightest eigenstate of the mass matrix, identified as a physical neutrino, has a mass in the range

$$[50, 100] \text{ meV}, \quad (3.58)$$

and in addition that the corresponding eigenstate is mostly composed of the left-handed doublet component  $\nu$  (i.e. the state arising from  $(\nu e)^T$ ). In order to do so, we compute the decomposition of the eigenstate in the original basis

$$|\nu_{light}\rangle = \alpha|\nu\rangle + \dots \quad (3.59)$$

and impose  $\alpha$  to be the largest of the coefficients. As discussed in the previous section, the prevalence of  $\nu$  as the largest component of  $\nu_{light}$  will depend greatly on the parameters of the mass matrix that mix different states, i.e. Dirac masses. For definiteness, we shall also require that the second lightest mass eigenstate (essentially the lightest non-neutrino-like neutralino) to be at least 100 GeV.

For each example, we only allow the particular desired Kolda-Martin operator while preventing all tree-level Yukawas involving states of the extra vector-like family. Furthermore,

unless otherwise stated we assume that all quadratic terms in Eq. (3.30) involving large VEVs are turned off. As expected within the  $M$  Theory framework, the disallowed tree-level couplings are regenerated through moduli VEVs, and so the respective coupling strength was set to be of  $\mathcal{O}(10^{-15})$ . Along the same line, the  $\mu$ -terms generated by moduli VEVs were set to  $\mathcal{O}(1)$  TeV.

Below we will show our findings for the only promising cases, which are  $(n, k) = (2, 0), (2, 1), (3, 0)$ . The other  $(n, k)$  assignments either returned to little points or no viable correlation to enhance  $\alpha$ . For example, cases  $(3, 1)$  and  $(4, 0)$  are not realised because  $N_X, \bar{N}_X \simeq 10^{15.5}$  GeV and the B-RPV coupling  $\kappa_m$  is generically greater than 1 GeV, spoiling the mass of the physical neutrino. As we will see below, the only viable regions of the parameter space coincide with a naturally suppressed B-RPV parameter.

### 3.4.1 $\nu$ component of the lightest state

From the discussion above, we expect the value of  $\alpha$  to be correlated with some parameters of the theory. Namely, we expect  $\alpha$  to be enhanced if  $b_{11}$  is not suppressed and if the B-RPV couplings  $\kappa$ -s, given in Equations (3.37), (3.38) and (3.39), are much smaller than any other masses involving Higgsinos. Since any disallowed tree-level coupling can be regenerated through moduli VEVs with a  $\lambda \simeq 10^{-15}$  suppression, we started our numerical study by looking at the behaviour of  $\alpha$  as we let  $b_{11}$  vary in the range

$$b_{11} \in [10^{-15}, 1], \quad (3.60)$$

which, in conjugation with a non-vanishing  $N_X, \bar{N}_X$  VEVs will lead to non-vanishing  $\mu_{11}$  as defined in Eq. (3.56).

In order to assess the strength of the B-RPV terms allowed in the regions of the parameter space that return good neutrinos, we also registered values of  $\kappa$  parameters at each point which returned the neutrino mass inside the bounds stated.

#### (2, 0) and (2, 1) cases

For these two Kolda-Martin implementation cases, the three  $(N, N_X, \bar{N}_X)$  VEVs are all of order  $\mathcal{O}(10^{10.5})$  GeV. As such, we allowed these VEVs to take values around

$$N, N_X, \bar{N}_X \in [10^{9.5}, 10^{11.5}] \text{ GeV} \quad (3.61)$$

to cover the range of expected values. Since with these values the mass matrix is very similar for both (2, 0) and (2, 1) cases, we present them together.

As a consequence of the values of the VEVs above, the  $\mu_{11}$  Dirac mass between  $\nu_X, \bar{\nu}_X$ ,

defined in Eq. (3.56), will take values spanning

$$\mu_{11} = b_{11} \frac{N_X \bar{N}_X}{m_{pl}} = b_{11} [10, 10^5] \text{ GeV} \quad (3.62)$$

which means that, only for non-suppressed  $b_{11}$  we expect

$$\mu_{11} \gg \mu_{Xm}^L \quad (3.63)$$

as required to split  $\nu$  from  $\nu_X$ , as discussed in section 3.3.1.

The above considerations indicate us that the mechanism to split  $\nu$  from  $\nu_X$  will only work for large values of  $b_{11}$ . This can be seen in Figures 3.1a and 3.1b, where a slight agglomeration of points around  $(\alpha, b_{11}) \simeq (1, 1)$  can be identified.

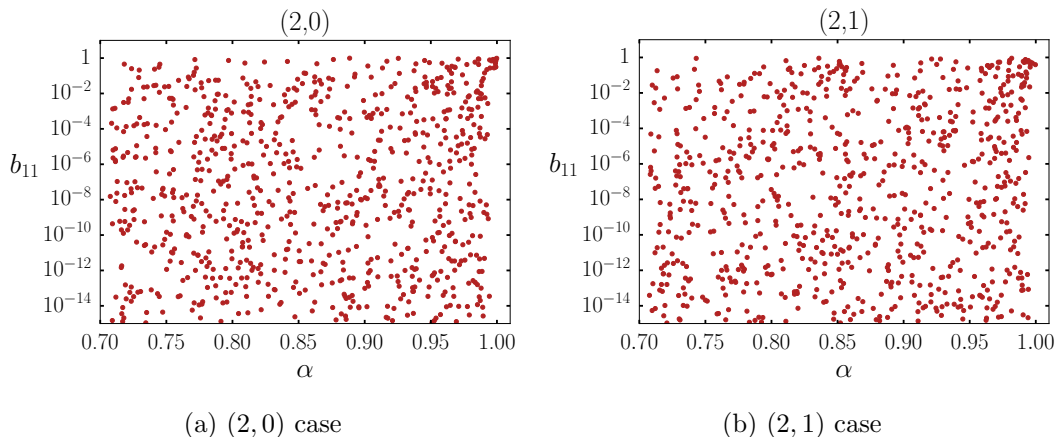


Figure 3.1: Scatter plots showing the amplitude  $\alpha$  of the left-handed doublet state  $\nu$  in the lightest mass eigenstate  $\nu_{light}$  as  $b_{11}$  varies for the (2, 0) and (2, 1) cases. The points are fairly evenly distributed with a slight clustering near the desired value of  $\alpha \approx 1$  for  $b_{11} \approx 1$ .

On the other hand, we find that the  $\kappa_m$  parameter, representing the potentially most dangerous B-RPV term, is mostly bounded to be smaller than 1 GeV, as is shown in Figures 3.2a and 3.2b. Although such small values of  $\kappa_m$  are welcome, the fact that there is no clear preference for  $\kappa_m \gtrsim 10^{-2}$  GeV suggests this class of models is challenged by BBN constraints, cf. Eq. (2.64).

### (3, 0) case

For the (3, 0) Kolda-Martin realisation, we found much promising results. Since the  $N_X$ ,  $\bar{N}_X$  VEVs are expected to be around  $\mathcal{O}(10^{14,25})$  GeV, if we allow them to be in the range

$$N_X, \bar{N}_X \in [10^{13,25}, 10^{15,25}] \text{ GeV} \quad (3.64)$$

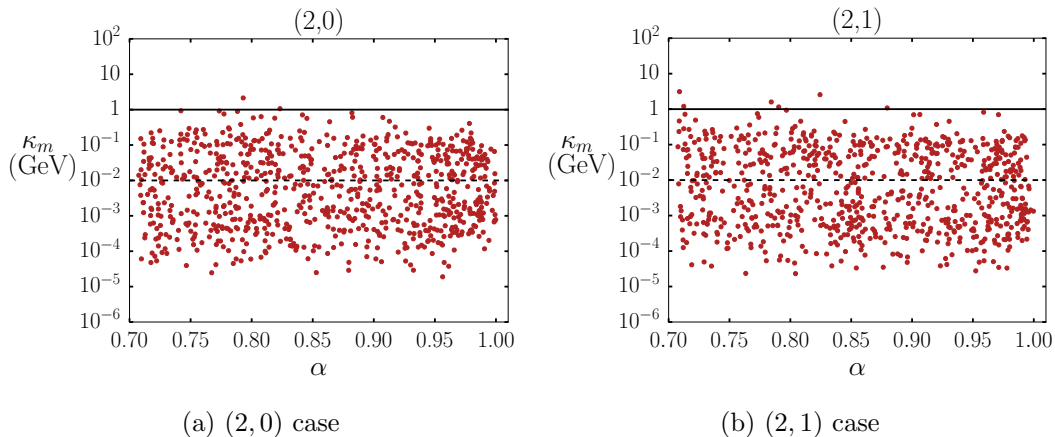


Figure 3.2: Scatter plots showing the amplitude  $\alpha$  of the left-handed doublet state  $\nu$  in the lightest mass eigenstate  $\nu_{light}$  as  $\kappa_m$  varies for the (2, 0) and (2, 1) cases. The points are fairly evenly distributed with a slight clustering near the desired value of  $\alpha \approx 1$ . The horizontal dashed line represents the bound on the LSP lifetime, cf. Eq. (2.64).

we find

$$\mu_{11} \in b_{11} [10^{8.25}, 10^{12.25}] \text{ GeV} \quad (3.65)$$

which implies that it is natural to achieve

$$\mu_{11} \gg \mu_{Xm}^L \quad (3.66)$$

and consequently  $\nu$  will decouple easily from the other  $\nu$ -type states.

The above expectations are confirmed by the numerical results, and the lightest state will be mostly composed of  $\nu$  even for values of  $b_{11}$  below  $\mathcal{O}(1)$ . This behaviour can be seen in Fig. 3.3a.

Interestingly, in the  $(\alpha, \kappa_m)$  plane, shown in Fig. 3.3b we can see again that the mass matrix prefers  $\kappa_m < 1$  GeV in order to reproduce a mostly- $\nu$  lightest state. This confirms result of [69–71] that B-RPV needs to be sufficiently suppressed in order to achieve good physical neutrinos. Furthermore, all the good points also suggest  $\kappa_m \gtrsim 10^{-2}$  GeV, satisfying the requirement for successful BBN physics, cf. Eq. (2.64).

### 3.4.2 Matter Neutrino Yukawas and B-RPV couplings

From the above analysis we learned that for the (2, 0), (2, 1) and (3, 0) cases we expect a non-suppressed  $b_{11}$  to enhance the component of  $\nu$  in the lightest state. As such, we will now consider this coupling to be of order 1 and re-run the analysis for these cases, with the goal being to assess what typical values  $\kappa_m$  and  $y_\nu$  should take for a successful implementation of the proposed Kolda-Martin mechanism.



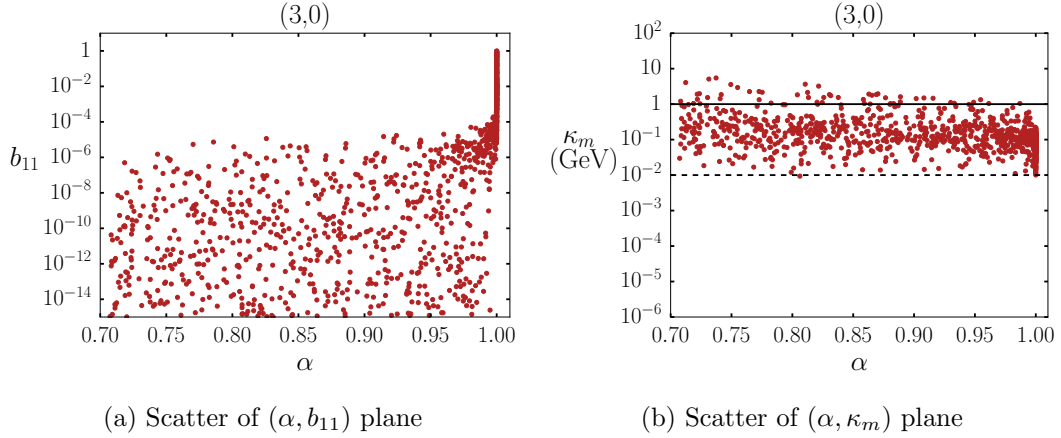


Figure 3.3: Scatter plots showing the amplitude  $\alpha$  of the left-handed doublet state  $\nu$  in the lightest mass eigenstate  $\nu_{light}$  as  $\kappa_m$  varies for the (3,0) case. The points are fairly evenly distributed except for a significant clustering near the desired value of  $\alpha \approx 1$  for larger values of  $b_{11}$ . The horizontal dashed line represents the bound on the LSP lifetime, cf. Eq. (2.64). The right panel shows that nearly all the points satisfy  $\kappa_m \gtrsim 10^{-2}$  GeV.

### (2,0) and (2,1) cases

In Figures 3.4a and 3.4b we see that the preferred points are those with  $y_\nu \lesssim 10^{-10}$ . This suggests that for these cases, the see-saw mechanism does not take a great role in explaining the light neutrino masses.

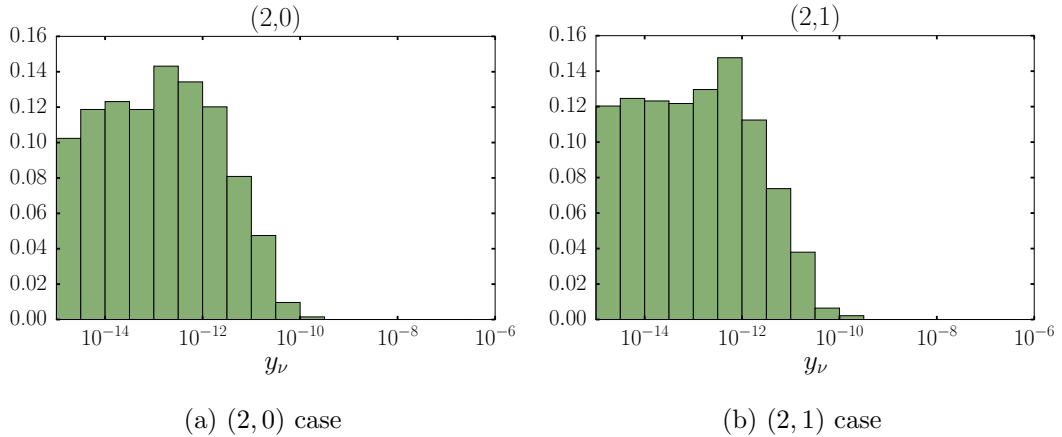


Figure 3.4: Histograms for the values of  $y_\nu$  for the (2,0) and (2,1) cases with unsuppressed  $b_{11}$

In Figures 3.5a and 3.5b we see that for these cases, the B-RPV parameter  $\kappa_m$  is naturally very small. This result is easy to understand, considering the main contribution to  $\kappa_m$ , provided in Eq. (3.37), to be

$$\kappa_m \simeq y_\nu \langle N \rangle,$$

and given the range of values that we are allowing the VEVs to take,  $\kappa_m$  is expected to be small. Unfortunately, some points returning good neutrino physics also return  $\kappa_m < 10^{-2}$  GeV, which means that these parameter points spoil BBN, cf. Eq. (2.64). Although not shown here one can also find that  $\kappa_X, \kappa_{\bar{X}}$  parameters, which mix  $L_X, \bar{L}_X$  with  $H_u, H_d$  respectively, are also constrained to be smaller than 1 GeV.

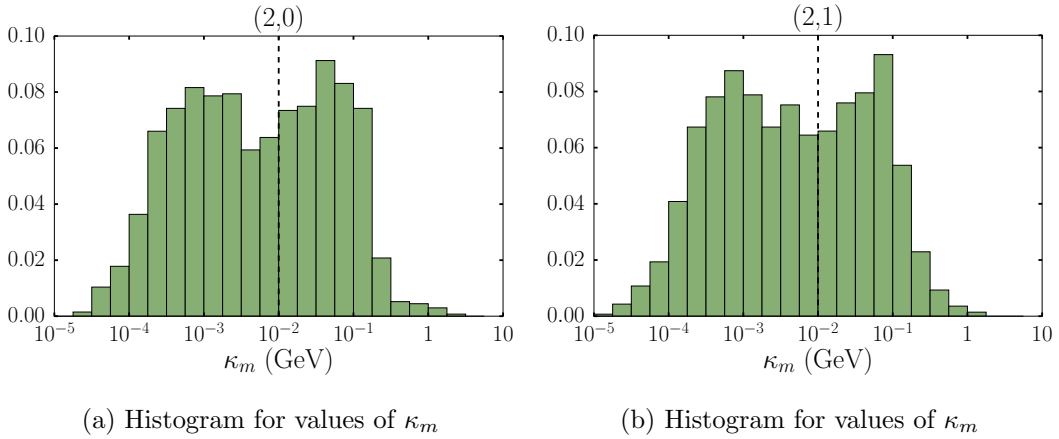


Figure 3.5: Histograms for the values of  $y_\nu$  and  $\kappa_m$  for the (2,1) case with unsuppressed  $b_{11}$ . The vertical dashed line represents the bound on the LSP lifetime, cf. Eq. (2.64).

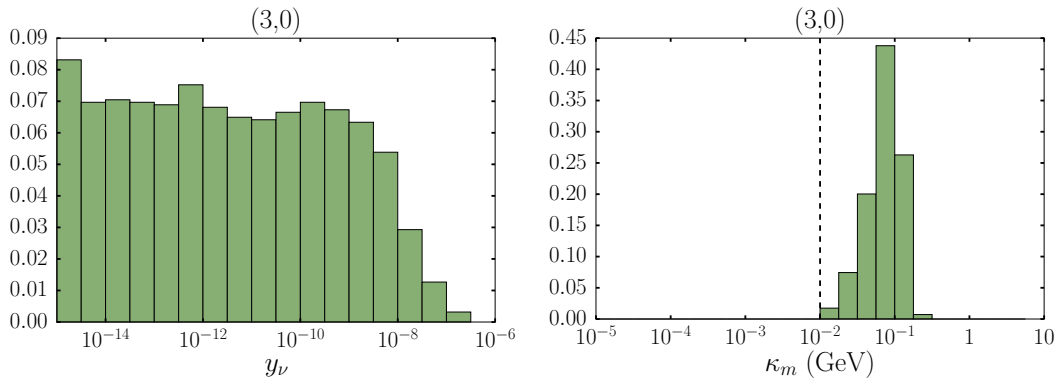
### (3,0) case

For this realisation of the Kolda-Martin mechanism, the results are slightly different but in line with our expectations. In Fig. 3.6a we can see that the matter Yukawa coupling is allowed to take values larger than in the previous case. This indicates that the see-saw mechanism is having an effect on reducing the contribution of the matter neutrino Dirac mass to the lightest eigenstate.

In Fig. 3.6b we see that  $\kappa_m$  is bound to be smaller than 1 GeV. The fact that  $\kappa_m$  takes larger values for (3,0) case than for the  $n = 2$  cases is easily understandable. The main contributions to  $\kappa_m$  are

$$\kappa_m \simeq y_\nu N + \lambda N_X \quad (3.67)$$

where the VEVs are expected as in Table 3.1. These contributions are in general greater than those in  $n = 2$  cases, but they are still bounded to be smaller than 1 GeV. This is fortunate, as  $\kappa_m \gtrsim 10^{-2}$  GeV and hence this class of models retain the successful predictions of BBN, cf. Eq. (2.64). As before, although not shown here also finds that  $\kappa_X, \kappa_{\bar{X}}$  parameter are also constrained to be smaller than 1 GeV.



(a) Histogram for values of  $y_\nu$

(b) Histogram for values of  $\kappa_m$ . The vertical dashed line represents the bound on the LSP lifetime, cf. Eq. (2.64).

Figure 3.6: Histograms for the values of  $y_\nu$  and  $\kappa_m$  for the  $(3, 0)$  case with unsuppressed  $b_{11}$

### 3.5 Conclusions and Discussion

In this chapter we have studied the origin of neutrino mass from  $SO(10)$  SUSY GUTs arising from  $M$  Theory compactified on a  $G_2$ -manifold. We have seen that this problem is linked to the problem of  $U(1)_X$  gauge symmetry breaking, which appears in the  $SU(5) \times U(1)_X$  subgroup of  $SO(10)$ , and remains unbroken by the Abelian Wilson line breaking mechanism. In order to break the  $U(1)_X$  gauge symmetry, we considered a (generalised) Kolda-Martin mechanism. Our results show that it is possible to break the  $U(1)_X$  gauge symmetry without further SUSY breaking while achieving high-scale VEVs that play a crucial role in achieving the desired value of neutrino mass.

The subsequent induced R-parity violation provides an additional source of neutrino mass, in addition to that arising from the seesaw mechanism from non-renormalisable terms. The resulting  $11 \times 11$  neutrino mass matrix was analysed for one neutrino family and it was shown how a phenomenologically acceptable neutrino mass can emerge. This happens easily for the  $(n, k) = (2, 0), (2, 1)$  and  $(3, 0)$  cases of the Kolda-Martin mechanism we developed. For these classes of models, not only is the neutrino masses phenomenologically viable, but also the physical light neutrino eigenstate is almost entirely composed of the left-handed (weakly charged) state  $\nu$  in the same doublet as the electron  $(\nu, e)$ , as desired. Furthermore, our analysis showed that the B-RPV parameters, which play an important role in neutrino masses and low-energy dynamics, are in the required range, being smaller than 1 GeV. Finally, we notice that the  $(n, k) = (3, 0)$  type of Kolda-Martin mechanism, and substantial number of parameter points in  $(n, k) = (2, 0)$  and  $(2, 1)$  cases preserve the successful predictions of BBN by allowing the LSP to decay quickly in early universe.

In conclusion, we have shown that  $SO(10)$  SUSY GUTs from  $M$  Theory on  $G_2$  manifolds provides a phenomenologically viable framework, in which the rank can be broken in the

effective theory below the compactification scale, leading to acceptable values of neutrino mass, arising from a combination of the seesaw mechanism and induced R-parity breaking contributions. In principle the mechanism presented here could be extended to three neutrino families and eventually could be incorporated into a complete theory of flavour, based on  $M$  Theory  $SO(10)$ , however such questions are beyond the scope of this work.

# Chapter 4

## Electroweakinos

### 4.1 Introduction

In the current chapter we are going to study the possibility of discovery of charginos/neutralinos in the  $WZ$  channel at a proposed 100 TeV proton-proton collider<sup>1</sup>. In the MSSM, which is likely to be a low-energy limit of string/M Theory, the chargino-neutralino sector is particularly important for several phenomenological reasons. Firstly, this sector contains Higgsinos, whose mass parameter,  $\mu$ , plays a crucial role in electroweak symmetry breaking. If the MSSM provides a solution to the gauge hierarchy problem, at least some of the charginos and neutralinos must be present not too far from the electroweak scale. Secondly, many SUSY breaking scenarios suggest that one of the neutralinos becomes the lightest SUSY particle (LSP). If the lightest neutralino is stable, for example due to a discrete symmetry like R-parity, it might be a promising candidate for dark matter. A stable neutralino also plays a crucial role in the collider phenomenology since the decay of supersymmetric particles will always produce the LSP, leading to a distinctive missing energy signature.

The ATLAS and CMS experiments at the CERN Large Hadron Collider (LHC) have put considerable effort into looking for charginos and neutralinos in the LHC data. In hadron colliders the expected limit and discovery reach for the charginos and neutralinos are considerably weaker compared to those for squarks and gluinos. For the  $\tilde{\chi}_1^\pm \tilde{\chi}_2^0 \rightarrow W^\pm \tilde{\chi}_1^0 Z \tilde{\chi}_1^0$  simplified model with  $m_{\tilde{\chi}_1^\pm} = m_{\tilde{\chi}_2^0}$  and  $m_{\tilde{\chi}_1^0} = 0$  GeV, the current limit, based on 2016 Run 2 data, is  $m_{\tilde{\chi}_1^\pm} \gtrsim 650$  GeV [94, 95]. The clean experimentally, but suppressed by branching ratios, three-lepton channel alone gives a weaker bound of about  $m_{\tilde{\chi}_1^\pm} \gtrsim 500$  GeV. Studies have been also performed into the projected experimental reach of the 14 TeV LHC using the same simplified model. In particular, the ATLAS collaboration expects [96] the  $5\text{-}\sigma$  discovery reach (95% CL limit) in the three-lepton channel for the chargino mass of about 550 (880) GeV with  $\mathcal{L} = 300 \text{ fb}^{-1}$  and 800 (1100) GeV with  $\mathcal{L} = 3000 \text{ fb}^{-1}$ . Similar sensitivities are expected

---

<sup>1</sup>In fact there are two proposals of a  $\sqrt{s} = 100$  TeV hadron machine. First one is CERN based FCC-hh, see <https://fcc.web.cern.ch>, and second is China's IHEP based SppC, see <http://cepc.ihep.ac.cn>

by CMS collaboration as well [97]. For massive neutralinos ( $m_{\tilde{\chi}_1^0} > 0$  GeV) or models with  $\text{BR}(\tilde{\chi}_2^0 \rightarrow h\tilde{\chi}_1^0) > 0$ , the limit and discovery reach become weaker and are well below those required by typical dark matter model.

Following the recent discussion of the next generation of circular colliders several physics cases at proton-proton colliders with  $\sqrt{s} \simeq 100$  TeV have already been studied [98–116]. For review see [117] and a recent CERN Yellow Report [118]. In particular, the limit and discovery reach for coloured SUSY particles have been studied in the context of simplified models assuming a 100 TeV proton-proton collider with  $3000 \text{ fb}^{-1}$  of integrated luminosity [98]. Searches for the mono-jet [104], vector boson fusion [111] as well as the mono-photon, soft lepton and disappearing track signatures [108, 109] have been studied in the similar setup for production of the pure  $W$ -inos (Higgsinos), assuming they are the main component of the LSP.

In this chapter, based on the publication [17], we study chargino-neutralino search at a 100 TeV collider assuming  $3000$  ( $1000$ )  $\text{fb}^{-1}$  luminosity exploiting the  $WZ$  channel. Instead of employing a simplified model approach, we work on a model which may arise as a limit of concrete UV complete scenarios. Partially motivated by string/M-Theory results, see Sec. 1.4.2, as well as anomaly mediation SUSY breaking scenarios and split supersymmetry [119–124], we assume that all SUSY particles apart from gauginos are decoupled and one of the neutralinos becomes the lightest SUSY particle. In particular we assume  $M_2 > \mu > 0$  and  $M_2 - \mu \gg m_Z$ , where  $M_2$  is the  $W$ -ino mass and  $\mu$  is the Higgsino mass. In this scenario Higgsins form the main component of the lighter charginos and neutralinos ( $\tilde{\chi}_1^\pm, \tilde{\chi}_1^0, \tilde{\chi}_2^0 \sim \tilde{H}^\pm, \tilde{H}_1^0, \tilde{H}_2^0$ ) and  $W$ -inos compose the heavier charginos and neutralinos ( $\tilde{\chi}_1^\pm, \tilde{\chi}_3^0 \sim \tilde{W}^\pm, \tilde{W}^0$ ). This choice of the mass hierarchy provides the highest discovery reach as production cross sections of Winos are higher than that of Higgsinos. The results we present can also be easily extended to the opposite scenario  $M_2 < \mu$  that appears to be more generic in models from M Theory on  $G_2$  [11]. We will also assume that the lightest neutralino is stable, or at least stable enough comparing to the collider time scale so that it escapes detection leaving a distinctive missing energy signature <sup>2</sup>.

They are other groups that have studied experimental reach of chargino-neutralino searches in multi-lepton channels at a 100 TeV collider [115, 116]. In particular, authors of [116] also investigate models that can arise from a UV complete theory. Apart from the Wino–Higgsino scenario with Higgsino being the LSP, as studied in this chapter, they report on other possible cases, when Wino or Bino is the LSP. In their analysis they have also included other than the 3 lepton search channel, investigating the opposite/same-sign di-leptons and four lepton channels as well. The prime advantage of our study, however, is that we include possible

---

<sup>2</sup>We have seen in chapter 3 that the LSP might not be stable in models arising from string/M Theory as R-parity violation can be present. Also, in [74] it was found that a generic string/M-theory model (with or without RPV) has the lightest visible neutralino decaying into a hidden sector. Depending on the specific scenario non-standard SUSY searches might be more appropriate [69]

detector effects using `Delphes 3` [125] fast detector simulation. In [115], on the other hand, a different approach, based on that of Collider Reach [126], was taken. The experimental reach of a future collider there is estimated based on current collider limits extrapolated to higher centre of mass energy assuming appropriate scaling of signal and background events acceptances and efficiencies. This approach means only signal cross sections are needed to place limits. No event simulations are required.

The rest of the chapter is organised as follows. In section 4.2, we describe the model setup and study the production cross sections and branching ratios of charginos and neutralinos. After clarifying our simulation setup in section 4.3, various kinematic distributions for signal and background are studied in section 4.4, which will be used to design optimal event selection cuts for the chargino-neutralino search. In section 4.5, we present the result of our analysis and derive the limit and discovery reach in the  $M_2 - \mu$  parameter plane. The conclusions are given in section 4.6.

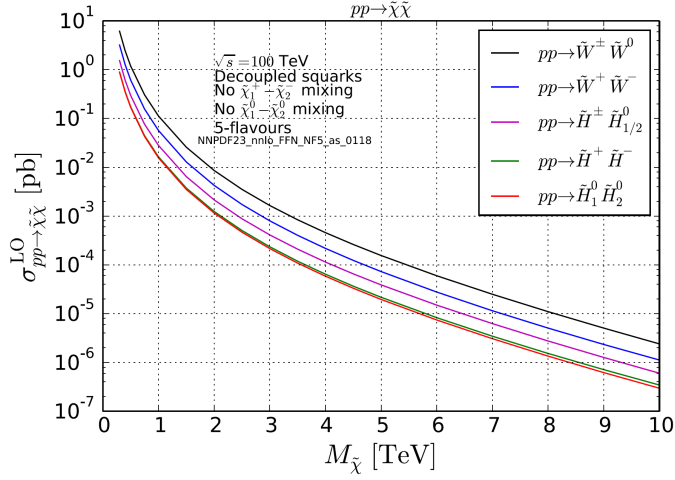
## 4.2 The cross sections and branching ratios

### 4.2.1 The model setup

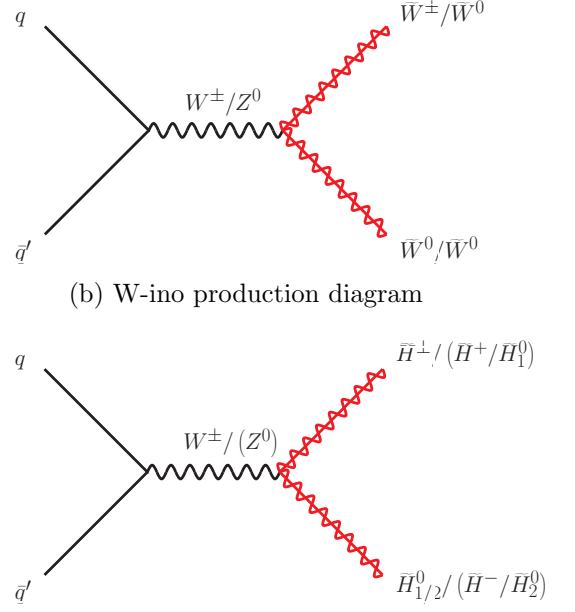
As mentioned before, in this chapter we focus on the models with  $M_2 > \mu > 0$  and  $M_2 - \mu \gg m_Z$ , where the  $\mu$  is the mass of the Higgsinos and  $M_2$  is the mass of the  $W$ -inos since the  $W$ -ino production cross section is larger than the Higgsino cross section. We assume that all the other SUSY particles, including the  $B$ -ino, are decoupled and all SUSY breaking parameters are real for simplicity. In this situation the mixing between  $W$ -ino and Higgsino is negligible; the two Higgsino doublets are the lightest charginos and the two lightest neutralinos (which are almost degenerate) and the  $W$ -inos (SU(2) triplet) are the second lightest charginos and the third lightest neutralino (almost mass degenerate):

$$\begin{aligned} \tilde{\chi}_1^\pm, \tilde{\chi}_1^0, \tilde{\chi}_2^0 &\sim \tilde{H}^\pm, \tilde{H}_1^0, \tilde{H}_2^0 && \text{with } m_{\tilde{\chi}_1^\pm} \simeq m_{\tilde{\chi}_1^0} \simeq m_{\tilde{\chi}_2^0} \simeq |\mu|, \\ \tilde{\chi}_2^\pm, \tilde{\chi}_3^0 &\sim \tilde{W}^\pm, \tilde{W}^0 && \text{with } m_{\tilde{\chi}_2^\pm} \simeq m_{\tilde{\chi}_3^0} \simeq |M_2|, \end{aligned} \quad (4.1)$$

where  $\tilde{H}_{1/2}^0 = \frac{1}{\sqrt{2}}(\tilde{H}_u^0 \mp \tilde{H}_d^0)$  is the neutral Higgsino mass eigenstate. With this setup, the remaining free parameters are  $M_2$ ,  $\mu$  and  $\tan\beta$ . We use  $\tan\beta = 10$  throughout our numerical study. However, the impact of  $\tan\beta$  on the production cross section and branching ratio of the charginos and neutralinos that are  $W$ -ino or Higgsino like is almost negligible unless  $\tan\beta$  is extremely small. We therefore believe our results including the chargino-neutrino mass reach are still useful for other values of  $\tan\beta$ .



(a) LO production cross sections



(b) W-ino production diagram

(c) Higgsino production diagram

Figure 4.1: (a) The leading order cross sections for the  $W$ -ino and Higgsino pair productions at a 100 TeV proton-proton collider with decoupled squarks and sleptons. Corresponding, dominant  $W$ -ino (b) and Higgsino (c) pair-production diagrams are also presented.

## 4.2.2 The cross sections

We show the leading order (LO) cross sections for the  $W$ -ino and Higgsino pair productions at a 100 TeV proton-proton collider in Fig. 4.1a. The cross sections are calculated using MadGraph5 [127]. Since squarks are decoupled, the  $W$ -inos and Higgsinos are produced via the  $s$ -channel diagrams exchanging off-shell  $W^\pm$  and  $Z$  bosons, see Figures 4.1b and 4.1c. For the pure  $W$ -inos and Higgsinos, there is no associated  $W$ -ino-Higgsino production process. Pair production of the same neutralino states,  $\widetilde{W}^0\widetilde{W}^0$ ,  $\widetilde{H}_1^0\widetilde{H}_1^0$ ,  $\widetilde{H}_2^0\widetilde{H}_2^0$ , are also absent.

One can see that the  $\widetilde{W}^\pm\widetilde{W}^0$  production mode has the largest cross section. The LO cross section varies from  $10^3$  fb to  $10^{-2}$  fb for the  $W$ -ino mass from 500 GeV to 8 TeV.

## 4.2.3 The branching ratios

The  $W$ -ino-Higgsino interaction is derived from the kinetic terms of Higgsinos.

$$\begin{aligned}
 \mathcal{L} &\supset \left[ H_u^\dagger e^V H_u + H_d^\dagger e^V H_d \right]_{\theta^4} \\
 &\supset \sqrt{2}g(H_u^* \widetilde{W}^a T^a \widetilde{H}_u - H_d^* \widetilde{W}^a T^a \widetilde{H}_d) + \text{h.c.}
 \end{aligned}
 \tag{4.2}$$



The Higgs and Higgsino fields can be written in terms of the Goldstone bosons and the mass eigenstates as:

$$\begin{aligned} \begin{pmatrix} H_u^+ \\ H_u^0 \end{pmatrix} &= \begin{pmatrix} \sin \beta \cdot \phi^+ + \dots \\ \frac{1}{\sqrt{2}}(\cos \alpha \cdot h + i \sin \beta \cdot \phi^0) + \dots \end{pmatrix}, & \begin{pmatrix} \tilde{H}_u^+ \\ \tilde{H}_u^0 \end{pmatrix} &\simeq \begin{pmatrix} \tilde{H}^+ \\ \frac{1}{\sqrt{2}}(\tilde{H}_1^0 + i\tilde{H}_2^0) \end{pmatrix}, \\ \begin{pmatrix} H_d^0 \\ H_d^- \end{pmatrix} &= \begin{pmatrix} \frac{-1}{\sqrt{2}}(\sin \alpha \cdot h + i \cos \beta \cdot \phi^0) + \dots \\ -\cos \beta \cdot \phi^- + \dots \end{pmatrix}, & \begin{pmatrix} \tilde{H}_d^0 \\ \tilde{H}_d^- \end{pmatrix} &\simeq \begin{pmatrix} \frac{1}{\sqrt{2}}(\tilde{H}_1^0 - i\tilde{H}_2^0) \\ \tilde{H}^- \end{pmatrix}, \end{aligned} \quad (4.3)$$

where  $h$  is the SM like Higgs boson, and  $\phi^0$  and  $\phi^\pm$  are the Goldstone bosons to be eaten by the SM gauge bosons,  $Z$  and  $W^\pm$ , respectively. The angles  $\alpha$  and  $\beta$  represent the mixing for the neutral and charged Higgs mass matrices.

In the large  $\tan \beta$  limit, we have  $\cos \alpha / \sin \alpha \simeq (-\sin \beta) / \cos \beta$ , and one can see that the  $h\tilde{W}\tilde{H}$ ,  $\phi^0\tilde{W}\tilde{H}$  and  $\phi^\pm\tilde{W}\tilde{H}$  have the same coupling. In this limit one can find the following results using the Goldstone equivalence theorem [128].

$$\begin{aligned} \text{BR}(\tilde{W}^\pm) &\simeq \begin{cases} 0.5 & \rightarrow W^\pm \tilde{H}_1^0 \text{ or } W^\pm \tilde{H}_2^0 \\ 0.25 & \rightarrow h\tilde{H}^\pm \\ 0.25 & \rightarrow Z\tilde{H}^\pm \end{cases} \\ \text{BR}(\tilde{W}^0) &\simeq \begin{cases} 0.5 & \rightarrow W^\pm \tilde{H}^\mp \\ 0.25 & \rightarrow h\tilde{H}_1^0 \text{ or } h\tilde{H}_2^0 \\ 0.25 & \rightarrow Z\tilde{H}_1^0 \text{ or } Z\tilde{H}_2^0 \end{cases} \end{aligned} \quad (4.4)$$

The different CP properties between  $h$  and  $\phi^0$ , and  $\tilde{H}_1^0$  and  $\tilde{H}_2^0$  result in the different rates for  $\tilde{W}^0 \rightarrow h\tilde{H}_1^0$  and  $\tilde{W}^0 \rightarrow Z\tilde{H}_1^0, h\tilde{H}_2^0$ . These rates are given by

$$\begin{aligned} \text{BR}(\tilde{W}^\pm \rightarrow W^\pm \tilde{H}_1^0) &\simeq \text{BR}(\tilde{W}^\pm \rightarrow W^\pm \tilde{H}_2^0), \\ \text{BR}(\tilde{W}^0 \rightarrow h\tilde{H}_{1/2}^0) &\simeq \text{BR}(\tilde{W}^0 \rightarrow Z\tilde{H}_{2/1}^0), \\ \frac{\text{BR}(\tilde{W}^0 \rightarrow Z\tilde{H}_1^0)}{\text{BR}(\tilde{W}^0 \rightarrow h\tilde{H}_1^0)} &\simeq \frac{1 - 2|\mu/M_2|}{1 + 2|\mu/M_2|}. \end{aligned} \quad (4.5)$$

Fig. 4.2 shows the branching ratios of  $\tilde{W}^\pm$  and  $\tilde{W}^0$ , which have been calculated using SUSY-HIT [129]. One can see that the branching ratios approach Eq. (4.4) in the large  $M_2$  limit. For the region where  $|M_2 - \mu|$  is close to the masses of SM bosons, the decay mode into  $W^\pm$  enhances since it has the largest phase space factor.

Since the charged and neutral  $W$ -inos are almost mass degenerate, it may not be possible to resolve  $\tilde{W}^\pm \rightarrow XY$  and  $\tilde{W}^0 \rightarrow X'Y'$  in hadron colliders if  $XY$  is equal to  $X'Y'$  up to soft activities. Similarly, four degenerate Higgsinos would not be resolvable, since  $\tilde{H}^\pm$  and  $\tilde{H}_2^0$  usually decay promptly into  $\tilde{H}_1^0$  and their decay products are too soft to be detected. We therefore categorise the processes into distinguishable groups in terms of the SM bosons

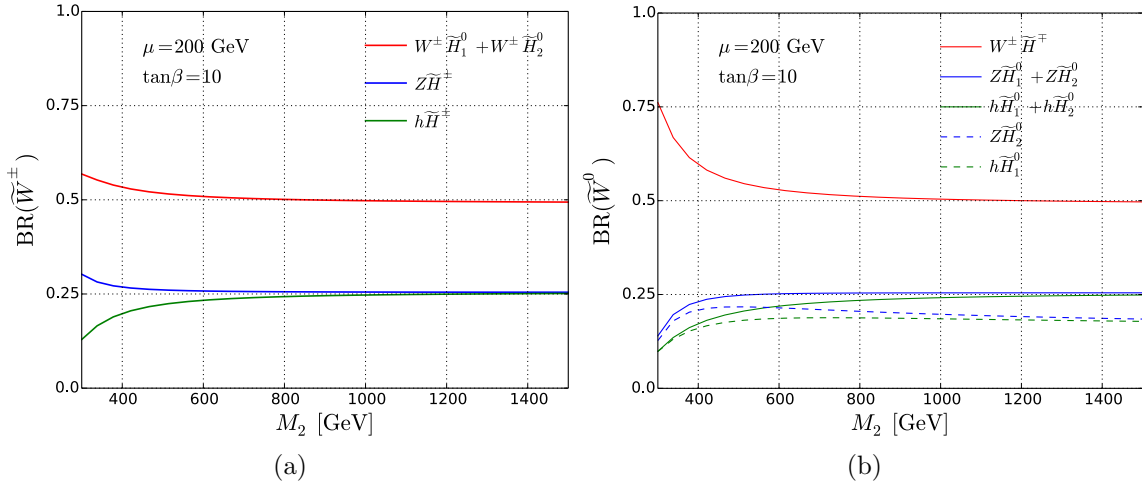


Figure 4.2: The branching ratios of  $\widetilde{W}^\pm$  (a) and  $\widetilde{W}^0$  (b) as functions of  $M_2$ . The  $\mu$  parameter is fixed at 200 GeV. The SUSY particles other than  $W$ -inos and Higgsinos are decoupled.

appearing in the final states. For example,  $\chi'\chi' \rightarrow WZ\chi\chi$  process ( $WZ$  mode) includes  $\widetilde{W}^+\widetilde{W}^- \rightarrow (W^\pm\widetilde{H}_{1/2}^0)(Z\widetilde{H}^\mp)$ ,  $\widetilde{W}^\pm\widetilde{W}^0 \rightarrow (W^\pm\widetilde{H}_{1/2}^0)(Z\widetilde{H}_{1/2}^0)$ ,  $(Z\widetilde{H}^\pm)(W^\pm\widetilde{H}^\mp)$  and  $\widetilde{W}^0\widetilde{W}^0 \rightarrow (W^\pm\widetilde{H}^\mp)(Z\widetilde{H}_{1/2}^0)$ . We show the cross sections of the all 6 distinguishable modes,  $WZ$ ,  $Wh$ ,  $WW$ ,  $ZZ$ ,  $Zh$  and  $hh$  modes, in the  $M_2 - \mu$  plane in Fig. 4.3.

One can see that the modes containing at least one  $W$  have considerably larger cross sections compared to the others at the same mass point. In particular, the  $WZ$  mode is promising<sup>3</sup> because one can reduce the QCD and  $t\bar{t}$  backgrounds significantly by requiring three high  $p_T$  leptons (See Fig. 4.4). Taking advantage of this we henceforth study the expected discovery reach and exclusion limit for chargino-neutralino production in the fully leptonic  $WZ$  mode<sup>4</sup>.

In Fig. 4.5, we show the cross section of the  $WZ$  mode after taking account of the branching ratios of the gauge bosons into  $3\ell + \nu$ . The black curve represents the limit beyond which less than 5 signal events ( $\chi'\chi' \rightarrow WZ\chi\chi \rightarrow 3\ell\nu\chi\chi$ ) are produced, assuming the integrated luminosity of  $3000 \text{ fb}^{-1}$ . This provides a rough estimate of the theoretically maximum possible exclusion limit assuming zero background with perfect signal efficiency.

<sup>3</sup>The  $Wh$  mode is also interesting. See [95, 130–135] for some recent LHC studies and results as well as [115] for an estimated reach of a 100 TeV collider.

<sup>4</sup>Due to higher branching ratio of  $W$  to jets, lepton plus jet searches ( $2l + 2j$ ) in the  $W(\rightarrow jj)Z(\rightarrow ll)$  mode can be more sensitive than the  $3l$  ones [95, 135]. Nonetheless, the  $3l$  case analysed here should be a good estimate of the sensitivity of a 100 TeV collider in the chargino-neutralino sector.

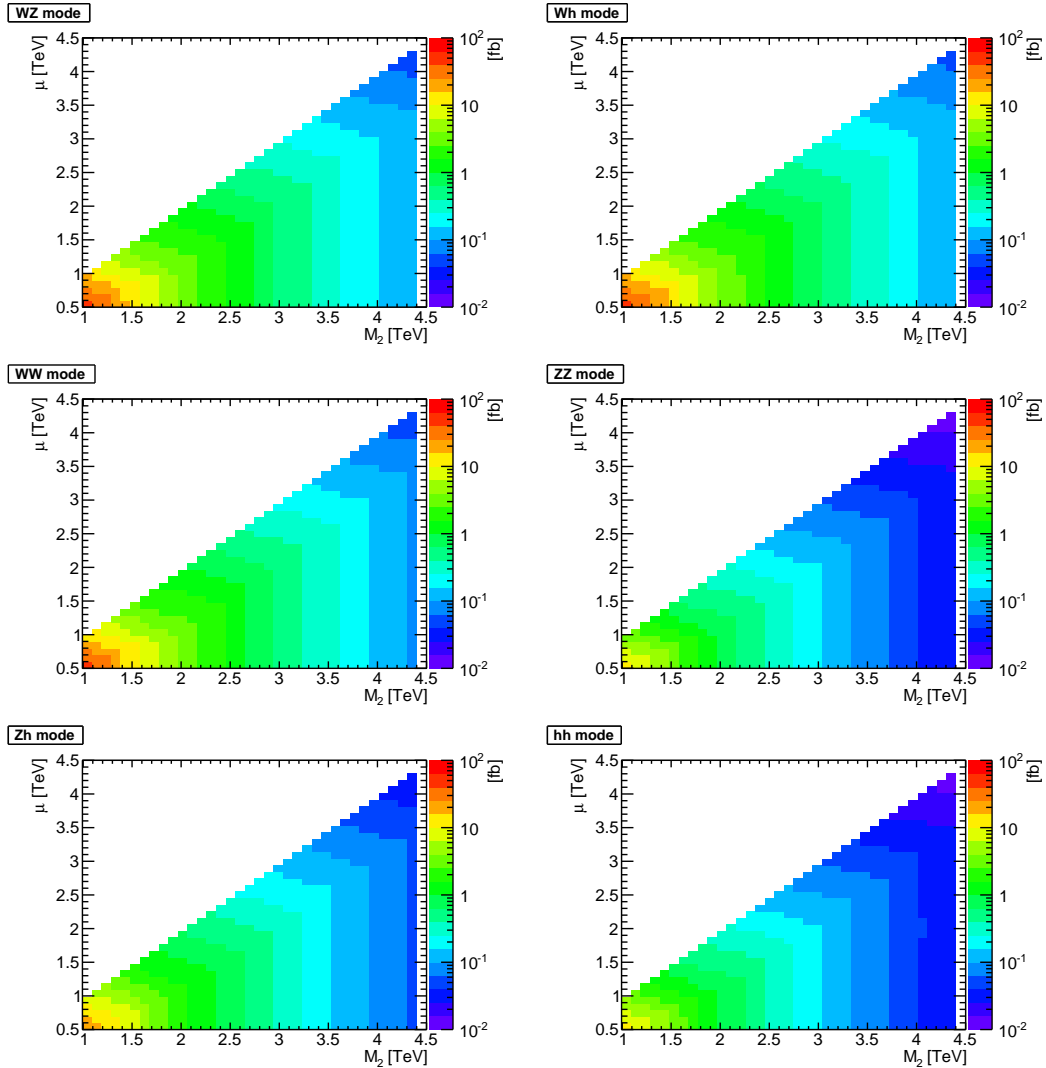


Figure 4.3: The cross sections of the 6 distinguishable modes,  $\chi'\chi' \rightarrow XY\chi\chi$  with  $XY = WZ, Wh, WW, ZZ, Zh$  and  $hh$ , as functions of  $M_2$  and  $\mu$ . SUSY particles other than  $W$ -inos and Higgsinos are decoupled.

### 4.3 The simulation setup

We use the **Snowmass** background samples [136] to estimate the Standard Model (SM) backgrounds. We include the relevant SM processes, which are summarised in Table 4.1.

For signal events we first generate chargino and neutralino production events using **MadGraph 5** [127] with the MSSM parameters and decay widths obtained by **SUSY-HIT** [129] and **BRIDGE** [137] respectively. **MadGraph 5** is a general purpose matrix-element-based event generator, capable of computing leading order and, in strong  $\alpha_s$ , next-to-leading order amplitudes for arbitrary processes. Provided with Feynman rules of a model, **MadGraph 5** generates all relevant, for processes studied, Feynman diagrams and helicity amplitudes. Equipped with an

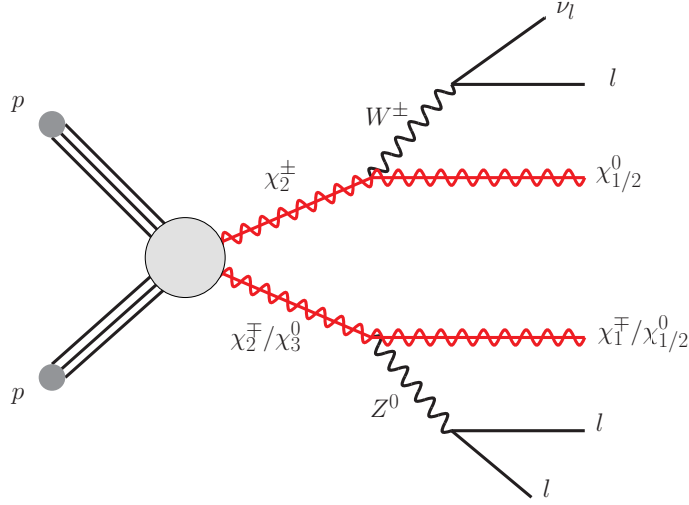


Figure 4.4: The three-lepton event topology of the  $WZ$  mode. In the model considered here  $\chi_2^\pm$ ,  $\chi_3^0$  are predominantly W-inos, and  $\chi_1^\pm$ ,  $\chi_{1/2}^0$  are predominantly Higgsinos. Because of small mass splittings between different Higgsinos (different W-inos) they are assumed to be indistinguishable experimentally.

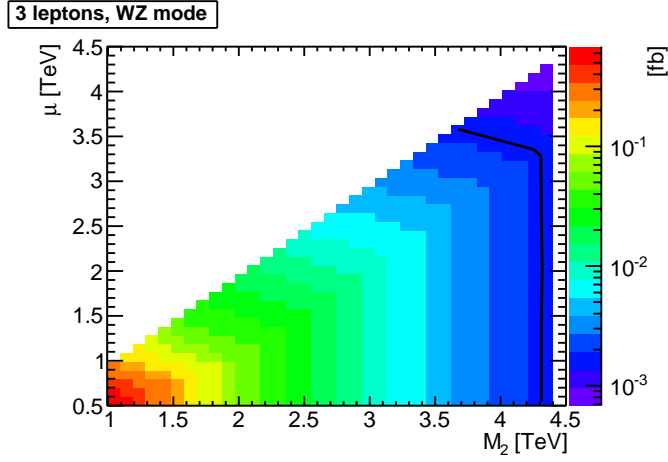


Figure 4.5: The cross section of  $\chi'\chi' \rightarrow WZ\chi\chi \rightarrow 3\ell\nu\chi\chi$  as a function of  $M_2$  and  $\mu$ . The black curve represents the limit beyond which less than 5 signal events are produced, assuming the integrated luminosity of  $3000 \text{ fb}^{-1}$ .

interface to parton distribution libraries it can then calculate cross sections and generate parton-level events. In our studies we use `MadGraph`'s build-in MSSM model with mass and mixing parameters calculated with `SUSY-HIT` spectrum generator. `SUSY-HIT` works on so called phenomenological MSSM (pMSSM) [138, 139], a subset of the general MSSM parameter space, with 22 free parameters defined at either low or high energy scale. `SUSY-HIT` can

run to an arbitrary scale with the renormalization group evolution (RGE) with up to two-loop level accuracy, implementing the radiative EWSB and calculating the pole masses and mixing between different mass-eigenstates. Although **SUSY-HIT** is also capable of calculating decay widths and branching ratios for SUSY particles, we are using a separate software, **BRIDGE**, that is also able to handle decays of unstable particles. **BRIDGE** is a decay width and branching ratio calculator for an arbitrary physics model. It is capable of handling 2 and 3 body decays and it attempts to preserve the angular structure of events using proper helicity amplitudes for each decay.

We consider two production processes for our signal sample,  $pp \rightarrow \chi_2^+ \chi_2^-$  and  $pp \rightarrow \chi_2^\pm \chi_3^0$ , where  $\chi_2^\pm \sim \widetilde{W}^\pm$  and  $\chi_3^0 \sim \widetilde{W}^0$ , with the dominant production diagram shown in Fig. 4.1b. The parton-level samples generated with **MadGraph 5** are then passed to **BRIDGE** to have the charginos and neutralinos decay. We then only accept the events with  $W$  and  $Z$  in the final states, and pass those events once again to **BRIDGE** to let  $W$  and  $Z$  decay leptonically. Finally we simulate the effects of parton shower, hadronization and detector resolutions using **Pythia 6** [140] and **Delphes 3** [125]. **Pythia 6** is a multi-purpose Monte-Carlo event generator. It is capable of performing initial and final state parton shower, generating underlying events, performing hadronisation and decay of unstable particles, to name the most important features, producing complete events as expected in particle collider experiments. The hadron-level events, output of **Pythia 6**, can be then run through a detector simulation software in order to model a detector response. Since no specific detector design is available for a 100 TeV collider at the moment we use a simplified detector simulation provided by **Delphes 3** tuned according to the **Snowmass** detector framework [136]. **Delphes 3** takes into account the effect of magnetic field on charged particles, the granularity of the calorimeters and sub-detector resolutions. Instead of performing detailed physics modeling, as for example done in **GEANT4**-based simulations [141], that is heavy computationally, **Delphes 3** parameterises the response of different detector components for fast processing speed. **Delphes 3** based results are less-reliable than dedicated detector response studies, but with no specific detector design for a 100 TeV collider this gives reasonable handle on potential detector effects. The **Snowmass** detector framework assumes the performance of a future collider detector to be at least as good as the performance of **ATLAS** and **CMS** detectors.

## 4.4 The kinematic distributions

In this section we show some kinematic distributions for the background and signal events. We consider the  $WZ$  mode for signal and diboson ( $VV$ ) and top-pair plus gauge boson ( $t\bar{t}V$ ) processes for backgrounds. The signal distributions are generated at a benchmark point:  $M_2 = 1.4$  TeV,  $\mu = 200$  GeV. Throughout this section we use a notation denoting the  $i$ -th hardest lepton (electron or muon) by  $\ell_i$  (namely,  $p_T(\ell_i) > p_T(\ell_j)$  for  $i < j$ ).

Name	Snowmass	Relevant sub-processes	$\sigma_{\text{total}}^{\text{NLO}}$ [pb]
diboson	VV	$W^+W^-, W^\pm Z, ZZ$	430.5
top-pair + gauge boson	ttV	$t\bar{t}W^\pm, t\bar{t}Z, t\bar{t}h$	219.9
top + gauge boson	tV	$tW^\pm, \bar{t}W^\pm$	182.5
triple gauge boson	VVV	$W^+W^-W^\pm, W^+W^-Z, W^\pm ZZ, ZZZ$	36.4

Table 4.1: The Standard Model background included in the analysis. For each background category, we only list sub-processes relevant in the 3 lepton analysis. Reported cross sections include all sub-processes in corresponding background categories.

Fig. 4.6a shows the normalised distributions of the leading lepton pseudo-rapidity,  $\eta_{\ell_1}$ , for signal (black) and background (red for VV and green for ttV). The distributions are obtained at a parton level without selection cuts apart from  $p_T(\ell_1) > 10$  GeV to understand the bare distribution before taking the detector acceptance into account. One can see that the leptons in the background tend to be more forward compared to the signal leptons. The production threshold is much lower for the backgrounds and more asymmetric momentum configurations are allowed for the initial partons. If one of the initial partons has a much larger momentum than the other, the system is boosted in the direction of the beam pipe and the leptons tend to be produced in the forward region.<sup>5</sup> Another effect is as follows. Unlike the signal, production of the backgrounds have a contribution from  $t$ -channel diagrams. In 100 TeV colliders, the SM gauge bosons can effectively be regarded as “massless” particles and there is an enhancement in the region of the phase space where the gauge bosons are produced in the forward region.

Fig. 4.6b shows the  $p_T$  distributions of the three hardest leptons. The distributions are obtained after taking the hadronization and detector effects into account and requiring at least 3 leptons (with  $p_T > 10$  GeV,  $|\eta| < 2.5$ ), of which two are same flavour and opposite sign (SFOS). As can be seen, the  $p_T$ -spectrum of background leptons has peaks below 100 GeV, whilst the signal peaks at around 300, 150 and  $\lesssim 50$  GeV for the leading, second leading and third leading leptons for our benchmark point.

We also show the  $E_T^{\text{miss}}$  distributions in Fig. 4.6c, where we use the same event sample as those in Fig. 4.6b. The main source of the  $E_T^{\text{miss}}$  in the background are the neutrinos produced from  $W$  and  $Z$  decays and the distribution has a peak around 30 – 40 GeV. Above this peak, the background  $E_T^{\text{miss}}$  distribution falls quickly. On the other hand, a large  $E_T^{\text{miss}}$  can be produced from the signal from the decays of heavy charginos and neutralinos. The typical scale of  $E_T^{\text{miss}}$  is given by  $\sim M_2/2$ . As can be seen, the signal distribution has a peak around 500 GeV. This indicates that a hard cut on  $E_T^{\text{miss}}$  will greatly help to improve the signal to background ratio.

<sup>5</sup>For the  $W^+Z$  background, the initial state is often  $u$  and  $\bar{d}$ . If the partonic collision energy is much smaller than the proton-proton collision energy, it is more likely to find a valence quark  $u$  carrying a larger fraction of the proton momentum compared to the sea quark  $\bar{d}$ .

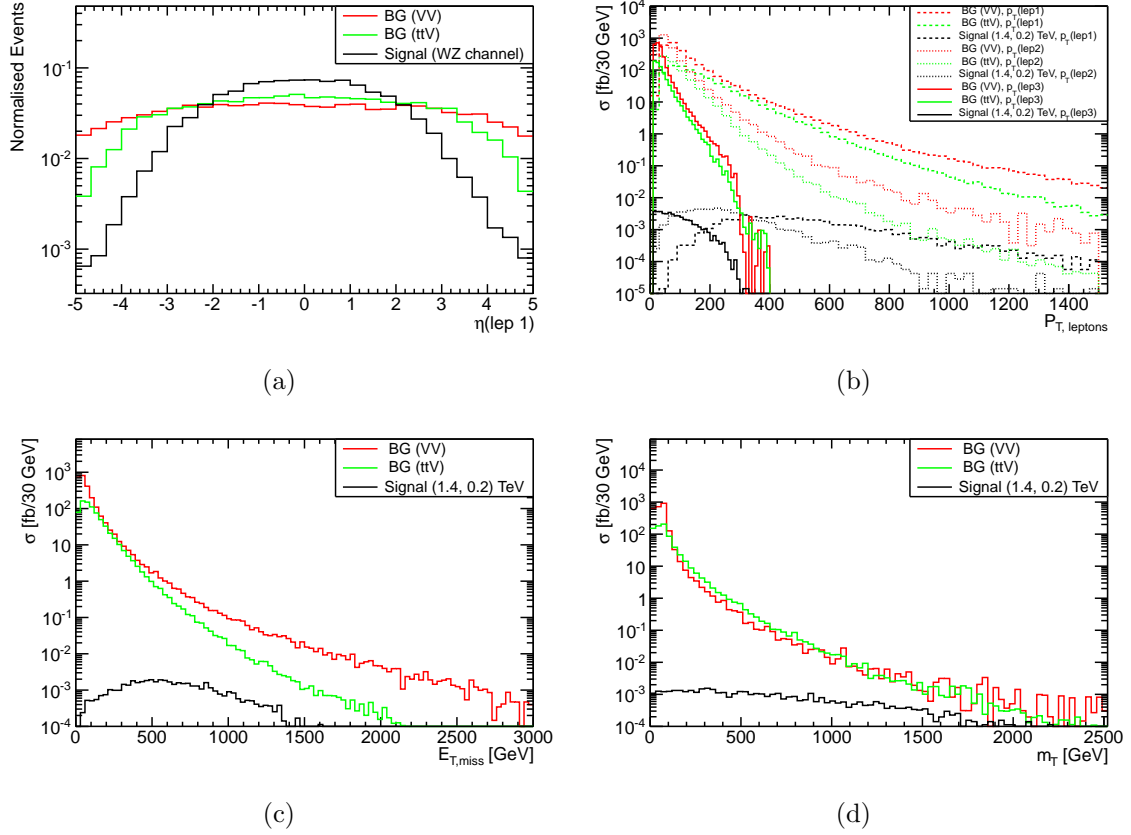


Figure 4.6: The distributions of **(a)** the leading lepton pseudo-rapidity,  $\eta_{\ell_1}$ , **(b)**  $p_T$  of the three hardest leptons, **(c)** the missing transverse energy,  $E_T^{\text{miss}}$ , **(d)** the transverse mass,  $m_T$ . The backgrounds are diboson (VV) and associated top-pair plus vector boson production (ttV). The signal events are generated at our benchmark point,  $M_2 = 1.4 \text{ TeV}$  and  $\mu = 200 \text{ GeV}$ , and only  $WZ$  mode is considered. The parton level events are used for **(a)**, whilst the detector level events after applying the 3 lepton + SFOS cuts are used for **(b)**, **(c)** and **(d)**.

We show the transverse mass  $m_T$  distributions in Fig. 4.6d, where the event samples are again the same as those used in Fig. 4.6b. We define  $m_T \equiv \sqrt{2|p_T(\ell')||E_T^{\text{miss}}|(1 - \cos \Delta\phi)}$ , where  $\ell'$  is the hardest lepton amongst those not chosen as the SFOS lepton pair and  $\Delta\phi$  is the azimuthal difference between the  $\ell'$  and the direction of  $\vec{p}_T^{\text{miss}}$ . In the  $WZ$  background, this distribution has an endpoint at  $m_W$  and above the endpoint the distribution drops very sharply. In the signal events, the distributions are much broader, as can be seen in Fig. 4.6d. A harsh cut on  $m_T$  would also be very helpful to reject a large fraction of background without sacrificing too many signal events.

Signal Region	3 lepton $p_T$ [GeV]	$E_T^{\text{miss}}$ [GeV]	$m_T$ [GeV]
Loose	> 100, 50, 10	> 150	> 150
Medium	> 250, 150, 50	> 350	> 300
Tight	> 400, 200, 75	> 800	> 1100

Table 4.2: The event selection cuts required in the signal regions. These cuts are applied on top of the preselection cuts.

## 4.5 The limit and discovery reach

### 4.5.1 The event selection

Our event selection consists of two parts: *preselection* and *signal region (SR) selection*. The *preselection* requirement is:

- exactly three isolated leptons with  $p_T > 10$  GeV and  $|\eta| < 2.5$ ,
- a same-flavour opposite-sign (SFOS) lepton pair with  $|m_{\ell\ell}^{\text{SFOS}} - m_Z| < 10$  GeV,
- no  $b$ -tagged jet.

With the first condition one can effectively reject the QCD, hadronic  $t\bar{t}$  and single gauge boson backgrounds. The definition of lepton isolation and some discussion around it is given in Appendix A.2. The second condition is introduced to remove the leptonic SM processes without  $Z$  bosons, such as  $t\bar{t}W^\pm$  and  $W^+W^-W^\pm$ . The last condition is effective to reduce the SM backgrounds containing top quarks. In the simulation we use the  $b$ -tagging efficiency of about 70%, which is set in the `Delphes` card used in the `Snowmass` backgrounds.

In order to obtain as large coverage as possible in the  $M_2 - \mu$  parameter plane, we define three signal regions: *Loose*, *Medium*, *Tight*. These signal regions are defined in Table 4.2. The selection cuts are inspired by the kinematical distributions shown in Fig. 4.6. The *Loose* region, which has the mildest cuts, is designed to constrain the degenerate mass region ( $M_2 \gtrsim \mu$ ), whereas the *Tight* region, which has the hardest cuts, targets the hierarchical mass region ( $M_2 \gg \mu$ ). The *Medium* region is also necessary to extend the coverage in the intermediate mass region.

The visible cross section (the cross section for the events satisfying the event selection requirements) for each signal region is shown in Appendix A.3. The information for the detailed breakdown of the background contribution and the visible cross section at each step of the selection is also shown. The number of total background events are expected to be 38400, 810 and 12.3 for the *Loose*, *Medium* and *Tight* signal regions, respectively, at 3000  $\text{fb}^{-1}$  of integrated luminosity.



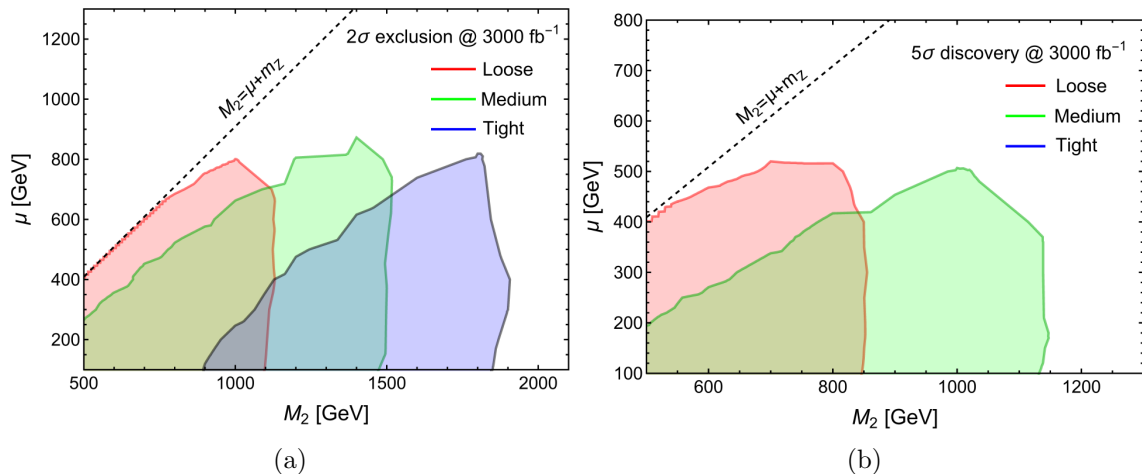


Figure 4.7: The exclusion limits (a) and the discovery reaches (b) obtained from three signal regions. The integrated luminosity of  $3000 \text{ fb}^{-1}$  is assumed.

#### 4.5.2 The result

In Fig. 4.7a, we show the  $2\sigma$  exclusion limits in the  $\mu - M_2$  parameter plane obtained by the different signal regions. The shaded regions have  $S/\sqrt{B} \geq 2$ , where  $S$  and  $B$  are the number of expected signal and background events falling into the signal regions, respectively. For signal we use a constant  $k$ -factor of 1.3 across the parameter plane. One can see that the three signal regions are complementary and  $M_2$  can be constrained up to  $\sim 1.8 \text{ TeV}$  for  $\mu \lesssim 800 \text{ GeV}$ .

Fig. 4.7b shows the  $5\sigma$  discovery reach ( $S/\sqrt{B} \geq 5$ ) obtained from the different signal regions. As can be seen, the *Loose* and *Medium* signal regions provide the discovery reach up to about 850 and 1.1 TeV, respectively, for  $\mu \lesssim 450 \text{ GeV}$ . On the other hand, the *Tight* signal region does not have sensitivity to  $S/\sqrt{B} \geq 5$ .

We show in Fig. 4.8a the global  $2\sigma$  exclusion limits for integrated luminosities of  $3000 \text{ fb}^{-1}$  (red) and  $1000 \text{ fb}^{-1}$  (blue). The global exclusion limit is obtained by choosing the signal region that provides the largest  $S/\sqrt{B}$  for each mass point. The shaded regions around the solid curves represent the uncertainty when varying the background yields by  $\pm 30\%$ . One can see that changing the background by  $30\%$  results in a  $\sim 100 \text{ GeV}$  shift in  $M_2$  for the  $\mu \ll M_2$  region.  $M_2$  can be constrained up to  $1.8 \text{ TeV}$  with  $\mu \lesssim 800 \text{ GeV}$  for  $3000 \text{ fb}^{-1}$ , which can be compared with the projected chargino neutralino mass limit of  $1.1 \text{ TeV}$  for the high luminosity LHC with  $3000 \text{ fb}^{-1}$  obtained by ATLAS [96]. For  $1000 \text{ fb}^{-1}$  the limit on  $M_2$  is about  $1.5 \text{ TeV}$  with  $\mu \lesssim 400 \text{ GeV}$  as can be seen in Fig. 4.8a.

Fig. 4.8b shows the global  $5\sigma$  discovery reach for  $3000 \text{ fb}^{-1}$  (red) and  $1000 \text{ fb}^{-1}$  (blue) with the  $30\%$  uncertainty bands for background. One can see that charginos and neutralinos can be discovered up to  $M_2 \lesssim 1.1 \text{ TeV}$  with  $\mu \lesssim 500 \text{ GeV}$  for  $3000 \text{ fb}^{-1}$  integrated luminosity,

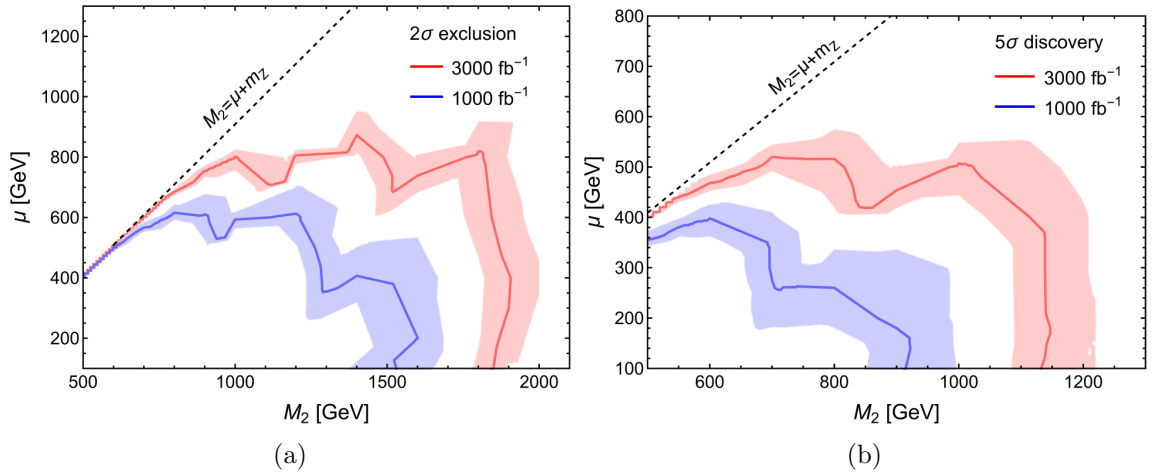


Figure 4.8: The global exclusion limits **(a)** and the discovery reaches **(b)** for 3000 fb<sup>-1</sup> (red) and 1000 fb<sup>-1</sup> (blue). The shaded region represent the uncertainty when varying the background yield by 30 %.

which can be compared with the projected ATLAS value of 0.8 TeV for the high luminosity LHC [96]. For 1000 fb<sup>-1</sup>, charginos and neutralinos can be discovered up to 900 GeV with  $\mu \lesssim 250$  GeV.

Note that in our simulation we include both the  $WZ$  and  $ZZ$  modes in the signal sample, though the contribution from  $ZZ$  mode is typically less than about 5 % after the selection cuts. We have also investigated the contribution from the other modes and found these to be of order  $\sim 10$  % or less, predominantly from  $Zh$ . This can therefore be considered as a small uncertainty on the discovery limit.

## 4.6 Conclusion

We studied the prospect of chargino and neutralino searches at a 100 TeV  $pp$  collider assuming 3000 (1000) fb<sup>-1</sup> of integrated luminosity. Our particular focus was the case where the Higgsinos form the lightest SUSY states (the lightest charginos and the two lightest neutralinos, which are almost mass degenerate) and  $W$ -inos form the second lightest states (the heavier charginos and the third lightest neutralino, which are almost mass degenerate). The other SUSY particles including  $B$ -ino are assumed to be decoupled, which is partly motivated by the current LHC results as well as popular scenarios of SUSY breaking and its mediation. We have shown that in this situation the LO production cross sections of 2 TeV  $W$ -inos are as large as 100 fb<sup>-1</sup> and the branching ratio of  $W$ -inos follows a simple formula, which can be derived from the Goldstone equivalence theorem.

From a study of kinematic distributions of signal and background we found harsh cuts on lepton  $p_T$  ( $> 50 - 400$  GeV),  $E_T^{\text{miss}}$  ( $> 150 - 800$  GeV) and  $m_T$  ( $> 150 - 1100$  GeV)

are beneficial to improve the signal and background ratio and designed three complementary signal regions. Using these three signal regions, we found the  $5\sigma$  discovery reach ( $2\sigma$  exclusion limit) for the chargino-neutralino mass is 1.1 (1.8) TeV for  $\mu \lesssim 500$  (800) GeV, which can be compared with the projected LHC reach (limit) of 0.8 (1.1) TeV obtained by ATLAS [96]. For  $1000 \text{ fb}^{-1}$  the discovery reach (exclusion limit) for the chargino-neutralino mass is found to be 0.9 (1.5) TeV for  $\mu \lesssim 250$  (400) GeV.

We would also like to comment on other hierarchies in the chargino-neutralino spectrum. In this study we have focused on a particular hierarchy ( $|M_2| \gg |\mu|$ ) of the  $W$ -ino and Higgsino states. If the LSP is a  $W$ -ino and the Higgsinos are not decoupled, one can consider the Higgsino pair production process followed by the decay of Higgsinos into the  $W$ -inos. As can be seen from Fig. 4.1a, the chargino-neutralino production has the largest cross section similarly to the  $W$ -ino production case, though the size of the cross section is about 5 times smaller compared to the  $W$ -ino production. Moreover the same argument based on the Goldstone equivalence theorem still holds for the Higgsino decay modes and leads to  $Br(\tilde{H}_{1/2}^0 \rightarrow Z\tilde{W}^0)/Br(\tilde{H}_{1/2}^0 \rightarrow h\tilde{W}^0) \sim 1$ . Therefore, the most promising channel in this scenario is again  $WZ$  + missing energy final state and they are effectively searched for by the 3-lepton analysis we have proposed in this chapter<sup>6</sup>. The same argument applies for the  $B$ -ino LSP case with non-decoupled Higgsinos.

We should also point out that parallel to our work similar studies has been done by [116]. The authors considered a variable:  $H_T(\text{jets})/M_{eff}$ , where  $H_T(\text{jets})$  is the scalar sum of all reconstructed jet  $p_T$ 's and  $M_{eff}$  is the sum of all reconstructed object  $p_T$ 's. This ratio is very useful to discriminate the chargino-neutralino signal from background. We have checked that adding this variable to our event selection improves our exclusion limit (discovery reach) by 200 (300) GeV if the detector simulation is taken into account and the effective lepton separation of  $\Delta R = 0.3$  is used. The authors of [116] used a milder lepton isolation criteria and their study is without a detector simulation.

---

<sup>6</sup>For other search channels in the context of a 100 TeV collider, see [115, 116].

## Chapter 5

# Summary and outlook

In this thesis models arising from M Theory compactified on  $G_2$  holonomy manifolds are considered. Against common lore that string/M theory bares no predictive power, developments of recent years showed that quite the contrary, a few robust assumptions in the string/M theory framework can lead to testable predictions.

In chapter 1 we review theoretical ingredients and generic features of  $G_2$  compactification of M Theory that lead to feasible low-energy theories. In particular, below compactification scale one effectively deals with  $N = 1$  supersymmetric theories with gauge and matter fields as well as scalar fields being remnants of compactification – moduli and axions. Strong dynamics of a hidden sector stabilises moduli fields and breaks supersymmetry. Gravity mediates the SUSY breaking to the visible sector, leading to all soft scalar masses and trilinear couplings being proportional to the gravitino mass  $m_{3/2}$ . Gaugino masses, on the other hand, not receiving direct contributions from the hidden sector, are suppressed compared to  $m_{3/2}$  by about two orders of magnitude. Cosmology constraints moduli mass to be about  $m_{3/2} \sim \mathcal{O}(10 \text{ TeV})$  leading to a distinct particle spectrum with heavy ( $\mathcal{O}(10 \text{ TeV})$ ) sparticles and light gauginos ( $\mathcal{O}(100 \text{ GeV})$ ).

Equipped with general results of M Theory on  $G_2$ , in chapter 2 we explore phenomenology of GUT models in string/M Theory framework with primary focus on solving the infamous doublet-triplet splitting problem. We start with known results of  $SU(5)$  GUT models, before embarking on study of  $SO(10)$  SUSY GUTs. In both cases a discrete symmetry non-commuting with the GUT group is used to solve the doublet-triplet splitting problem, however in the  $SU(5)$  case triplets can be made heavy, while in the  $SO(10)$  case they remain light and can only be decoupled from matter by suppression of colour triplets Yukawas. In order to restore the gauge coupling unification, spoiled by light triplets, we include an extra vector-like pair  $\mathbf{16}_X + \overline{\mathbf{16}}_X$ . We argue that these extra multiplets, also required to break the additional  $U(1)_X$  gauge symmetry, inevitably lead to R-parity violating operators. We find that the constraints on RPV operators from proton lifetime and LSP decays are naturally satisfied, however, their contribution to neutrino masses, without extra suppression, is potentially too

large. We also comment on possibility of relaxing strict relations on parameters (e.g. soft masses, Yukawas) imposed by  $SO(10)$  structure using effective matter multiplets constructed with the help of the discrete symmetry.

In chapter 3 we provide details of a mechanism that breaks the extra  $U(1)_X$  gauge symmetry in our  $SO(10)$  SUSY GUT model. The mechanism is similar to that of Kolda-Martin where higher order terms in the superpotential induce vacuum expectation values for the scalar right-handed neutrino components  $N_X, \bar{N}_X$  of the vector like pair  $\mathbf{16}_X + \bar{\mathbf{16}}_X$ . The symmetry breaking induces R-parity violating interactions which together with other contributions, e.g. those coming from the see-saw mechanism, have impact on neutrino masses. The case of a single neutrino family is studied in great details and we presented several scenarios that result in phenomenologically viable neutrino masses and RPV terms being under control. We conclude that the  $SO(10)$  SUSY GUT model from M Theory on  $G_2$  manifolds provides a phenomenologically viable results with interesting predictions (e.g. light vector like pair, RPV) for physics at the LHC and other experiments.

In chapter 4 the prospect of discovering charginos and neutralinos at a future hadron collider with  $\sqrt{s} = 100$  TeV is investigated. Following general results of M Theory compactified on  $G_2$  manifolds one expects gauginos to be lightest supersymmetric particles. Since scalar superpartners are potentially more than an order of magnitude heavier, gauginos are likely to be first beyond SM particles to be discovered. In our study we consider models where Higgsinos form the main component of the LSP while W-inos are next lightest supersymmetric particles ( $M_2 > \mu$ ), however it is straight forward to consider reverse situation. With sfermions decoupled, pair produced W-inos decay exclusively into  $W, Z$  or SM Higgs accompanied with Higgsinos. Motivated by a clean experimental signature we focus on  $WZ$  channel with gauge bosons decaying leptonically that results in the 3-leptons plus MET signature we search for. We design simple but effective signal regions which we apply on the results of (simplified) detector-level simulations and evaluate discovery reach and exclusion limits. We conclude that with  $3000 \text{ fb}^{-1}$  of integrated luminosity, W-inos could be discovered (excluded) up to 1.1 (1.8) TeV if the spectrum is not compressed.

Finally, let us comment on possible directions for future studies in the field of string/M theory phenomenology. First of all, there is a huge mathematical challenge of finding explicit examples of compact  $G_2$  holonomy manifolds with all the singularities required for phenomenological purposes. Although dualities with other string corners strongly suggest that such examples should exist, there are not known currently. From phenomenological perspective it is still not clear to what extent M Theory can explain the structure of Yukawa couplings we observe. What can it tell about the Cabibbo–Kobayashi–Maskawa and Pontecorvo–Maki–Nakagawa–Sakata matrices? Those questions are particularly relevant to address in full glory for the  $SO(10)$  case considered here, where light states from the vector-like pair are likely to cause, observable in the near future, deviation from SM expectations. Still

open is the question what the dark matter is made from. String/M theory framework provides at least three different possibilities: visible sector supersymmetric particles, hidden sector particles and/or axions, each with their own properties and signatures. With new generation of experiments in energy, precision and cosmology frontiers either proposed or already entering service we should be able to start seeing answers for above and many more questions in the near future.

# Appendices

## A.1 Charge fields Wilson Line absorption

In this section we will present a relation between Wilson line breaking pictures based on a 5D toy model compactified along a 5<sup>th</sup> dimensional circle  $S^1$  of radius  $R$ , i.e. the space is  $M^4 \times S^1$ . On the one hand, a Wilson line corresponds to a non-trivial background gauge field  $B_4$  (along the fifth dimension), that cannot be gauged away in  $M^4 \times S^1$ . From the point of view of a covering space  $M^4 \times R^1$ , however, one can gauge away the background field  $B_M$ , however being left with charge fields absorbing the Wilson line as in Eq. (2.5).

Let's assume that we have a model on  $M^4 \times S^1$  with the (GUT) gauge group  $G = SU(5)$  that we want to break to SM's  $H = SU(3)_C \times SU(2)_L \times U(1)_Y$ . We have a gauge field  $A_M$ , naturally transforming in the adjoint representation of  $SU(5)$  and a field  $\psi$  in the fundamental representation. The Wilson line  $\mathcal{W}$  that breaks the gauge group appropriately to SM can be written as:

$$\mathcal{W} = \text{diag} \left( e^{i2\theta}, e^{i2\theta}, e^{i2\theta}, e^{-i3\theta}, e^{-i3\theta} \right), \quad (\text{A.1})$$

where  $\theta$  is a constant. The fundamental group of  $S^1$  being isomorphic to group  $(\mathbb{Z}, +)$  is not finite, but can be generated by a single element to which Eq. (A.1) corresponds. As  $\pi_1(S^1)$  is not finite, there might **not** be an integer  $N$  such that  $W^N = 1$ .

The Wilson line Eq. (A.1) can be generated from a flat background field  $B$  non zero along extra-dimensional component:

$$B_4 = \text{diag} \left( \frac{2\theta}{2\pi R}, \frac{2\theta}{2\pi R}, \frac{2\theta}{2\pi R}, \frac{-3\theta}{2\pi R}, \frac{-3\theta}{2\pi R} \right), \quad (\text{A.2})$$

following the definition of Wilson lines, Eq. (2.1):

$$\mathcal{W} = \exp \left( i \int_0^{2\pi R} B_4 dx_4 \right). \quad (\text{A.3})$$

From the point of view of the covering space  $R^1$  of the circle  $S^1 = R^1/L$ , where  $L : x \rightarrow$

---

<sup>1</sup>This example is inspired by Section 7 in [142]

$x + 2\pi R$ , fields satisfy periodic boundary conditions:

$$\begin{aligned}\psi(x_\mu, x_4 + 2\pi R) &= \psi(x_\mu, x_4), \\ A_4(x_\mu, x_4 + 2\pi R) &= A_4(x_\mu, x_4).\end{aligned}\tag{A.4}$$

The background field  $B_4$  can be written as a pure gauge:

$$B_4 = i\Lambda^{-1}(x_4)\partial_4\Lambda(x_4),\tag{A.5}$$

with

$$\Lambda(x_4) = \text{diag}(e^{i\frac{2\theta x_4}{2\pi R}}, e^{i\frac{2\theta x_4}{2\pi R}}, e^{i\frac{2\theta x_4}{2\pi R}}, e^{i\frac{-3\theta x_4}{2\pi R}}, e^{i\frac{-3\theta x_4}{2\pi R}}).\tag{A.6}$$

Now, we can apply a gauge transformation  $\Omega(x_4) = \Lambda(x_4)$  transforming fields according to their representations:

$$\begin{aligned}\psi(x_\mu, x_4) &\rightarrow \psi'(x_\mu, x_4) = \Omega(x_4)\psi(x_\mu, x_4), \\ A_4(x_\mu, x_4) &\rightarrow A'_4(x_\mu, x_4) = A_4(x_\mu, x_4) - \Omega^\dagger(x_4)\partial_4\Omega(x_4).\end{aligned}\tag{A.7}$$

This transformation  $\Omega(x_4)$  clearly gauge away the background field  $B_M$ , however, it does not satisfy the periodic boundary condition, but pick up the phase  $\mathcal{W}$ , Eq. (A.1), under a periodic translation  $x_4 \rightarrow x_4 + 2\pi R$ :

$$\Omega(x_4 + 2\pi R) = \mathcal{W}\Omega(x_4).\tag{A.8}$$

This changes the boundary condition for fields transforming in fundamental representation, e.g.:

$$\psi(x_\mu, x_4 + 2\pi R) = \mathcal{W}\psi(x_\mu, x_4),\tag{A.9}$$

leading to absorption of the phase  $\mathcal{W}$  by those fields, breaking representation and in turn breaking the GUT group.

## A.2 The lepton isolation requirement

In hadron colliders, leptons (electrons and muons) may arise from heavy hadron decays. Those ‘‘background’’ leptons are usually found together with other particles around them. The leptons originating from gauge boson decays can therefore be distinguished from the background leptons by investigating activity around the lepton. For this check, *Delphes 3*



uses an isolation variable,  $I$ , defined as

$$I(\ell) = \frac{\sum_{i \neq \ell}^{\Delta R < R, p_T(i) > p_T^{\min}} p_T(i)}{p_T(\ell)}, \quad (\text{A.10})$$

where the numerator sums the  $p_T$  of all particles (except for the lepton itself) with  $p_T > p_T^{\min}$  lying within a cone of radius  $R$  around the lepton. If  $I(\ell)$  is smaller than  $I_{\min}$ , the lepton is said to be isolated, otherwise gets rejected as background. The `Snowmass` samples were generated using `Delphes 3` with the lepton isolation parameters of  $R = 0.3$ ,  $p_T^{\min} = 0.5$  and  $I_{\min} = 0.1$ .

A 100 TeV collider can explore charginos and neutralinos with their mass scale of a few TeV. If the mass hierarchy between  $W$ -ino states and Higgsino states are much higher than the gauge bosons mass scale, the  $W$  and  $Z$  produced from the  $W$ -ino decays will be highly boosted. If such a boosted  $Z$  decays into a pair of same-flavour opposite-sign (SFOS) leptons, those two leptons can be highly collimated, and one may be rejected by the isolation criteria defined above.

To see the impact of this effect, we show the  $\Delta R_{\text{SFOS}}$  (the distance between the SFOS pair<sup>2</sup>) distributions in Fig. A.1. In Fig. A.1, the background sample consists of the most relevant processes,  $WZ$  and  $ttZ$ , which we have generated using `MadGraph 5` and `Pythia 6`.<sup>3</sup> For signal, we examine three benchmark points:  $(M_2, \mu)/\text{GeV} = (800, 200)$ ,  $(1200, 200)$  and  $(1800, 200)$ . The particle level samples are passed to `Delphes 3` with the same detector setup as used in `Snowmass` but with  $R = 0.05$  for the lepton isolation cone radius.

Fig. A.1a shows the  $\Delta R_{\text{SFOS}}$  distributions after the preselection cuts. As can be seen, signal events are more concentrated around the small  $\Delta R_{\text{SFOS}}$  values, while background has rather flat distribution. One can also see that smaller  $\Delta R_{\text{SFOS}}$  is preferred for model points with larger mass hierarchy.

In Fig. A.1b we present the same distributions of  $\Delta R_{\text{SFOS}}$  but with the requirement of  $E_T^{\text{miss}} > 500$  GeV and  $m_T > 200$  GeV on top of the preselection cuts. As can be seen, the distributions are more concentrated for signal and background compared to the distributions with only preselection cuts. This is because the harsh cuts on  $E_T^{\text{miss}}$  and  $m_T$  call for large  $\sqrt{\hat{s}}$  for the partonic collision, leading to more boosted  $Z$  for both signal and background events. One can see that the significant fraction of events has a SFOS lepton pair lying within  $\Delta R_{\text{SFOS}} < 0.3$  of each other, and it is expected that the `Snowmass` lepton isolation criteria with  $R = 0.3$  would reject some fraction of signal and background events.

One can see the detrimental impact of the rather large lepton isolation criteria  $R = 0.3$

<sup>2</sup>To be explicit,  $\Delta R_{\text{SFOS}} = \sqrt{(\Delta\phi_{\text{SFOS}})^2 + (\Delta\eta_{\text{SFOS}})^2}$ , where  $\Delta\phi_{\text{SFOS}}$  and  $\Delta\eta_{\text{SFOS}}$  are the azimuthal and pseudo-rapidity differences between the SFOS lepton pair.

<sup>3</sup>In the  $WZ$  sample, two extra partons are matched with the parton shower radiation with the MLM merging scheme [143].

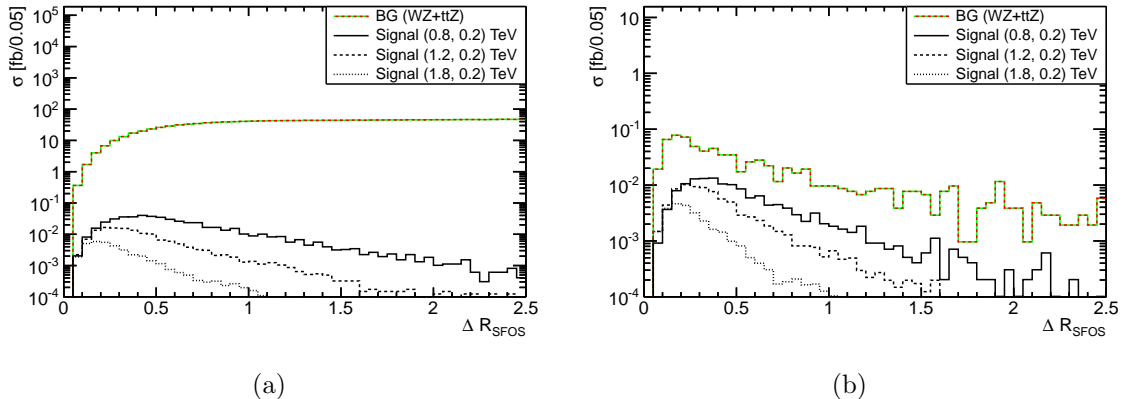


Figure A.1: The distributions of  $\Delta R_{\text{SFOS}}$ , the distance between the SFOS lepton pair, **(a)** after preselection cuts, **(b)** after additional cuts:  $E_T^{\text{miss}} > 500$  GeV and  $m_T > 200$  GeV. For both plots, detector simulation has been done by `Delphes 3` using the same detector setup as the one used in `Snowmass` samples but with  $R = 0.05$ .

on our discovery reach in Fig. A.2 where we present the acceptance of signal events (for the Loose SR) for different  $(M_2, \mu)$  model points. The acceptance drops as the mass difference between Higgsinos and W-inos increases (producing more boosted  $Z$ ) along the arrow marked  $\Delta R$ . We therefore believe that employing smaller lepton isolation cone radius will improve the chargino-neutralino mass reach to some extent, although a dedicated study in this direction is beyond the scope of this work.

### A.3 The visible cross sections

In this section we report the visible cross sections (the cross section after cuts) for each step of the selection cuts for different processes. Four sets of samples are considered for the SM background, which are defined in Table 4.1. We show the results for three benchmark model points for signal:  $(M_2, \mu)/\text{GeV} = (800, 200)$ ,  $(1200, 200)$  and  $(1800, 200)$ . The (visible) cross sections with k-factor = 3 are shown in fb for all tables in this section. Table A.1 shows the (visible) cross sections for the cuts employed in the *preselection* stage. Table A.2, A.3 and A.4 show the visible cross sections for the cuts used in *Loose*, *Medium* and *Tight* signal regions, respectively. The last columns in Tables A.2, A.3 and A.4 show  $S/\sqrt{B}$  assuming  $3000 \text{ fb}^{-1}$  of integrated luminosity for the three different benchmark points.

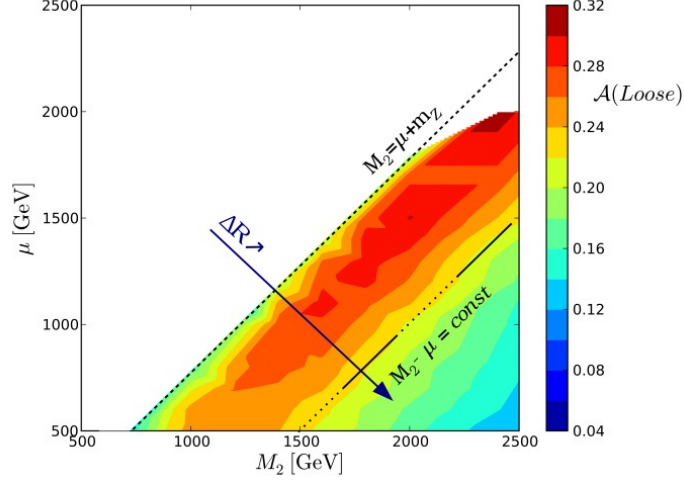


Figure A.2: The acceptance of signal events for the Loose SR for different data points. The higher the mass difference  $M_2 - \mu$ , the smaller lepton isolation ( $\Delta R$ ) and the worst reconstruction efficiency. This is inherited with the **Snowmass** detector card.

Process	No cut	= 3 lepton	$ m_{\ell\ell}^{\text{SFOS}} - m_Z  < 10$	no- $b$ jet
VV	3025348	2487	2338	2176
ttV	220161	792	552	318
tV	2764638	68.9	6.07	4.12
VVV	36276	76.1	56.2	56.2
BG total	6046422	3424	2952	2554
$(M_2, \mu) = (800, 200)$	1.640	0.588	0.565	0.534
$(M_2, \mu) = (1200, 200)$	0.397	0.124	0.119	0.111
$(M_2, \mu) = (1800, 200)$	0.0863	0.0190	0.0179	0.0170

Table A.1: The (visible) cross sections (in fb) for the cuts employed in the *preselection*. The column marked "No cut" shows the cross sections for the background processes (defined in Table 4.1) and the cross section times branching ratio into 3 leptons via  $WZ$  for signal benchmark points.

Process	$p_T^\ell > (100, 50, 10)$	$E_T^{\text{miss}} > 150$	$m_T > 150$	$S/\sqrt{B}$
VV	647	106	5.1	
ttV	176	41.2	6.6	
tV	0.665	0.391	0.0793	
VVV	23.4	6.0	1.06	
BG total	847	153	12.8	
$(M_2, \mu) = (800, 200)$	0.506	0.465	0.381	5.82
$(M_2, \mu) = (1200, 200)$	0.109	0.103	0.090	1.38
$(M_2, \mu) = (1800, 200)$	0.0168	0.0164	0.0150	0.234

Table A.2: The visible cross sections (in fb) used in the *Loose* signal region. The last column shows  $S/\sqrt{B}$  assuming the  $3000 \text{ fb}^{-1}$  luminosity for different benchmark points.

Process	$p_T^\ell > (250, 150, 50)$	$E_T^{\text{miss}} > 350$	$m_T > 300$	$S/\sqrt{B}$
VV	33.8	3.13	0.106	
ttV	9.84	0.780	0.119	
tV	0.037	0.0213	0.00132	
VVV	1.87	0.291	0.0442	
BG total	45.6	4.22	0.271	
$(M_2, \mu) = (800, 200)$	0.170	0.107	0.0845	8.89
$(M_2, \mu) = (1200, 200)$	0.0572	0.0463	0.0408	4.30
$(M_2, \mu) = (1800, 200)$	0.0099	0.0088	0.0081	0.845

Table A.3: The visible cross sections (in fb) used in the *Medium* signal region. The last column shows  $S/\sqrt{B}$  assuming the  $3000 \text{ fb}^{-1}$  luminosity for different benchmark points.

Process	$p_T^\ell > (400, 200, 75)$	$E_T^{\text{miss}} > 800$	$m_T > 1100$	$S/\sqrt{B}$
VV	5.65	0.123	0.00166	
ttV	1.03	0.0056	0.00092	
tV	0.015	0.0001	0	
VVV	0.350	0.0109	0.00153	
BG total	7.05	0.140	0.00411	
$(M_2, \mu) = (800, 200)$	0.0460	0.0020	0.0012	1.00
$(M_2, \mu) = (1200, 200)$	0.0238	0.0070	0.0052	4.45
$(M_2, \mu) = (1800, 200)$	0.0053	0.0031	0.0026	2.22

Table A.4: The visible cross sections (in fb) used in the *Tight* signal region. The last column shows  $S/\sqrt{B}$  assuming the  $3000 \text{ fb}^{-1}$  luminosity for different benchmark points.

# Bibliography

- [1] S. L. Glashow, *Partial-symmetries of weak interactions*, *Nuclear Physics* **22** (1961), no. 4 579 – 588.
- [2] S. Weinberg, *A model of leptons*, *Phys. Rev. Lett.* **19** (Nov, 1967) 1264–1266.
- [3] A. Salam, *Weak and electromagnetic interactions*, in *Elementary particle theory* (N. Svartholm, ed.), pp. 367–377, Almquist & Wiksell.
- [4] K. Becker, M. Becker, and J. Schwarz, *String theory and M-theory: A modern introduction*, .
- [5] P. Candelas, G. T. Horowitz, A. Strominger, and E. Witten, *Vacuum Configurations for Superstrings*, *Nucl. Phys.* **B258** (1985) 46–74.
- [6] G. Papadopoulos and P. K. Townsend, *Compactification of  $D = 11$  supergravity on spaces of exceptional holonomy*, *Phys. Lett.* **B357** (1995) 300–306, [[hep-th/9506150](#)].
- [7] M. R. Douglas, *The Statistics of string / M theory vacua*, *JHEP* **0305** (2003) 046, [[hep-th/0303194](#)].
- [8] H. Ooguri and C. Vafa, *On the Geometry of the String Landscape and the Swampland*, *Nucl.Phys.* **B766** (2007) 21–33, [[hep-th/0605264](#)].
- [9] B. S. Acharya and M. R. Douglas, *A Finite landscape?*, [hep-th/0606212](#).
- [10] B. S. Acharya, K. Bobkov, G. L. Kane, P. Kumar, and J. Shao, *Explaining the Electroweak Scale and Stabilizing Moduli in M Theory*, *Phys.Rev.* **D76** (2007) 126010, [[hep-th/0701034](#)].
- [11] B. S. Acharya, K. Bobkov, G. L. Kane, J. Shao, and P. Kumar, *The  $G(2)$ -MSSM: An M Theory motivated model of Particle Physics*, *Phys. Rev.* **D78** (2008) 065038, [[arXiv:0801.0478](#)].
- [12] B. S. Acharya, G. Kane, and P. Kumar, *Compactified String Theories – Generic Predictions for Particle Physics*, *Int. J. Mod. Phys.* **A27** (2012) 1230012, [[arXiv:1204.2795](#)].

- [13] S. Kachru, R. Kallosh, A. D. Linde, and S. P. Trivedi, *De Sitter vacua in string theory*, *Phys.Rev.* **D68** (2003) 046005, [[hep-th/0301240](#)].
- [14] V. Balasubramanian, P. Berglund, J. P. Conlon, and F. Quevedo, *Systematics of moduli stabilisation in Calabi-Yau flux compactifications*, *JHEP* **0503** (2005) 007, [[hep-th/0502058](#)].
- [15] B. S. Acharya, K. Božek, M. Crispim Romão, S. F. King, and C. Pongkitivanichkul, *SO(10) Grand Unification in M theory on a G2 manifold*, *Phys. Rev.* **D92** (2015), no. 5 055011, [[arXiv:1502.01727](#)].
- [16] B. S. Acharya, K. Božek, M. Crispim Romão, S. F. King, and C. Pongkitivanichkul, *Neutrino mass from M Theory SO(10)*, *JHEP* **11** (2016) 173, [[arXiv:1607.06741](#)].
- [17] B. S. Acharya, K. Božek, C. Pongkitivanichkul, and K. Sakurai, *Prospects for observing charginos and neutralinos at a 100 TeV proton-proton collider*, *JHEP* **02** (2015) 181, [[arXiv:1410.1532](#)].
- [18] S. P. Martin, *A Supersymmetry primer*, [hep-ph/9709356](#). [Adv. Ser. Direct. High Energy Phys.18,1(1998)].
- [19] P. West, *Introduction to Supersymmetry and Supergravity*. World Scientific, 1986.
- [20] J. Wess and J. Bagger, *Supersymmetry and Supergravity*. Princeton series in physics. Princeton University Press, 1992.
- [21] B. S. Acharya, K. Bobkov, G. Kane, P. Kumar, and D. Vaman, *An M theory Solution to the Hierarchy Problem*, *Phys.Rev.Lett.* **97** (2006) 191601, [[hep-th/0606262](#)].
- [22] B. S. Acharya and K. Bobkov, *Kahler Independence of the G(2)-MSSM*, *JHEP* **1009** (2010) 001, [[arXiv:0810.3285](#)].
- [23] D. J. H. Chung, L. L. Everett, G. L. Kane, S. F. King, J. D. Lykken, and L.-T. Wang, *The Soft supersymmetry breaking Lagrangian: Theory and applications*, *Phys. Rept.* **407** (2005) 1–203, [[hep-ph/0312378](#)].
- [24] P. Kumar, *Compactified String Theories — Generic Predictions for Particle Physics*, *Adv. Ser. Direct. High Energy Phys.* **22** (2015) 277–324.
- [25] M. K. Gaillard, *Perspective on the weakly coupled heterotic string*, *Adv. Ser. Direct. High Energy Phys.* **22** (2015) 23–47.
- [26] J. H. Schwarz, *Lectures on superstring and M theory dualities: Given at ICTP Spring School and at TASI Summer School*, *Nucl. Phys. Proc. Suppl.* **55B** (1997) 1–32, [[hep-th/9607201](#)].

- [27] B. S. Acharya and S. Gukov, *M theory and singularities of exceptional holonomy manifolds*, *Phys. Rept.* **392** (2004) 121–189, [[hep-th/0409191](#)].
- [28] B. S. Acharya, *M theory, Joyce orbifolds and superYang-Mills*, *Adv. Theor. Math. Phys.* **3** (1999) 227–248, [[hep-th/9812205](#)].
- [29] B. S. Acharya, *On Realizing  $N=1$  superYang-Mills in M theory*, [hep-th/0011089](#).
- [30] B. S. Acharya and E. Witten, *Chiral fermions from manifolds of  $G(2)$  holonomy*, [hep-th/0109152](#).
- [31] M. Atiyah and E. Witten, *M theory dynamics on a manifold of  $G(2)$  holonomy*, *Adv. Theor. Math. Phys.* **6** (2003) 1–106, [[hep-th/0107177](#)].
- [32] S. B. Giddings, S. Kachru, and J. Polchinski, *Hierarchies from fluxes in string compactifications*, *Phys. Rev.* **D66** (2002) 106006, [[hep-th/0105097](#)].
- [33] B. S. Acharya, *A Moduli fixing mechanism in M theory*, [hep-th/0212294](#).
- [34] B. S. Acharya, F. Denef, and R. Valandro, *Statistics of M theory vacua*, *JHEP* **06** (2005) 056, [[hep-th/0502060](#)].
- [35] B. S. Acharya, G. Kane, and E. Kuflik, *Bounds on scalar masses in theories of moduli stabilization*, *Int. J. Mod. Phys.* **A29** (2014) 1450073, [[arXiv:1006.3272](#)].
- [36] B. S. Acharya, K. Bobkov, and P. Kumar, *An M Theory Solution to the Strong CP Problem and Constraints on the Axiverse*, *JHEP* **1011** (2010) 105, [[arXiv:1004.5138](#)].
- [37] A. Brignole, L. E. Ibanez, and C. Munoz, *Soft supersymmetry breaking terms from supergravity and superstring models*, *Adv. Ser. Direct. High Energy Phys.* **21** (2010) 244–268, [[hep-ph/9707209](#)].
- [38] E. Witten, *Deconstruction,  $G(2)$  holonomy, and doublet triplet splitting*, [hep-ph/0201018](#).
- [39] E. Witten, *Symmetry Breaking Patterns in Superstring Models*, *Nucl.Phys.* **B258** (1985) 75.
- [40] R. N. Mohapatra and M. Ratz, *Gauged Discrete Symmetries and Proton Stability*, *Phys.Rev.* **D76** (2007) 095003, [[arXiv:0707.4070](#)].
- [41] H. M. Lee, S. Raby, M. Ratz, G. G. Ross, R. Schieren, et al., *A unique  $Z_4^R$  symmetry for the MSSM*, *Phys.Lett.* **B694** (2011) 491–495, [[arXiv:1009.0905](#)].

- [42] G. Dvali, *Light color triplet Higgs is compatible with proton stability: An Alternative approach to the doublet - triplet splitting problem*, *Phys.Lett.* **B372** (1996) 113–120, [[hep-ph/9511237](#)].
- [43] W. Kilian and J. Reuter, *Unification without doublet-triplet splitting*, *Phys.Lett.* **B642** (2006) 81–84, [[hep-ph/0606277](#)].
- [44] J. Reuter, *SUSY multi-step unification without doublet-triplet splitting*, [arXiv:0709.4202](#).
- [45] R. Howl and S. King, *Minimal  $E(6)$  Supersymmetric Standard Model*, *JHEP* **0801** (2008) 030, [[arXiv:0708.1451](#)].
- [46] Y. Hosotani, *Dynamical mass generation by compact extra dimensions*, *Physics Letters B* **126** (1983), no. 5 309 – 313.
- [47] E. Witten, *Symmetry breaking patterns in superstring models*, *Nuclear Physics B* **258** (1985) 75 – 100.
- [48] D. C. Lewellen, *Embedding higher-level kac-moody algebras in heterotic string models*, *Nuclear Physics B* **337** (1990), no. 1 61 – 86.
- [49] J. Ellis, J. L. Lopez, and D. Nanopoulos, *Constraints on grand unified superstring theories*, *Physics Letters B* **245** (1990), no. 3 375 – 383.
- [50] I. Antoniadis, J. Ellis, J. Hagelin, and D. Nanopoulos, *Supersymmetric flipped  $su(5)$  revitalized*, *Physics Letters B* **194** (1987), no. 2 231 – 235.
- [51] A. Hebecker and J. March-Russell, *The structure of GUT breaking by orbifolding*, *Nucl. Phys.* **B625** (2002) 128–150, [[hep-ph/0107039](#)].
- [52] L. J. Hall, H. Murayama, and Y. Nomura, *Wilson lines and symmetry breaking on orbifolds*, *Nucl. Phys.* **B645** (2002) 85–104, [[hep-th/0107245](#)].
- [53] H. Georgi, *LIE ALGEBRAS IN PARTICLE PHYSICS. FROM ISOSPIN TO UNIFIED THEORIES*, *Front. Phys.* **54** (1982) 1–255.
- [54] G. Giudice and A. Masiero, *A Natural Solution to the  $\mu$  Problem in Supergravity Theories*, *Phys.Lett.* **B206** (1988) 480–484.
- [55] B. S. Acharya, G. Kane, E. Kuflik, and R. Lu, *Theory and Phenomenology of  $\mu$  in  $M$  theory*, *JHEP* **1105** (2011) 033, [[arXiv:1102.0556](#)].
- [56] C. Patrignani and P. D. Group, *Review of particle physics*, *Chinese Physics C* **40** (2016), no. 10 100001.



- [57] S. P. Martin and M. T. Vaughn, *Two loop renormalization group equations for soft supersymmetry breaking couplings*, *Phys. Rev.* **D50** (1994) 2282, [[hep-ph/9311340](#)].  
[Erratum: *Phys. Rev.*D78,039903(2008)].
- [58] C. F. Kolda and S. P. Martin, *Low-energy supersymmetry with D term contributions to scalar masses*, *Phys. Rev.* **D53** (1996) 3871–3883, [[hep-ph/9503445](#)].
- [59] P. Minkowski,  *$\mu \rightarrow e\gamma$  at a Rate of One Out of  $10^9$  Muon Decays?*, *Phys. Lett.* **B67** (1977) 421–428.
- [60] M. Gell-Mann, P. Ramond, and R. Slansky, *Complex Spinors and Unified Theories*, *Conf. Proc.* **C790927** (1979) 315–321, [[arXiv:1306.4669](#)].
- [61] T. Yanagida, *HORIZONTAL SYMMETRY AND MASSES OF NEUTRINOS*, *Conf. Proc.* **C7902131** (1979) 95–99.
- [62] R. N. Mohapatra and G. Senjanovic, *Neutrino Mass and Spontaneous Parity Violation*, *Phys. Rev. Lett.* **44** (1980) 912.
- [63] J. Schechter and J. W. F. Valle, *Neutrino Masses in  $SU(2) \times U(1)$  Theories*, *Phys. Rev.* **D22** (1980) 2227.
- [64] M. B. Green and J. H. Schwarz, *Anomaly Cancellation in Supersymmetric  $D=10$  Gauge Theory and Superstring Theory*, *Phys. Lett.* **149B** (1984) 117–122.
- [65] M. Dine, N. Seiberg, and E. Witten, *Fayet-iliopoulos terms in string theory*, *Nuclear Physics B* **289** (1987) 589 – 598.
- [66] J. J. Atick, L. J. Dixon, and A. Sen, *String calculation of fayet-iliopoulos d-terms in arbitrary supersymmetric compactifications*, *Nuclear Physics B* **292** (1987) 109 – 149.
- [67] T. Pantev and M. Wijnholt, *Hitchin’s Equations and M-Theory Phenomenology*, *J. Geom. Phys.* **61** (2011) 1223–1247, [[arXiv:0905.1968](#)].
- [68] E. Witten, *Anomaly cancellation on  $G(2)$  manifolds*, [hep-th/0108165](#).
- [69] R. Barbier et al., *R-parity violating supersymmetry*, *Phys. Rept.* **420** (2005) 1–202, [[hep-ph/0406039](#)].
- [70] T. Banks, Y. Grossman, E. Nardi, and Y. Nir, *Supersymmetry without R-parity and without lepton number*, *Phys.Rev.* **D52** (1995) 5319–5325, [[hep-ph/9505248](#)].
- [71] B. S. Acharya, G. L. Kane, P. Kumar, R. Lu, and B. Zheng, *R-Parity Conservation from a Top Down Perspective*, *JHEP* **1410** (2014) 1, [[arXiv:1403.4948](#)].

- [72] H. K. Dreiner, *An Introduction to explicit R-parity violation*, *Adv.Ser.Direct.High Energy Phys.* **21** (2010) 565–583, [[hep-ph/9707435](#)].
- [73] P. Svrcek and E. Witten, *Axions In String Theory*, *JHEP* **0606** (2006) 051, [[hep-th/0605206](#)].
- [74] B. S. Acharya, S. A. R. Ellis, G. L. Kane, B. D. Nelson, and M. J. Perry, *The lightest visible-sector supersymmetric particle is likely to be unstable*, [arXiv:1604.05320](#).
- [75] B. S. Acharya, S. A. R. Ellis, G. L. Kane, B. D. Nelson, and M. Perry, *Categorisation and Detection of Dark Matter Candidates from String/M-theory Hidden Sectors*, [arXiv:1707.04530](#).
- [76] T. Araki, T. Kobayashi, J. Kubo, S. Ramos-Sanchez, M. Ratz, et al., *(Non-)Abelian discrete anomalies*, *Nucl.Phys.* **B805** (2008) 124–147, [[arXiv:0805.0207](#)].
- [77] L. J. Hall, R. Rattazzi, and U. Sarid, *The Top quark mass in supersymmetric SO(10) unification*, *Phys. Rev.* **D50** (1994) 7048–7065, [[hep-ph/9306309](#)].
- [78] R. Rattazzi, U. Sarid, and L. J. Hall, *Yukawa unification: The good, the bad and the ugly*, in *Yukawa couplings and the origins of mass. Proceedings, 2nd IFT Workshop, Gainesville, USA, February 11-13, 1994*, 1994. [hep-ph/9405313](#).
- [79] H. Murayama, M. Olechowski, and S. Pokorski, *Viable  $t - b - \tau$  Yukawa unification in SUSY SO(10)*, *Phys. Lett.* **B371** (1996) 57–64, [[hep-ph/9510327](#)].
- [80] H. Baer, M. A. Diaz, J. Ferrandis, and X. Tata, *Sparticle mass spectra from SO(10) grand unified models with Yukawa coupling unification*, *Phys. Rev.* **D61** (2000) 111701, [[hep-ph/9907211](#)].
- [81] D. Auto, H. Baer, C. Balazs, A. Belyaev, J. Ferrandis, et al., *Yukawa coupling unification in supersymmetric models*, *JHEP* **0306** (2003) 023, [[hep-ph/0302155](#)].
- [82] H. Baer, S. Kraml, and S. Sekmen, *Is 'just-so' Higgs splitting needed for  $t - b - \tau$  Yukawa unified SUSY GUTs?*, *JHEP* **0909** (2009) 005, [[arXiv:0908.0134](#)].
- [83] A. S. Joshipura and K. M. Patel, *Yukawa coupling unification in so(10) with positive  $\mu$  and a heavier gluino*, *Phys. Rev.* **D86** (2012) 035019, [[arXiv:1206.3910](#)].
- [84] R. Blumenhagen, M. Cvetič, and T. Weigand, *Spacetime instanton corrections in 4D string vacua: The Seesaw mechanism for D-Brane models*, *Nucl. Phys.* **B771** (2007) 113–142, [[hep-th/0609191](#)].
- [85] L. E. Ibanez and A. M. Uranga, *Neutrino Majorana Masses from String Theory Instanton Effects*, *JHEP* **03** (2007) 052, [[hep-th/0609213](#)].

- [86] M. Cvetič, R. Richter, and T. Weigand, *Computation of D-brane instanton induced superpotential couplings: Majorana masses from string theory*, *Phys. Rev.* **D76** (2007) 086002, [[hep-th/0703028](#)].
- [87] W. Buchmüller, K. Hamaguchi, O. Lebedev, S. Ramos-Sanchez, and M. Ratz, *Seesaw neutrinos from the heterotic string*, *Phys. Rev. Lett.* **99** (2007) 021601, [[hep-ph/0703078](#)].
- [88] J. P. Conlon and D. Cremades, *The Neutrino Suppression Scale from Large Volumes*, *Phys. Rev. Lett.* **99** (2007) 041803, [[hep-ph/0611144](#)].
- [89] A. E. Faraggi,  *$\nu_\tau$  Mass as Possible Evidence for a Superstring Inspired Standard Like Model*, *Phys. Lett.* **B245** (1990) 435–440.
- [90] A. E. Faraggi and E. Halyo, *Neutrino masses in superstring derived standard - like models*, *Phys. Lett.* **B307** (1993) 311–317, [[hep-th/9303060](#)].
- [91] C. Coriano and A. E. Faraggi, *String inspired neutrino mass textures in light of KamLAND and WMAP*, *Phys. Lett.* **B581** (2004) 99–110, [[hep-ph/0306186](#)].
- [92] M. Drees, *Intermediate Scale Symmetry Breaking and the Spectrum of Super Partners in Superstring Inspired Supergravity Models*, *Phys. Lett.* **B181** (1986) 279.
- [93] M. Hirsch, M. A. Diaz, W. Porod, J. C. Romao, and J. W. F. Valle, *Neutrino masses and mixings from supersymmetry with bilinear R parity violation: A Theory for solar and atmospheric neutrino oscillations*, *Phys. Rev.* **D62** (2000) 113008, [[hep-ph/0004115](#)]. [Erratum: *Phys. Rev.* D65,119901(2002)].
- [94] **ATLAS** Collaboration, M. Aaboud et al., *Search for electroweak production of supersymmetric particles in final states with two or three leptons at  $\sqrt{s} = 13$  TeV with the ATLAS detector*, [arXiv:1803.02762](#).
- [95] **CMS** Collaboration, A. M. Sirunyan et al., *Combined search for electroweak production of charginos and neutralinos in proton-proton collisions at  $\sqrt{s} = 13$  TeV*, [arXiv:1801.03957](#).
- [96] **ATLAS** Collaboration, *Search for Supersymmetry at the high luminosity LHC with the ATLAS experiment*, Tech. Rep. ATL-PHYS-PUB-2014-010, CERN, Geneva, 2014.
- [97] **CMS Collaboration** Collaboration, *Supersymmetry discovery potential in future LHC and HL-LHC running with the CMS detector*, Tech. Rep. CMS-PAS-SUS-14-012, CERN, Geneva, 2015.
- [98] T. Cohen, T. Golling, M. Hance, A. Henrichs, K. Howe, et al., *SUSY Simplified Models at 14, 33, and 100 TeV Proton Colliders*, *JHEP* **1404** (2014) 117, [[arXiv:1311.6480](#)].

- [99] T. Andeen, C. Bernard, K. Black, T. Childres, L. Dell’Asta, et al., *Sensitivity to the Single Production of Vector-Like Quarks at an Upgraded Large Hadron Collider*, [arXiv:1309.1888](#).
- [100] L. Apanasevich, S. Upadhyay, N. Varelas, D. Whiteson, and F. Yu, *Sensitivity of potential future pp colliders to quark compositeness*, [arXiv:1307.7149](#).
- [101] D. Stolarski, *Reach in All Hadronic Stop Decays: A Snowmass White Paper*, [arXiv:1309.1514](#).
- [102] T. Cohen, R. T. D’Agnolo, M. Hance, H. K. Lou, and J. G. Wacker, *Boosting Stop Searches with a 100 TeV Proton Collider*, *JHEP* **11** (2014) 021, [[arXiv:1406.4512](#)].
- [103] F. Yu, *Di-jet resonances at future hadron colliders: A Snowmass whitepaper*, [arXiv:1308.1077](#).
- [104] N. Zhou, D. Berge, L. Wang, D. Whiteson, and T. Tait, *Sensitivity of future collider facilities to WIMP pair production via effective operators and light mediators*, [arXiv:1307.5327](#).
- [105] S. Jung and J. D. Wells, *Gaugino physics of split supersymmetry spectrum at the LHC and future proton colliders*, *Phys.Rev.* **D89** (2014) 075004, [[arXiv:1312.1802](#)].
- [106] A. Fowlie and M. Raidal, *Prospects for constrained supersymmetry at  $\sqrt{s} = 33$  TeV and  $\sqrt{s} = 100$  TeV proton-proton super-colliders*, *Eur.Phys.J.* **C74** (2014) 2948, [[arXiv:1402.5419](#)].
- [107] S. A. R. Ellis, G. L. Kane, and B. Zheng, *Superpartners at LHC and Future Colliders: Predictions from Constrained Compactified M-Theory*, [arXiv:1408.1961](#).
- [108] M. Low and L.-T. Wang, *Neutralino Dark Matter at 100 TeV*, [arXiv:1404.0682](#).
- [109] M. Cirelli, F. Sala, and M. Taoso, *Wino-like Minimal Dark Matter and future colliders*, [arXiv:1407.7058](#).
- [110] D. Curtin, P. Meade, and C.-T. Yu, *Testing Electroweak Baryogenesis with Future Colliders*, *JHEP* **1411** (2014) 127, [[arXiv:1409.0005](#)].
- [111] A. Berlin, T. Lin, M. Low, and L.-T. Wang, *Neutralinos in Vector Boson Fusion at High Energy Colliders*, *Phys. Rev.* **D91** (2015), no. 11 115002, [[arXiv:1502.05044](#)].
- [112] J. Fan, P. Jaiswal, and S. C. Leung, *Jet Observables and Stops at 100 TeV Collider*, *Phys. Rev.* **D96** (2017), no. 3 036017, [[arXiv:1704.03014](#)].

- [113] H. Beauchesne, K. Earl, and T. Grégoire, *LHC constraints on Mini-Split anomaly and gauge mediation and prospects for LHC 14 and a future 100 TeV pp collider*, *JHEP* **08** (2015) 117, [[arXiv:1503.03099](#)].
- [114] C.-R. Chen, J. Hajer, T. Liu, I. Low, and H. Zhang, *Testing naturalness at 100 TeV*, *JHEP* **09** (2017) 129, [[arXiv:1705.07743](#)].
- [115] G. Grilli di Cortona, *Hunting electroweakinos at future hadron colliders and direct detection experiments*, *JHEP* **05** (2015) 035, [[arXiv:1412.5952](#)].
- [116] S. Gori, S. Jung, L.-T. Wang, and J. D. Wells, *Prospects for Electroweakino Discovery at a 100 TeV Hadron Collider*, [arXiv:1410.6287](#).
- [117] N. Arkani-Hamed, T. Han, M. Mangano, and L.-T. Wang, *Physics opportunities of a 100 TeV proton–proton collider*, *Phys. Rept.* **652** (2016) 1–49, [[arXiv:1511.06495](#)].
- [118] M. Mangano, *Physics at the FCC-hh, a 100 TeV pp collider*, [arXiv:1710.06353](#).
- [119] L. Randall and R. Sundrum, *Out of this world supersymmetry breaking*, *Nucl.Phys.* **B557** (1999) 79–118, [[hep-th/9810155](#)].
- [120] G. F. Giudice, M. A. Luty, H. Murayama, and R. Rattazzi, *Gaugino mass without singlets*, *JHEP* **9812** (1998) 027, [[hep-ph/9810442](#)].
- [121] T. Moroi and L. Randall, *Wino cold dark matter from anomaly mediated SUSY breaking*, *Nucl.Phys.* **B570** (2000) 455–472, [[hep-ph/9906527](#)].
- [122] N. Arkani-Hamed and S. Dimopoulos, *Supersymmetric unification without low energy supersymmetry and signatures for fine-tuning at the LHC*, *JHEP* **0506** (2005) 073, [[hep-th/0405159](#)].
- [123] G. Giudice and A. Romanino, *Split supersymmetry*, *Nucl.Phys.* **B699** (2004) 65–89, [[hep-ph/0406088](#)].
- [124] N. Arkani-Hamed, S. Dimopoulos, G. Giudice, and A. Romanino, *Aspects of split supersymmetry*, *Nucl.Phys.* **B709** (2005) 3–46, [[hep-ph/0409232](#)].
- [125] **DELPHES 3** Collaboration, J. de Favereau et al., *DELPHES 3, A modular framework for fast simulation of a generic collider experiment*, *JHEP* **1402** (2014) 057, [[arXiv:1307.6346](#)].
- [126] G. Salam and A. Weiler. <http://collider-reach.web.cern.ch/>.
- [127] J. Alwall, R. Frederix, S. Frixione, V. Hirschi, F. Maltoni, et al., *The automated computation of tree-level and next-to-leading order differential cross sections, and their matching to parton shower simulations*, *JHEP* **1407** (2014) 079, [[arXiv:1405.0301](#)].

- [128] S. Jung, *Resolving the existence of Higgsinos in the LHC inverse problem*, *JHEP* **1406** (2014) 111, [[arXiv:1404.2691](#)].
- [129] A. Djouadi, M. Muhlleitner, and M. Spira, *Decays of supersymmetric particles: The Program SUSY-HIT (SUSpect-SdecaY-Hdecay-Interface)*, *Acta Phys.Polon.* **B38** (2007) 635–644, [[hep-ph/0609292](#)].
- [130] H. Baer, V. Barger, A. Lessa, W. Sreethawong, and X. Tata, *Wh plus missing- $E_T$  signature from gaugino pair production at the LHC*, *Phys.Rev.* **D85** (2012) 055022, [[arXiv:1201.2949](#)].
- [131] T. Han, S. Padhi, and S. Su, *Electroweakinos in the Light of the Higgs Boson*, *Phys.Rev.* **D88** (2013) 115010, [[arXiv:1309.5966](#)].
- [132] D. Ghosh, M. Guchait, and D. Sengupta, *Higgs Signal in Chargino-Neutralino Production at the LHC*, *Eur.Phys.J.* **C72** (2012) 2141, [[arXiv:1202.4937](#)].
- [133] P. Byakti and D. Ghosh, *Magic Messengers in Gauge Mediation and signal for 125 GeV boosted Higgs boson*, *Phys.Rev.* **D86** (2012) 095027, [[arXiv:1204.0415](#)].
- [134] A. Papaefstathiou, K. Sakurai, and M. Takeuchi, *Higgs boson to di-tau channel in Chargino-Neutralino searches at the LHC*, [arXiv:1404.1077](#).
- [135] **ATLAS** Collaboration, *Search for electroweak production of supersymmetric particles in the two and three lepton final state at  $\sqrt{s} = 13$  TeV with the ATLAS detector*, Tech. Rep. ATLAS-CONF-2017-039, CERN, Geneva, Jun, 2017.
- [136] J. Anderson, A. Avetisyan, R. Brock, S. Chekanov, T. Cohen, et al., *Snowmass Energy Frontier Simulations*, [arXiv:1309.1057](#).
- [137] P. Meade and M. Reece, *BRIDGE: Branching ratio inquiry / decay generated events*, [hep-ph/0703031](#).
- [138] **MSSM Working Group** Collaboration, A. Djouadi et al., *The Minimal supersymmetric standard model: Group summary report*, in *GDR (Groupement De Recherche) - Supersymetrie Montpellier, France, April 15-17, 1998*, 1998. [hep-ph/9901246](#).
- [139] A. Djouadi, J.-L. Kneur, and G. Moultaka, *SuSpect: A Fortran code for the supersymmetric and Higgs particle spectrum in the MSSM*, *Comput. Phys. Commun.* **176** (2007) 426–455, [[hep-ph/0211331](#)].
- [140] T. Sjostrand, S. Mrenna, and P. Z. Skands, *PYTHIA 6.4 Physics and Manual*, *JHEP* **0605** (2006) 026, [[hep-ph/0603175](#)].

- [141] S. Agostinelli et al., *Geant4—a simulation toolkit*, *Nuclear Instruments and Methods in Physics Research Section A: Accelerators, Spectrometers, Detectors and Associated Equipment* **506** (2003), no. 3 250 – 303.
- [142] R. J. Szabo, *BUSSTEPP lectures on string theory: An Introduction to string theory and D-brane dynamics*, in *31st British Universities Summer School in Theoretical Elementary particle Physics (BUSSTEPP 2001) Manchester, England, August 28-September 12, 2001*, 2002. [hep-th/0207142](#).
- [143] M. L. Mangano, M. Moretti, F. Piccinini, and M. Treccani, *Matching matrix elements and shower evolution for top-quark production in hadronic collisions*, *JHEP* **0701** (2007) 013, [[hep-ph/0611129](#)].